geologica acta

Citation: Casas, J.M., Díez-Montes, A., Pujol-Solà, N., Beranoaguirre, A., Proenza, J.A., Sánchez-García, T., Álvaro, J.J., Murphy, J.B., 2025. From the Upper Ordovician unconformity to the core-mantle boundary: review of the Ordovician events in the Canigó massif, Pyrenees. Geologica Acta, 23.13, 1-48, I-II.
DOI: 10.1344/GeologicaActa2025.23.13
Online ISSN: 1696-5728

From the Upper Ordovician unconformity to the core-mantle boundary: A review of the Ordovician events in the Canigó massif, Pyrenees

Josep Maria Casas[1] Alejandro Díez-Montes[2] Núria Pujol-Solà[3] Aratz Beranoaguirre[4] Joaquín A. Proenza[5] Teresa Sánchez-García[6] J. Javier Álvaro[7] J. Brendan Murphy[8]

[1]Departament de Dinàmica de la Terra i de l'Oceà, Universitat de Barcelona
Martí Franquès s/n, 08028 Barcelona, Spain. E-mail: casas@ub.edu. ORCID: 0000-0001-7760-7028

[2]Instituto Geológico y Minero de España (CSIC)
Plaza de la Constitución 1, 37001 Salamanca, Spain. E-mail: al.diez@igme.es. ORCID: 0000-0003-3215-9174

[3]Departamento de Mineralogía y Petrología, Facultad de Ciencias, Universidad de Granada
Avda. Fuentenueva, s/n, 18071, Granada, Spain. E-mail: npujolsola@ugr.es. ORCID: 0000-0001-6378-6811

[4]Goethe-Universität Frankfurt Institut für Geowissenschaften Petrologie und Geochemie
Altenhöferallee 160438 Frankfurt am Main, Germany. E-mail: beranoaguirre@fierce.uni-frankfurt.de. ORCID: 0000-0002-1137-6498

[5]Departament de Mineralogia, Petrologia i Geologia Aplicada, Universitat de Barcelona
Martí i Franquès, s/n, 08028, Barcelona, Spain. E-mail: japroenza@ub.edu. ORCID: 0000-0001-8738-7305

[6]Instituto Geológico y Minero de España (CSIC)
Ríos Rosas 23, 28003 Madrid, Spain. E-mail: t.sanchez@igme.es. ORCID: 0000-0001-5826-420X

[7]Instituto de Geociencias (CSIC-UCM)
Dr. Severo Ochoa 7, 28040 Madrid, Spain. E-mail: jj.alvaro@csic.es. ORCID: 0000-0001-6294-1998

[8]Department of Earth and Environmental Sciences, St. Francis Xavier University
Antigonish, NS, Canada. E-mail: bmurphy@stfx.ca. ORCID: 0000-0003-2269-1976

ABSTRACT

We present a review of the stratigraphical, structural, geochemical, isotopic and geochronological data that document Ordovician events in the Canigó massif, eastern Pyrenees. Voluminous felsic magmatism, 15-20my in duration, occurred in the Mid to Late Ordovician, in two magmatic pulses that produced several laccolithic bodies, up to ca. 2000m in thickness, which became the protoliths of the various lithologies of the Canigó gneisses. There is also evidence of coeval basalt (now metabasites) with E-MORB affinities. Mid Ordovician uplift and erosion produced an Upper Ordovician (Sardic) unconformity. Synchronous extensional faults built propagation cleavage-free folds affecting a pre-Upper Ordovician succession and caused the erosion of up to 1500m of the underlying Cambrian-Lower Ordovician succession. Early Late Ordovician synsedimentary normal faults produced significant thickness variations in the Upper Ordovician successions. Compiled data match the Ordovician evolution described in Sardinia, Mouthoumet and Montagne Noire (Occitan Domain), but differs from the evolution of neighbouring areas, such as the Iberian, Armorican and Bohemian massifs, where thermal doming and magmatism developed earlier, in Furongian-Early Ordovician times, linked to the Toledanian unconformity. In the study area, uplift, erosion and extensional tectonics argue for a lithospheric uplift coeval with the development of felsic and basaltic (with E-MORB affinities) magmatism, and strongly suggests Mid to Late Ordovician plume activity beneath this segment of NW Gondwanan. The proposed plume would be one of a cluster of plumes impacting the Gondwana periphery that probably migrated inwards into Gondwana. Plume activity may be related to an early Palaeozoic superplume event, that contributed to the birth and development of the Rheic Ocean throughout the Gondwana margin breakup.

KEYWORDS **Ordovician magmatism. Pyrenees. Canigó. Mantle plume. Sardic unconformity.**

INTRODUCTION

A series of tectonic and magmatic events characterized the geodynamic evolution of Gondwana during the early Palaeozoic. These events include a voluminous, mainly felsic, peraluminous magmatism that occurred along much of the Gondwana periphery (Dan *et al.*, 2022; García-Arias *et al.*, 2024; Murphy *et al.*, 2024; and references therein). Interpretation of this early Palaeozoic (Cambrian-Ordovician) magmatic event is key to understanding the geodynamic setting of Gondwana from the Ediacaran-Terreneuvian (Cadomian) accretionary tectonics to the late Palaeozoic amalgamation of Pangea which produced the Variscan-Alleghanian orogeny (Arenas *et al.*, 2014; Gutiérrez-Alonso e*t al.*, 2008; Murphy *et al.*, 2006; Nance *et al.*, 2010; Wu *et al.*, 2022). Despite its large volume and importance, no consensus exists on the origin of this magmatism, and several models have been proposed: i) subduction-related melts formed in a magmatic arc-to-back-arc setting (Castro *et al.*, 2009; Rubio-Ordóñez *et al.*, 2012; Valverde-Vaquero and Dunning, 2000), ii) post-collisional decompression melting of an earlier thickened continental crust linked to asthenospheric upwelling (Pereira *et al.*, 2022; Rodríguez *et al.*, 2022; Villaseca *et al.*, 2016), iii) partial melting of an immature lower crust comprised of metasedimentary and igneous rocks in response to either mafic underplating or mafic intrusion generated by mantle plume activity (Álvaro *et al.*, 2020; Bea *et al.*, 2007; Casas *et al.*, 2024; Dan *et al.*, 2022; Díez-Montes *et al.*, 2010; Marini, 1988; Murphy *et al.*, 2024; Žák *et al.*, 2023) and iv) extensional tectonics in the back-arc region after Gondwana assembly (García-Arias *et al.*, 2024). In some areas of the Gondwana margin, this magmatism is coeval with the formation of intra-Ordovician unconformities (Álvaro *et al.*, 2024a; Dan *et al.*, 2022; Lefebvre *et al.*, 2023). In the Iberian Massif, Casas *et al.* (2023) proposed that this magmatism was also linked to other events that include pronounced magnetic anomalies and significant thickness variations in Lower to Middle Ordovician sedimentary successions in adjacent areas. According to Casas *et al.* (2023) and Álvaro *et al.* (2024a), these events resulted from Furongian-Early Ordovician mantle plume activity located beneath the northwestern margin of Gondwana.

In the Pyrenees, the pre-Variscan basement rocks record Ordovician, mainly felsic, magmatism well represented in the Aston, Hospitalet, Canigó, Roc de Frausa and Albera massifs (Casas *et al.*, 2024; Castiñeiras *et al.*, 2008a; Clariana *et al.*, 2018; Cocherie *et al.*, 2005; Denèle *et al.*, 2009; Liesa *et al.*, 2011; Mezger and Gerdes, 2016). Moreover, a Mid(?) Ordovician folding episode has been described together with Upper Ordovician extensional tectonics and the development of an Upper Ordovician ("Sardic") angular unconformity (Casas, 2010; Casas and Fernández, 2007; Casas *et al.*, 2012; García-Sansegundo and Alonso, 1989; Puddu *et al.*, 2019; Santanach, 1972a, b).

In this paper we review published stratigraphical, structural, geochemical, isotopic and geochronological data of the Ordovician magmatic and tectonic events recorded in the pre-Variscan basement rocks of the Canigó massif, in the eastern Pyrenees (Fig. 1). We focus on this massif because it provides a complete record of bimodal Mid to Late Ordovician plutonic and volcanic magmatism. Moreover, the Canigó massif provides good exposures of the Ordovician deformational structures as well as a regional Upper Ordovician unconformity. We suggest these events collectively indicate mantle plume activity during the Mid to Late Ordovician beneath this segment of the Gondwanan margin, and that this plume activity was genetically linked to the export of terranes from the Gondwana margin during Cambrian-Ordovician times. This study is an example of how the compilation of field-based data can assess several proposed geodynamic scenarios purported to explain the early Palaeozoic Gondwana evolution.

GEOLOGICAL SETTING

Pre-Variscan basement rocks, ranging in age from late Ediacaran to pre-Variscan Carboniferous, crop out extensively in the central part of the Pyrenees, an Alpine E-W trending chain formed in the Late Cretaceous to Miocene after the collision between Iberia and Eurasia (Muñoz, 1992, 2019). The Canigó massif is one of the largest gneissic domes that crops out in the central part of the Pyrenees (Fig. 1; 2). It exhibits an E-W oriented antiformal megastructure (35km long, 20km wide), resulting from the superposition of late Variscan folds (Guitard, 1967) and an antiformal fold linked to an underlying Alpine thrust (Casas *et al.*, 2010) (Fig. 2). Superimposed on this structure are two sets of NE-SW and NW-SE oriented Oligocene-Neogene extensional faults (Fontboté and Guitard, 1958). The reactivation of some of these faults during the Pliocene (Maurel *et al.*, 2002) is responsible for the uplift of the massif (Fig. 2). Two of these faults, the Marialles and Mentet-Fillols faults, cut across the central part of the massif and the deepest crustal rocks recognized in the area are exposed in their footwall (Fig. 2). As a result, the Canigó massif exhibits one of the most complete pre-Silurian successions of the Pyrenees, ranging in age from late-Ediacaran to Late Ordovician.

In the Canigó massif, three megasequences can be recognized in the metasedimentary succession underlying the Upper Ordovician rocks, from bottom to top: the Balaig Series, the Canaveilles Group and the Jujols Group (Fig. 3). The Balaig Series (Guitard, 1953) is a 1500m thick

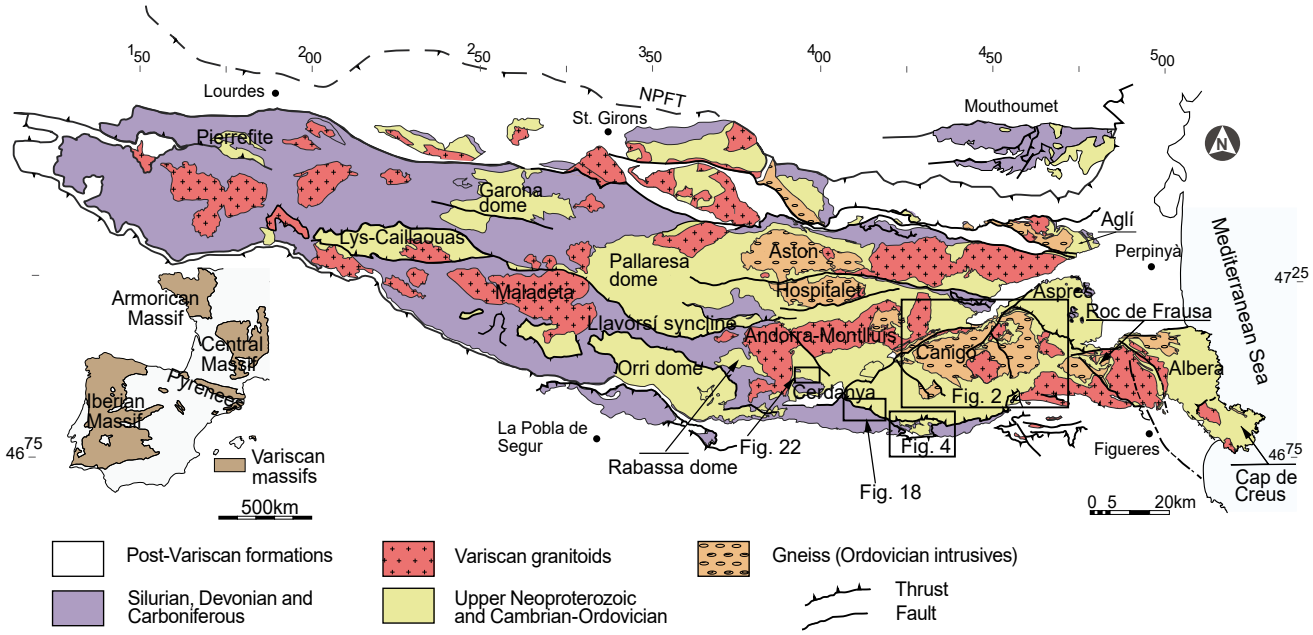

FIGURE 1. Geologic sketch of the eastern and central Pyrenees and Mouthoumet massifs with location of the Figures 2, 4, 18 and 22. NPFT: North Pyrenean Frontal Thrust. Geographical coordinates are provided in UTM.

unfossiliferous succession of mica-schists with marble, quartzite and metabasite intercalations. The protolith age of this series remains unresolved, although an age slightly older (>580Ma?) than the Cadomian magmatic rocks located in the overlying series seems likely (Álvaro *et al.*, in press; Casas *et al.*, 2015). The most remarkable metaigneous intercalation in the Balaig Series is the Casemí gneiss, a laccolithic body mainly made up of fine-grained granitic gneisses, up to 500m thick, that form the highest peaks of the massif. Underlying the Balaig series, the Cadí gneiss crops out locally in the footwall of the Mentet–Fillols fault and constitutes the deepest rocks recognizable in the Canigó massif (Fig. 2; 3).

The Canigó gneiss (see below) separates the Balaig Series from the overlying Canaveilles and Jujols group metasedimentary successions (Fig. 2; 3). The Canaveilles Group (former Canaveilles Series of Calvet, 1957, and redefined as Canaveilles Group by Padel *et al.*, 2018a), is a heterolithic unfossiliferous succession, up to 1500m thick, mainly composed of metapelites interbedded with quartzites, marbles, calc-silicate rocks, felsic metatuffs and metabasites. The lower part of this succession is lithologically and chemically similar to the Balaig Series and a radiometric age of interbedded metatuffs suggests an Ediacaran-Terreneuvian age for this sequence (552±10 to 565±9Ma, U-Pb on zircons, Casas *et al.*, 2015; Padel *et al.*, 2018b; Pujol-Solà *et al.*, 2022), and represents the Neoproterozoic/Cambrian boundary located in the upper part of the sequence (Álvaro *et al.*, in press).

Overlying the Canaveilles Group are the relatively monotonous shale-dominated rocks of the Err Formation (Padel *et al.*, 2018a), which constitute the basal formation of the Jujols Group (formerly defined as Jujols Schists Series by Cavet, 1957) (Fig. 3). The Err Formation is conformably overlain by limestones amb marbles of the Valcebollère Formation, which are of Cambrian Epoch 2 age according to Padel *et al.* (2018a), based on acritarchs recovered in equivalent limestones in the Aspres massif. Overlying these limestones, the Serdinya Formation constitutes the uppermost succession underlying the Upper Ordovician unconformity (Fig. 3). It mainly comprises grey to greenish shales alternating with centimetre to decimetre-thick sandstone beds and some quartzite beds at the top. Ichnoassemblages comprise the predominant *Cruziana* ichnofacies with brief occurrences of the *Skolithos* ichnofacies (Gámez *et al.*, 2012). Acritarchs recovered from the uppermost part of this formation indicate a broad Furongian–Early Ordovician age (Casas and Palacios, 2012), consistent with a maximum depositional age of ca. 475Ma based on the youngest detrital zircon population collected in the quartzites of the uppermost part of the Serdinya Formation in the southern slope of the Rabassa dome (Margalef *et al.*, 2016). Thus, the depositional age of the Jujols Group is bracketed between the Terreneuvian and the Furongian-Early Ordovician.

In the Canigó massif, the Upper Ordovician succession forms a broad fining-upward siliciclastic package (Cavet, 1957; Hartevelt, 1970), ranging from 100 to 1000m in

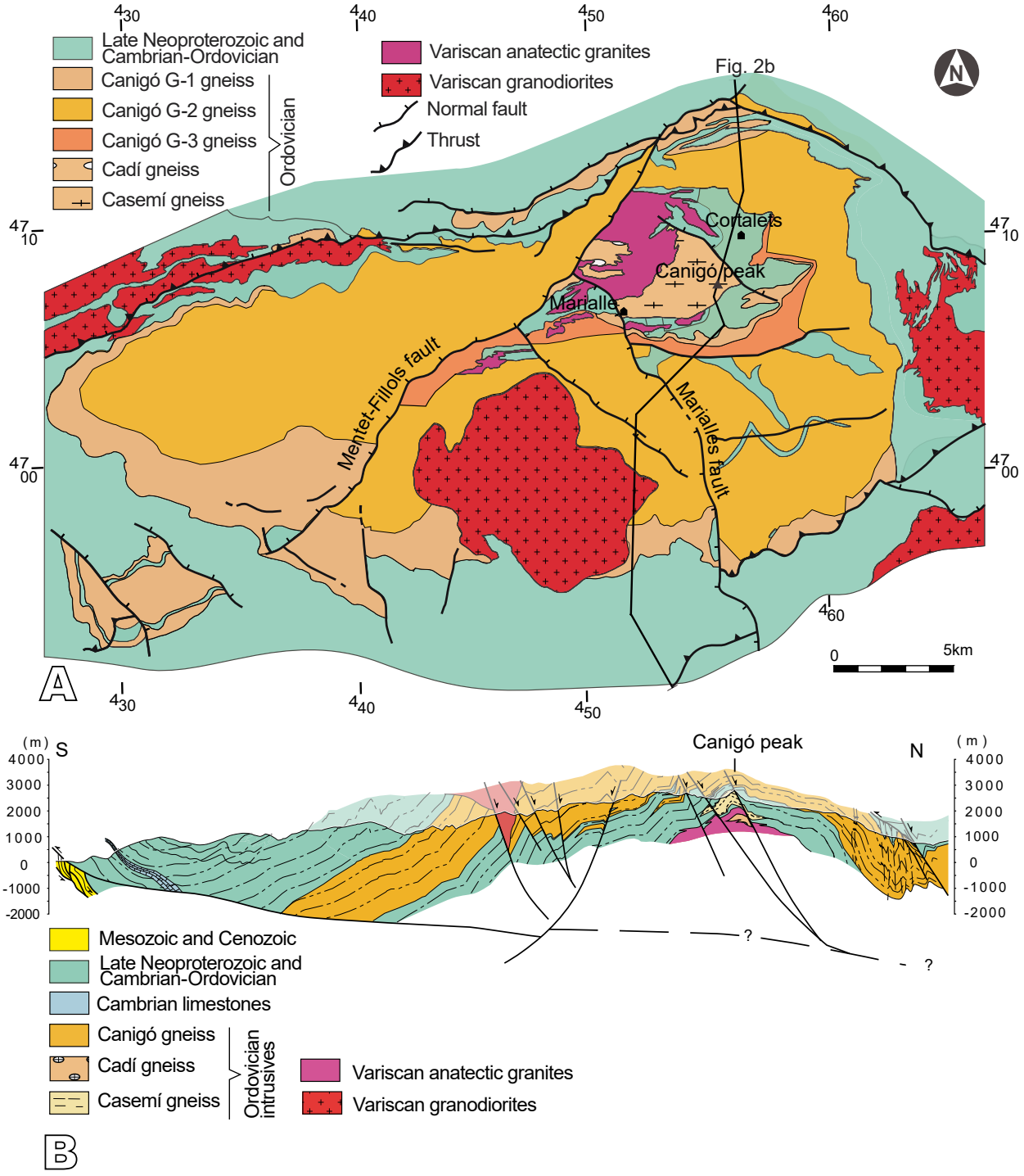

FIGURE 2. A) Geological map of the Canigó massif showing the location of the Marialles and Cortalets huts and the line of the cross-section illustrated in Figure 2B. Data after Guitard (1970), Santanach (1972b), Casas (1984) and Ayora and Casas (1986); B) Cross section through the Canigó massif, modified after Casas *et al.* (2010). Location on Figure 2A. Geographical coordinates are provided in UTM.

thickness, which unconformably overlies the pre–Upper Ordovician succession (Santanach, 1972a) (Fig. 3). In this succession Hartevelt (1970) distinguished five formations, from bottom to top, the Rabassa Conglomerate, Cava, Estana, Ansobell and Bar Quartzite formations. The Rabassa Conglomerate Formation is up to 100m thick and consists of variegated polymictic conglomerates, with heterometric clasts including vein quartz, quartzite and slate. Puddu *et al.* (2019) interpreted the conglomerates as alluvial and fluvial deposits locally affected by debris flows.

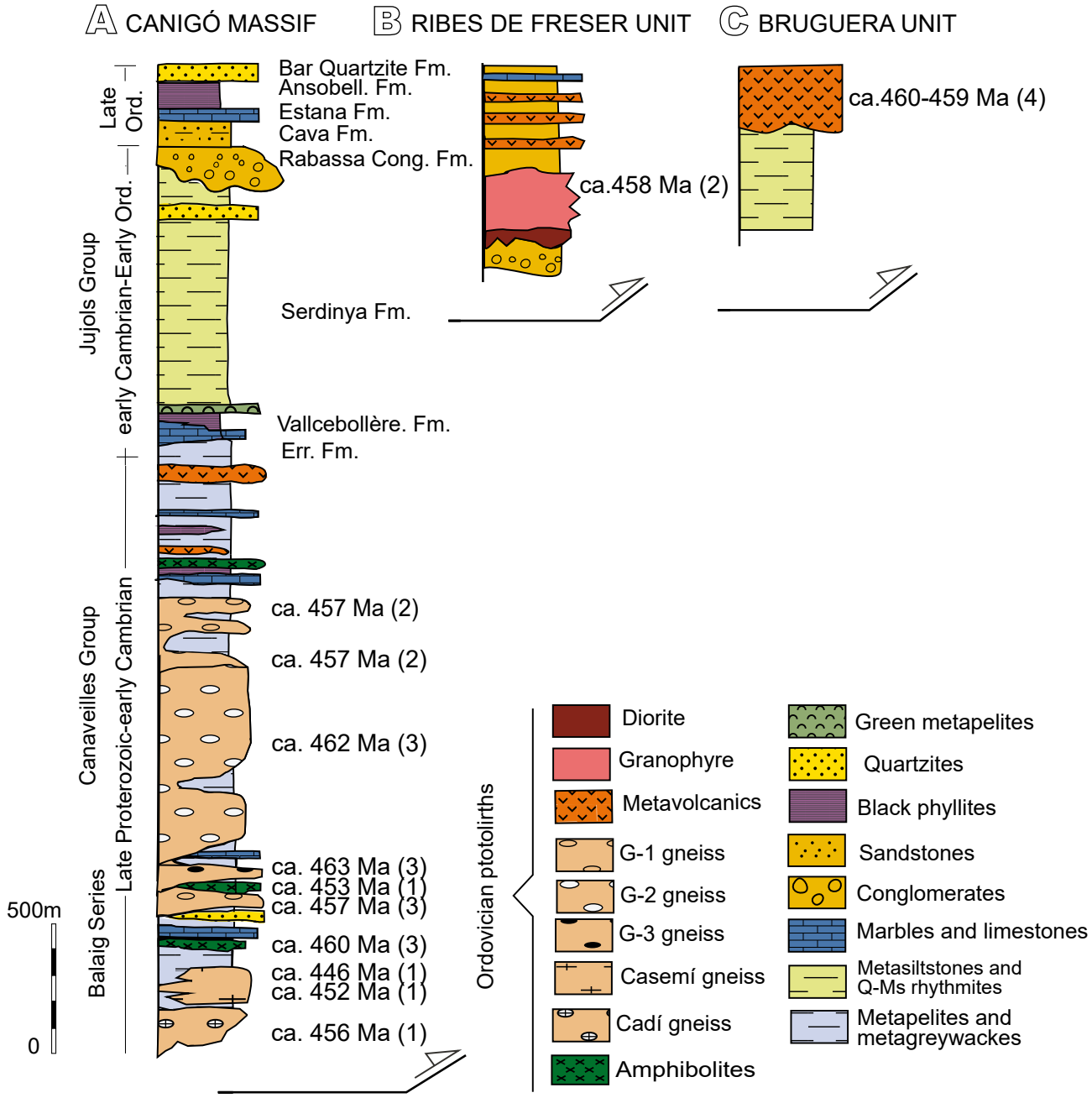

FIGURE 3. Synthetic stratigraphic logs of: A) Canigó massif; B) Ribes de Freser unit; C) Bruguera unit. Geochronological data of the protoliths of the Ordovician magmatic rocks after: (1) Casas *et al.* (2010); (2) Martínez *et al.* (2011); (3) Navidad *et al.* (2018) and (4) Martí *et al.* (2019). Stratigraphic data from Guitard (1970), Hartevelt (1970), Santanach (1972b), Muñoz (1985), Ayora and Casas (1986) and Puddu *et al.* (2018).

Hartevelt (1970) attributed the Rabassa conglomerates to the Sandbian (former Caradoc). The overlying Cava Formation, 0-850m thick, comprises conglomerates, sandstones and shales. According to Puddu *et al.* (2019), basal continental conglomerates and sandstones grade upward into sandstone–shale alternations that reflect the influence of marine shoreface-to-offshore conditions. One coquina layer interbedded with the dominant shale layers has yielded brachiopods (*Svobodaina havliceki*, *Rostricellula* sp. and *Rafinesquina* sp.; Puddu and Casas, 2011), trilobite and bryozoans that indicate a Katian (former late Caradoc–early Ashgill) age (Hartevelt, 1970; Gil-Peña *et al.*, 2004; Pereira *et al.*, 2024) of deposition. Traces of the ichnogenus *Arthrophycus* occur in fine-grained sandstones of the upper part of the formation (Belaústegui *et al.*, 2016). The Estana Formation, 0–200m thick, consists of limestones and marly limestones with abundant late–Katian brachiopods, bryozoans, echinoderms, conodonts and cornulitids (Gil-

Peña *et al.*, 2004; Sarmiento *et al.*, 2011; Vinn *et al.*, 2024). The top of the carbonate succession is unconformably overlain by the black-grey shales of the Hirnantian Ansobell Formation, 20–320m thick, in turn overlain by the 8–18m thick Hirnantian Bar Quartzite Formation (Štorch *et al.*, 2019). These formations are well exposed in the southern slope of the Canigó massif and in the Rabassa dome (Fig. 1), which constitutes the western edge of the Canigó massif and display some variations over a wide area of the central and eastern Pyrenees. The Andorra-Montlluís granodiorite separates the Rabassa dome from the rest of the Canigó massif (Hartevelt, 1970) (Fig. 1).

South of the Canigó massif, a second-order Alpine antiformal stack crops out in a kilometre-scale culmination in both sides of the Freser valley (Muñoz, 1985) (Fig. 4A), separated from the rest of the Canigó massif by the Alpine Ribes-Camprodon thrust (Muñoz, 1985) (Fig. 4B). The Ribes de Freser and Bruguera units are exposed in this antiformal stack that, in contrast to the Upper Ordovician succession cropping out in the rest of the Canigó massif, exposer voluminous Ordovician felsic-dominant magmatism. The Bruguera unit exhibits a 300m-thick unfossiliferous slate-dominant succession, assigned to the Cambrian–Lower Ordovician by Muñoz (1985) (Fig. 3; 4), overlain by a volcanic complex, described below. To the North, a North-dipping fault separates this unit from the Ribes de Freser unit, which contains a 200–600m-thick succession, mainly composed of Upper Ordovician volcanic, subvolcanic and volcano-sedimentary rocks interbedded with Sandbian-Katian strata and intruded by a subvolcanic granitic body (see below). Underlying the Buguera unit, the El Baell unit comprises a 500m-thick succession of limestones, marlstones and shales (the El Baell Formation, Puddu *et al.*, 2018). Conodonts and echinoderms allowed Robert (1980) to assign an early Katian (former Caradoc) age to the strata of this unit. Sánz-López and Sarmiento (1995) identified conodont faunas that suggest a late Katian depositional age and correlated them with strata described from the Estana Formation. Puddu *et al.* (2018) suggested that the drastic changes in thickness and facies linking the El Baell and Estana formations point to the onset of extensional tectonic pulses which may have controlled significant modifications in accommodation space and development of (half-) grabens, although the initial orientation of the faults controlling these grabens is difficult to establish due to overprinting by late Variscan and Alpine deformations.

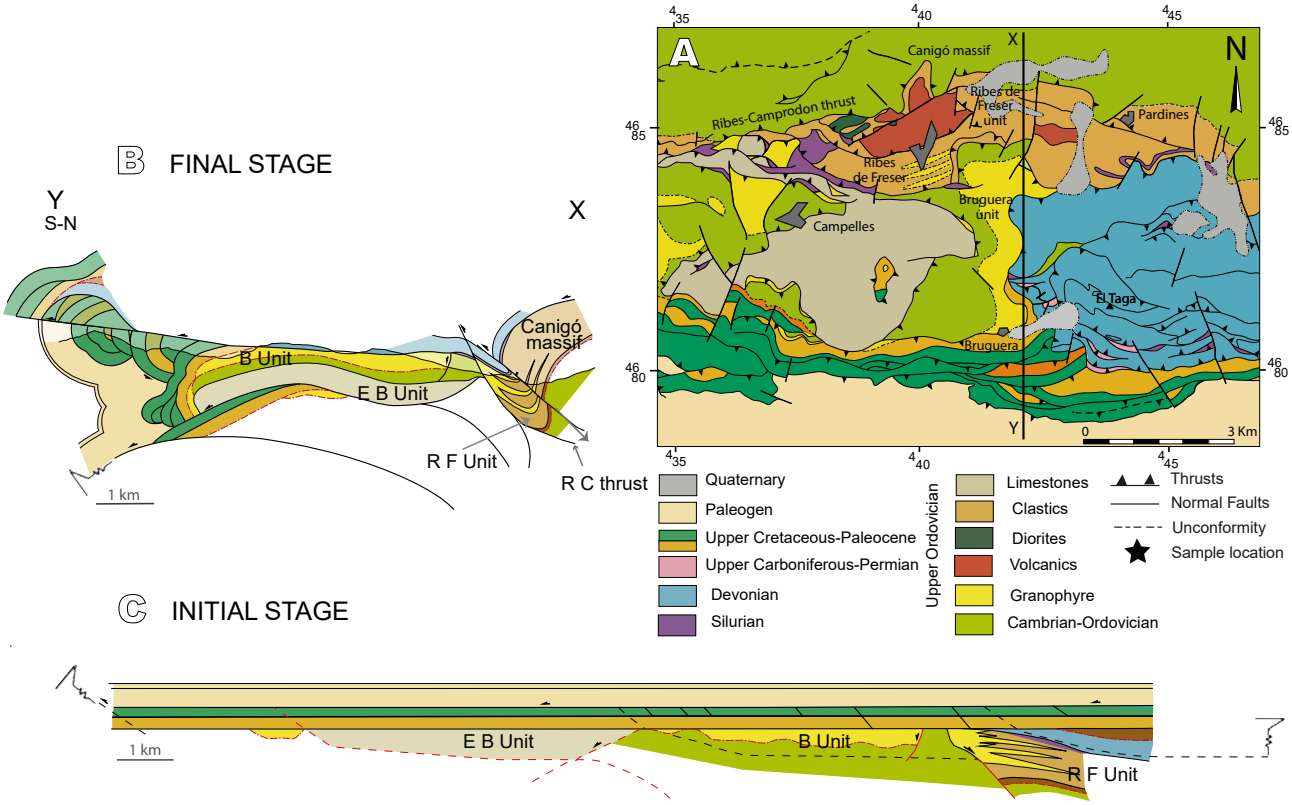

FIGURE 4. A) Geological map of the Ribes de Freser area. Black line X-Y indicates the trace of cross-section from B. Location on Figure 1; B) Balanced cross-section of the Ribes de Freser antiformal stack (B unit= Bruguera unit; E B= El Baell unit; R F unit= Ribes de Freser unit; R C thrust= Ribes Camprodon thrust). C) Restored section of the Ribes de Freser antiformal stack showing the initial location of the El Baell, Bruguera and Ribes de Freser units (modified after Casas *et al.*, 2024). Geographical coordinates are provided in UTM.

Restoration of the Alpine deformation situates the Ribes de Freser unit in a pre-Alpine northerly position, between the Bruguera unit to the South and the Canigó massif to the North (Fig. 4C).

ORDOVICIAN MAGMATISM

Canigó gneiss: Guitard's legacy

After discarding the prevailing ideas that gneisses were of metasomatic origin, Guitard (1955) pointed out that the Canigó gneiss is an orthogneiss resulting from the Variscan deformation, of either metavolcanic (fine-grained felsic gneisses) or metagranitic (augen gneisses) rocks (Guitard, 1963a, b, 1967). Moreover, Autran and Guitard (1969), Autran *et al.* (1966), Fonteilles and Guitard (1972, 1977, 1988), Guitard (1958, 1970, 1976; Guitard in Jaffrezo *et al.*, 1977) and Guitard *et al.* (1996, 1998), proposed that massive augen gneisses were derived from Variscan deformation and metamorphism of a Cadomian granitic basement, implying that: i) a major post-Cadomian unconformity exists, ii) the Canaveilles Series (*sensu* Cavet, 1957) represents a Cambrian sedimentary cover that unconformably overlies this basement and iii) the base of this discordant succession comprises felsic metavolcanic rocks. In this basement-cover model, a major recumbent fold is required to explain the reappearance of the Canaveilles metasedimentary rocks and the Canigó gneiss at the bottom of the succession, forming the Balaig Series and the Cadí gneiss respectively (Fig. 2; 3).

Although their model has been invalidated since the beginning of the 21st century because of the new geochronological data (see below), Guitard's exhaustive descriptions and detailed field mapping are a cornerstone when dealing with lithostratigraphy, structure and metamorphism of the Variscan basement rocks of the Pyrenees. In this sense, the identification of several types of gneiss in the Canigó massif made by Guitard (1970) based on petrographical criteria, is still valid. Briefly, this author recognized: i) G-1 gneiss, fine-grained leucogneisses ("leptynites" in French terminology) with thin augen gneiss intercalations and banded gneisses, located predominantly at the bottom and at the top of the main gneissic body (Figs. 5A; 6A); ii) G-2 gneiss, massive, coarse-grained porphyritic, rapakivi biotite gneiss, forming the main Canigó gneissic body, ranging from 1500 to 2000m in thickness (Fig. 5B; 6B); iii) G-3 gneiss, mesocratic, medium grained porphyritic biotite gneiss, located only at the bottom of the main gneissic body (Fig. 5C; 6C); iv) Casemí gneiss, a laccolithic body intercalated in the Balaig Series (Fig. 5D, E; 6D) and v) Cadí gneiss, granitic augen gneisses lithologically similar to the G-2 gneiss (Fig. 5F), constituting the deepest rocks exposed in the Canigó massif.

Origin of the Canigó gneiss protoliths: field evidence

Although the basement-cover model of Guitard and co-workers was widely accepted, mainly by French geologists, some field data from several zones cast doubt on the origin of the gneiss protolith and invited several authors to explore alternatives. Sebastián *et al.* (1982) suggested a plutonic and intrusive origin for the G-1 gneiss protolith in the Queralbs-Núria area, on the southern slope of the Canigó massif, based on petrological and field criteria (xenoliths, granophyric textures, and relics of contact metamorphism among others), and suggested a Late Ordovician age for the intrusion.

On the northern slope of the massif, near the towns of En and Nyer, Casas (1984) described some marble levels crosscut by the gneiss/metasediment contact (Fig. 7A), as well as abundant sills of orthogneisses within the micaschists close to the upper contact in the Bastimets peak area in the southern slope (Fig. 7B). Liesa (1988) found similar relationships in the neighbouring gneissic Roc de Frausa massif, and Alías *et al.* (2000) emphasized the irregular geometry of the basal contact of the gneiss in the central part of the massif, better explained by an intrusive contact than a folded (overturned) unconformity (Fig. 7C). Moreover, relics of contact metamorphism (pseudomorphs of cordierite porphyroblasts) deformed by the main Variscan foliation are common in a kilometre-scale septum located in the middle of the gneissic body (St.Guillem septum; Casas, 1984) and in the southern slope of the massif in the Ull de Ter area (Fig. 7D). Although all these field data suggest a gneiss/metasedimentary intrusive contact, taken separately these observations were not sufficiently robust at that time to challenge the basement-cover model. Later on, Barbey *et al.* (2001) compiled all these field data, and following Sebastián *et al.* (1982), proposed that the Canigó gneiss was derived from an intrusive Ordovician granite laccolith protolith deformed during the Variscan orogeny.

Origin of the Canigó gneiss protoliths: review of the radiometric age of the Canigó gneiss

The first geochronological data obtained for the protolith of the Aston augen gneiss yielded an Ordovician age (475Ma, whole rock Rb/Sr analysis; Jäger and Zwart, 1968) that clearly contradicted the basement-cover model. In contrast, radiometric ages available at that time for the Canigó gneiss (between ca. 580 and 524Ma, whole rock Rb/Sr; Vitrac-Michard and Allègre, 1975a, b) supported a Cadomian age for the Canigó metagranites, in accordance with the basement-cover model. Delaperrière and Soliva (1992) obtained a Silurian age for the Casemí gneiss (425±18Ma, zircon Pb evaporation), which was difficult to interpret because this age is unrelated to any other magmatic occurrence in the pre-Variscan rocks of

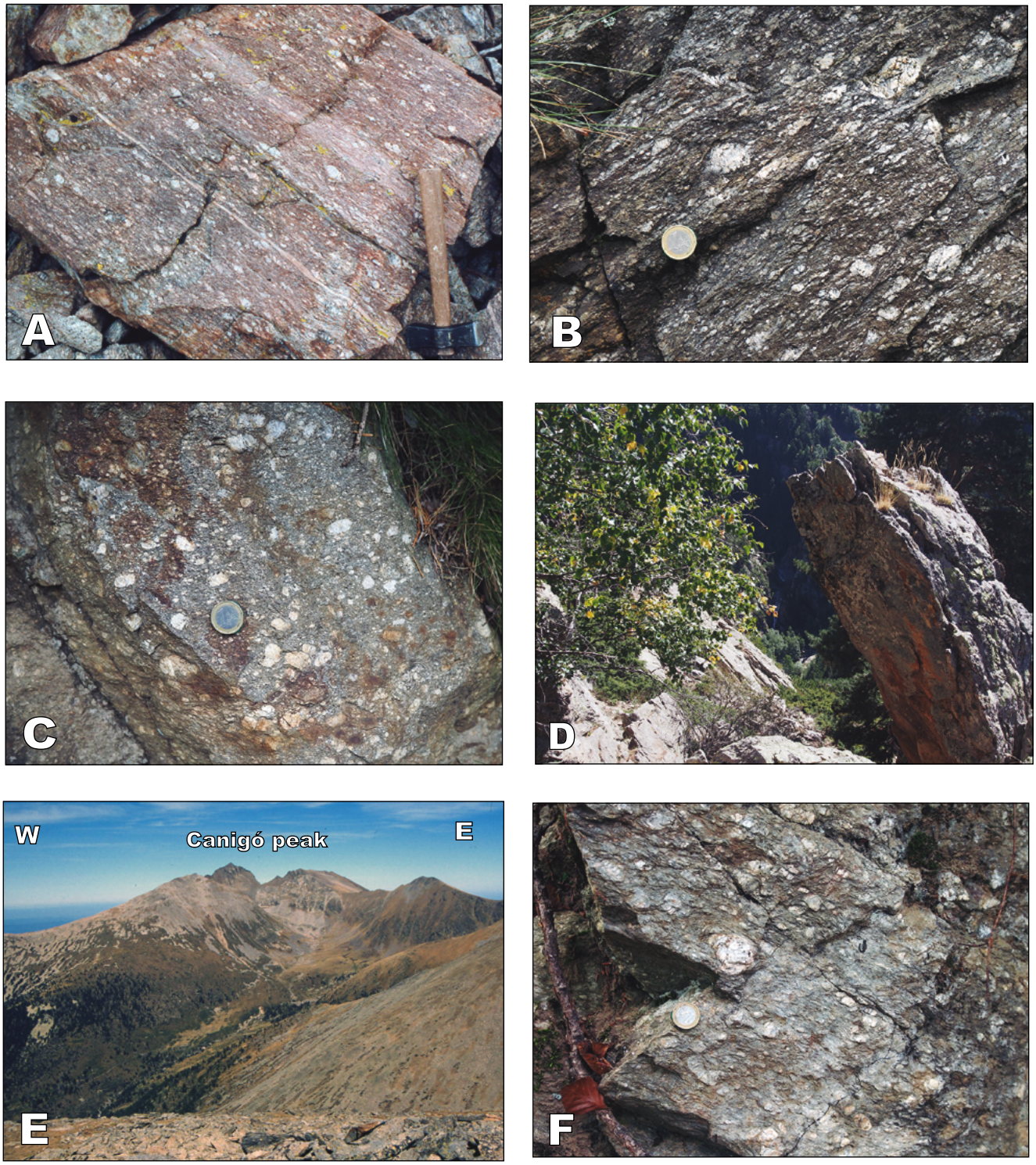

FIGURE 5. A) Field image of the Canigó G-1 type gneiss near Pic de Bastiments; B) G-2 type gneiss in the Saorra-Pi road; C) Canigó G-3 type gneiss in the Marialles-Pla Guillem road; D) Casemí type gneiss near Marialles hut; E) The Canigó peak (2784m) and the central part of the massif, mainly made up by the Casemí gneiss, view from the south (Pic de Tres Vents); F) Cadí type gneiss near Marquirol creek.

the Pyrenees. Using the same method, Delaperrière and Respaut (1995) obtained the first Ordovician age for the Canigó gneiss protolith (446±20Ma, Katian) of the G-1 type gneiss.

The results of the first modern in situ dating (SHRIMP: Sensitive High Resolution Ion Microprobe, Deloule *et al.* 2002) yielded an age of 475±10Ma for the protoliths of the gneiss. This age was calculated with zircons from three

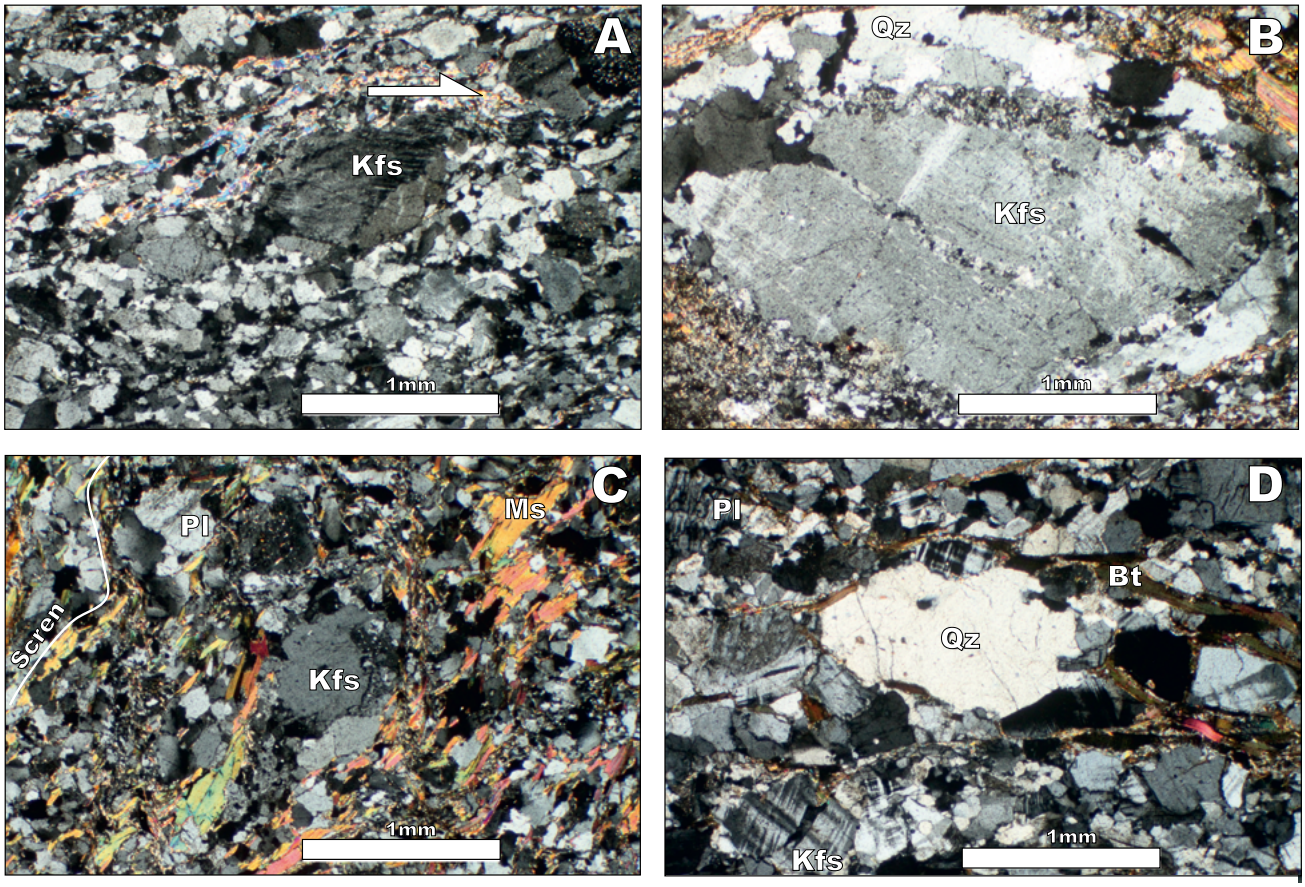

FIGURE 6. Thin-section photomicrographs of gneiss. A) Textural aspect of G-1 gneiss. Potassium feldspar phenocryst with undulating extinction and sigmoid shape; B) Potassium feldspar porphyroclast ("augen") in G-2 gneiss, with recrystallized quartz tails; C) G-3 gneiss with a foliation marked by micas; D) Textural aspect of the Casemí gneiss. Mineral abbreviations: Bt= Biotite, Kfs= K-feldspar, Ms= Muscovite, Pl= Plagioclase and Qz= Quartz. Scale bars: 1mm.

different samples representative of the G1- and G2-type gneisses, based on a few concordant results in an unspecified number of analyses. Their data set shows many concordant analyses, spanning from 575Ma to 334Ma, and the authors interpreted the age of 475Ma as the most plausible age of the protoliths. They inferred that ages older correspond to inherited Proterozoic components, while ages younger than 460Ma reflect lead-loss related to Late Carboniferous HT–LP metamorphism.

Early Ordovician ages were published by Cocherie *et al.* (2005) who, in addition to U-Pb SHRIMP ages, also analysed two samples by ID-TIMS (Isotope Dilution Thermal Ionization Mass Spectrometry). The latter were performed in a G2-type gneiss and a transitional G-1 gneiss. In both cases, five zircon fractions were analysed and the ages obtained were based on three fractions (including discordant results due to lead loss), whereas the other two fractions were outliers due to inherited components. The ages obtained by these authors exhibit relatively large uncertainties of ca. 2%; 471±8Ma and 467±7Ma for the G-2 and transitional gneisses G-1, respectively. On the other hand, the SHRIMP measurements on two samples from the G1-type gneisses yielded ages of 477±4Ma and 472±6Ma which are within the analytical uncertainty of those of Deloule *et al.* (2002). Cocherie *et al.* (2005) pointed out the difficulty of deciphering Pb loss, and interpreted some of the analyses to be outliers. However, they did not consider the possibility of any inherited component for other spot analyses. If all the analyses are deemed to belong to the same cloud of ellipses, and therefore, none of the analyses are excluded, the protolith age of the gneisses would be slightly younger. The same situation occurs in the study of Castiñeiras *et al.* (2008a), who dated an orthogneiss from the neighbouring Roc de Frausa massif (476±5Ma), which is equivalent to the Canigó G-2 gneiss. They discarded younger concordant analyses assuming Pb loss. In addition, analyses with reverse discordance were not excluded.

More recently, Navidad *et al.* (2018) analysed new samples from the G-1-, G-2- and G-3 type gneisses, as well as an amphibolite sill in the area. The data imply the same

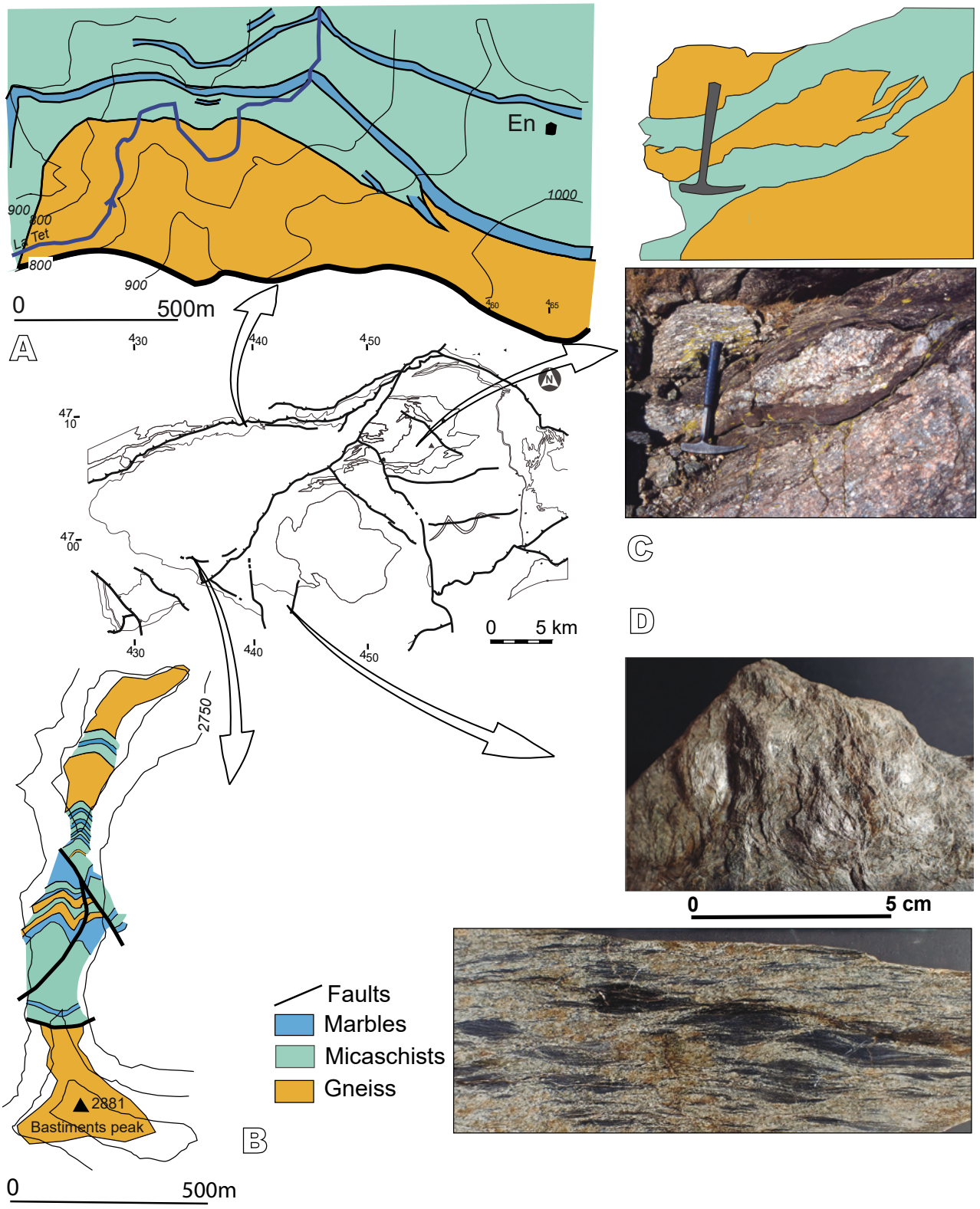

FIGURE 7. Sketch of the Canigó massif with location of outcrops pointing to an intrusive origin for the Canigó gneiss protoliths. A) Cartographic sketch near En town showing marble levels crosscut by the gneiss-metasediment contact; B) Cartographic sketch showing sills of orthogneiss within the mica-schists close to the upper gneiss-metasediment contact in the Bastiments peak area; C) Irregular geometry of the basal gneiss/Balaig mica-schists contact in the central part of the massif; D) Relics of contact metamorphism (pseudomorphs of cordierite porphyroblasts) deformed by main Variscan foliation in a section parallel (up) and normal (down) to the main Variscan foliation in the Ull de Ter area, southern slope of the massif.

age within uncertainty of ca. 460-465Ma for the G-2 and G-3 gneisses (SHRIMP, 462±2 and 464±1Ma, respectively, Darriwilian), except for the G-1-type, which yielded a slightly younger age of 457Ma (SHRIMP, 457±2Ma, Sandbian). The latter age is in agreement with the age obtained by Casas *et al.* (2010) for the Cadí gneisses (SHRIMP, 456±5 Ma, Sandbian), which are emplaced into the lower part of the pre-Upper Ordovician succession of the Canigó massif. Additionally, Casas *et al.* (2010) also dated the Casemí gneisses, with ages of ca. 446-451Ma (SHRIMP, 446±5Ma and 451±5Ma, Katian). Also, Late Ordovician ages for the G-1 type gneiss (SHRIMP, 457±4 and 457±5Ma, Sandbian) were obtained by Martínez *et al.* (2011). These ages contrast with the Early Ordovician age proposed by Cocherie *et al.* (2005) for the G-1 type gneiss protolith.

All the aforementioned data lack the expanded (or method-related) uncertainty. According to Schaltegger *et al.* (2015), the absolute age resolution (2σ) of the SHRIMP technique is about 1-2%. This means that the minimum uncertainty for an Ordovician zircon is at least ca. 5Ma. If so, all published data for the G-2 and G-3 Canigó gneisses overlap with a coherent age of ca. 465-470Ma, which lies in the range of the ID-TIMS ages published by Cocherie *et al.* (2005).

Besides the work by Castiñeiras *et al.* (2008a) on the Roc de Frausa massif gneisses, the neighbouring Aston and Albera massifs have been dated by Mezger and Gerdes (2016) and Liesa *et al.* (2011), respectively. The results obtained in these massifs are equivalent to the Canigó massif, 470±3 and 467±2Ma respectively, and signify Mid Ordovician magmatic activity.

Overall, the ages published show that the magmatic activity at the Canigó massif was active for ca. 15-20m.y., from the Mid Ordovician. However, the possibility of two magmatic events, one at ca. 465Ma and the second at ca. 450Ma, cannot be discarded.

Mafic metavolcanics

Although Ordovician felsic igneous rocks predominate, some metre-scale thick bodies of amphibolites (mafic rocks) interlayered in the Balaig mica-schists can be recognized in the central part of the massif.

Samples CG-07-04 and CG-24-04 correspond to a 2m thick metabasite sill located near the Cortalets hut (Fig. 2), adjacent to the gneiss/Balaig Series contact (Fig. 3). Both samples are well-foliated amphibolites made up of green hornblende, zoisite, titanite and scarce chlorite and plagioclase showing porphyro-nematoblastic texture formed by green hornblende porphyroblasts rimmed by prismatic hornblende that defines the main foliation. The porphyroblasts are replaced by clinozoisite, chlorite and biotite, with abundant titanite. This sample yielded a 460±3Ma (Darriwilian) crystallization age (LA-ICP-MS, Navidad *et al.*, 2018).

Samples CG-07-02 and CG-19-06 were collected near the Marialles hut (Fig. 2), on the road to Pla Guillem, also close to the gneiss/Balaig Series contact (Fig. 3). The outcrop is dominated by metre-scale metabasite composed of amphibole (hornblende), plagioclase and minor quartz. Biotite is scarce and accessory minerals include titanite. This sample yielded a 453±4Ma (Sandbian/Katian) age for the protolith (SHRIMP, Casas *et al.*, 2010).

Felsic metavolcanics and granophyre

The Ribes de Freser thrust unit, which forms the Alpine Freser valley antiformal stack, exhibits a 200–600m thick pre-Variscan basement succession, mainly composed of Upper Ordovician volcanic, subvolcanic and volcano-sedimentary rocks interbedded with Katian sedimentary rocks (Fig. 3B; 4B) (Ayora, 1980; Martí *et al.*, 1986; Muñoz, 1985; Robert, 1980; Robert and Thiebaut, 1976). A granitic body with granophyric texture, the Ribes de Freser granophyre, intrudes the lower part of the succession. This granophyre was first considered a Variscan magmatic body (Fontboté, 1949; Robert, 1980; Santanach, 1972b), although Ayora (1980) and Muñoz (1985) suggested a Late Ordovician age based on field relationships. A Late Ordovician (Sandbian) age was confirmed by Martínez *et al.* (2011), who obtained a SHRIMP U-Pb zircon radiometric age of 458±3Ma.

The Bruguera unit, separated from the Ribes de Freser unit by a set of North-dipping normal and reverse faults, exhibits a 300m-thick unfossiliferous slate-dominated pre-Variscan succession, assigned to the Cambrian–Lower Ordovician by Muñoz (1985) (Fig. 3C; 4). This succession is overlain by a volcanic complex (Fontboté, 1949; Morre-Biot and Robert 1976; Robert, 1980) that consists of 300-400m of rhyolitic ignimbrites that overlie andesites, variegated in colour and finely banded (Martí *et al.*, 2024; Morre-Biot and Robert, 1976; Muñoz, 1985). Although these authors attributed a Permian-Carboniferous age to this magmatism, recent U–Pb data on these volcanic rocks (LA-ICP-MS; Martí *et al.*, 2019) suggest a radiometric age of ca. 460-459 Ma (late Darriwilian-early Sandbian) (Fig. 3C). If we assume a Cambrian-Ordovician depositional age for the slate-dominated succession, the contact between the slates and the overlying volcanic succession may be equivalent to the Upper Ordovician unconformity described close to the study area (Santanach, 1972a; Puddu *et al.*, 2019).

On the eastern slope of the Canigó massif, in the Aspres area (Fig. 1), a 450±4Ma (Katian) age was obtained for felsic metavolcanic rocks (rhyodacite, the "Aspres Porphyrite" of French geologists), located on top of the Upper Ordovician conglomerates (U-Pb, LA-ICPMS, Laumonier *et al.*, 2015).

Geochemical and isotopic data

Geochemical data described below correspond to 35 whole-rock analyses of samples from the Canigó massif. Twenty of these analyses are new and correspond to 18 felsic samples of the five compositional types of the Ordovician Canigó orthogneisses, Ribes granite, Bruguera ignimbrite, 1 sample of the Cortalets metabasite and 1 sample of the Marialles metabasite (X-ray Fluorescence (XRF) and Inductively Coupled Plasma Mass Spectrometry (ICP-MS) analysis, ACTLABS, for details see Analytical procedure in the Supplementary material). Sample locations are given in Table I of the Appendix. In addition, we have included in our compilation 15 previously published whole-rock analyses of the Canigó gneisses and the Cortalets and the Marialles metabasites (Navidad *et al.*, 2010, 2018). Data from Guitard (1970) have also been included for comparison (Table I of the Supplementary material). Isotopic analyses include data from 24 samples, 16 previously published (Martínez *et al.*, 2011; Navidad *et al.*, 2018) and 8 new anlysis from this study, performed at the Centro de Geocronología y Geoquímica Isotópica from the Complutense University, Madrid (Table II of the Supplementary material; for details see Analytical procedure in the Appendix).

Felsic rocks

The Ordovician silicic magmatism (>63wt.% SiO_2) is felsic to moderately mafic (>0.5wt.% and <8wt.% FeO_t+MgO), alkali-rich (>6wt.% Na_2O+K_2O) and potassic (K_2O/Na_2O>1) (Table I of the Supplementary material; Fig. 8). Based on geochemical characteristics, three main groups of rocks can be distinguished (Fig. 8A-B). The first group comprises the G-2 and G-3 gneisses (ca. 462-464Ma), the Bruguera ignimbrite (ca. 459-460Ma) and the Cadí gneiss (ca. 456Ma). The second group includes the G-1 gneisses (ca. 457Ma), whereas the third consist of the Casemí gneisses and the Ribes granite (ca. 446-451 and 458Ma, respectively).

The samples of the first group are monzogranitic to granodioritic in composition in the Total Alkali Silica (TAS) and Winchester and Floyd (1977) diagrams, respectively (Fig. 8A-B). Although the Cadí gneiss samples (Sandbian in age) are similar in composition to the Middle Ordovician ones (G-2 and G-3 gneisses), the remaining Upper Ordovician samples have higher SiO_2 values, and are granitic in composition (G-1 and Casemí gneisses, and Ribes granite; Fig. 8A-B).

The Bruguera ignimbrite has a high loss on ignition (LOI; 2.7wt.%) and a high Chemical Index of Alteration (CIA= 73.8; Nesbitt and Young, 1982). These characteristics indicate significant mobility of the major elements, explaining why these samples are geochemically distinct from the rest of the samples in the group defined by the G-2+G-3+Cadí orthogneisses (Fig. 8A, C). In contrast, if we consider the immobile elements, the Bruguera ignimbrite sample plots within the cluster defined by the aforementioned gneisses (Group-1 in Fig. 8B).

In the B-A diagram (Fig. 8C; Debon and Le Fort, 1983, modified by Villaseca *et al.*, 1998; Aluminium Saturation Index calculated as molar $Al_2O_3/(Na_2O+K_2O+CaO-10/3\ P_2O_5)$, this magmatism is peraluminous (ASI>1.0) to strongly peraluminous (ASI>1.1). In the AFM diagram (Fig. 8D), the set of samples from the Canigó massif has a well-defined trend within the calc-alkaline field. In the Fe-number (Fig. 8E; Frost *et al.*, 2001) and Modified Alkali-Lime Index (MALI) diagrams (Fig. 8F; Frost and Frost, 2008), these rocks classify as alkali-calcic and calc-alkaline, and as magnesian (G-2, G-3 and Cadí samples) with a ferroan trend for the most silicic Upper Ordovician samples (G-1, Casemí and Ribes granite). In the Harker variation diagrams (Fig. 9), all major elements show marked negative trends with SiO_2, least mobile elements (TiO_2, Al_2O_3 FeO^t). K_2O, on the other hand, shows a positive trend. Concerning P_2O_5, the G-1 gneiss plots away from the trend defined by the rest of the lithologies.

All samples have high chondrite-normalized Rare Earth Element (REE) contents (ΣREE=115-270ppm), and are moderately enriched in light REE (LREE), relative to heavy REE (HREE) (Fig. 10A, C, E). The highest degree of HREE fractionation is shown by the samples of the second group (G-1 gneisses), with $(Gd/Yb)_N$= 2.3-4.4 (Fig. 10C). The rocks of the first group exhibit a lower degree of HREE fractionation, $(Gd/Yb)_N$= 1.4-1.8 (Fig. 10A), whereas the samples of the third group (Casemí gneiss and Ribes granite), are characterized by a HREE flat pattern $(Gd/Yb)_N$= 1.0-1.5 (Fig. 10E).

In the Primitive Mantle-normalized multi-element diagram (Fig. 10B, D, F), the three groups of rocks show similar patterns from Th to Sm, but some differences can be observed between Zr and Lu. All samples exhibit strong enrichment in Th, similar Ta, Nb negative anomalies and similar LREE fractionation. The Zr and Hf contents are similar in all rock groups, except for the Casemí gneisses, which show positive anomalies (Fig. 10F). All samples show negative Eu and Ti anomalies, which are especially pronounced in the G-1 and Casemí gneisses and the Ribes granite (Fig. 10B, F). The G-1 gneisses show the greatest fractionation of HREE and Y (Fig. 10D), whereas the rocks forming the third group

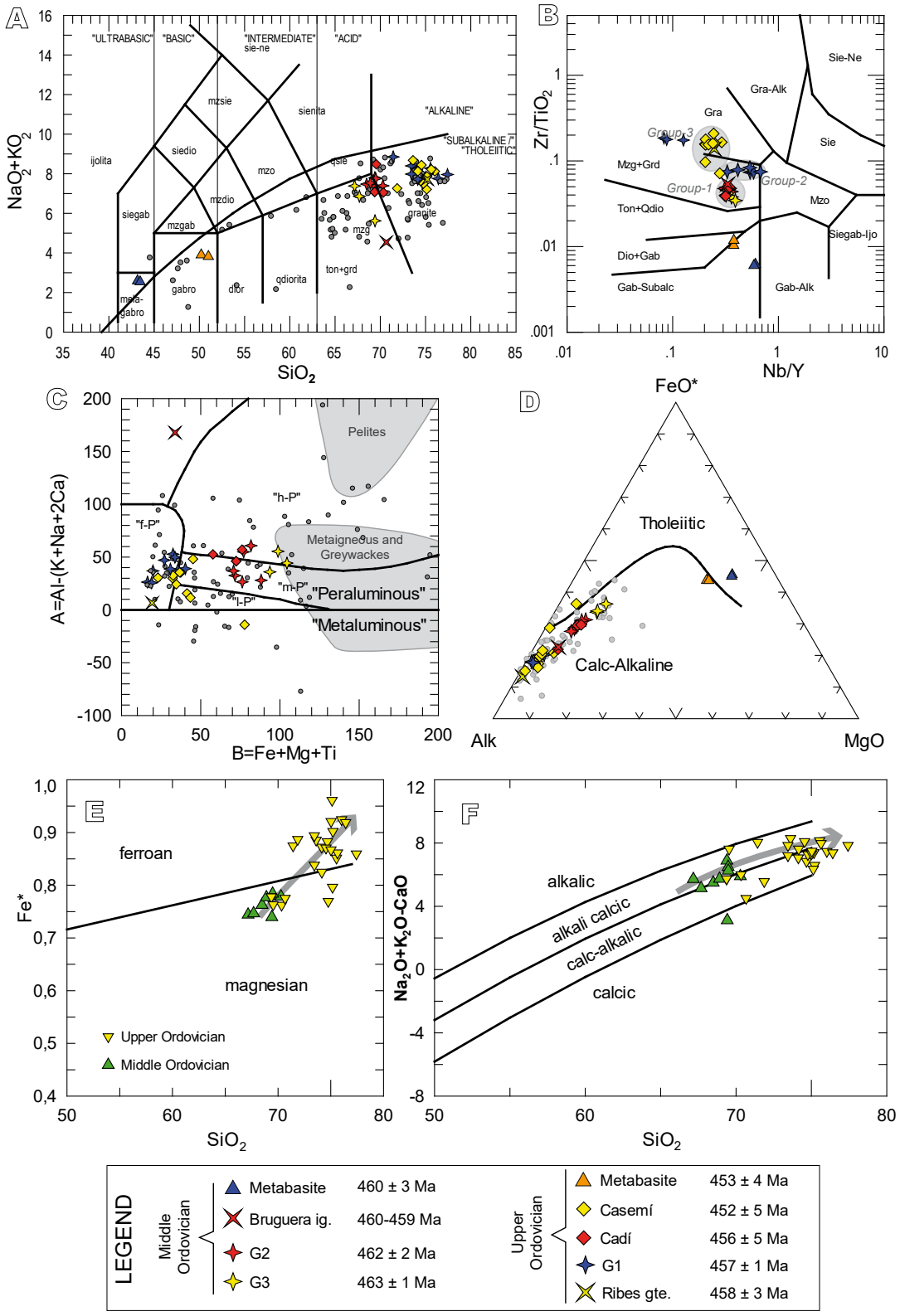

FIGURE 8. Geochemical diagrams. A) Total Alkali Silica (TAS) diagram from Le Bas *et al.* (1986); B) Zr/TiO_2 vs Nb/Y classification diagram of Winchester and Floyd (1977). The samples are concentrated in three groups of composite rocks, the first formed by samples of the Middle Ordovician gneiss (G-2 and G-3), Bruguera ignimbrites and Cadí gneiss. The second group is formed by the G-1 gneiss, and the third group comprises rocks of Late Ordovician age, Casemí gneiss and Ribes granite; C) B-A diagram of Debon and Le Fort (1983), modified by Villaseca *et al.* (1998); D) Alkalis, iron and magnesium (AFM) diagram; E) and F) Fe-number and Modified Alkali-Lime Index (MALI) (Na_2O+K_2O-CaO) diagrams (Frost *et al.*, 2001). All elements are normalized to 100% anhydrous. Data from filled circles after Guitard (1970).

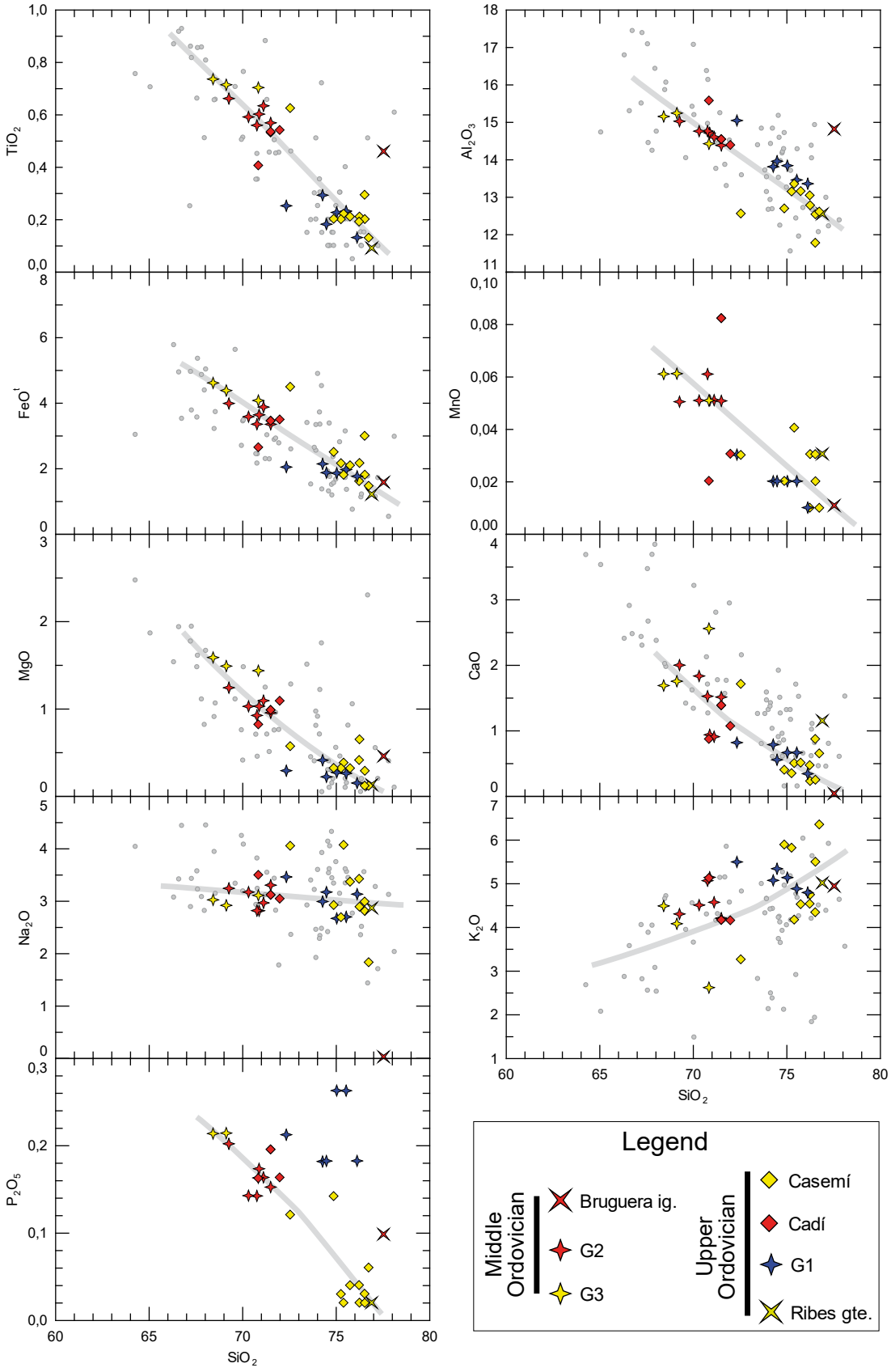

FIGURE 9. Harker diagrams for the Ordovician felsic magmatic rocks of the Canigó massif. Data from filled circles after Guitard (1970).

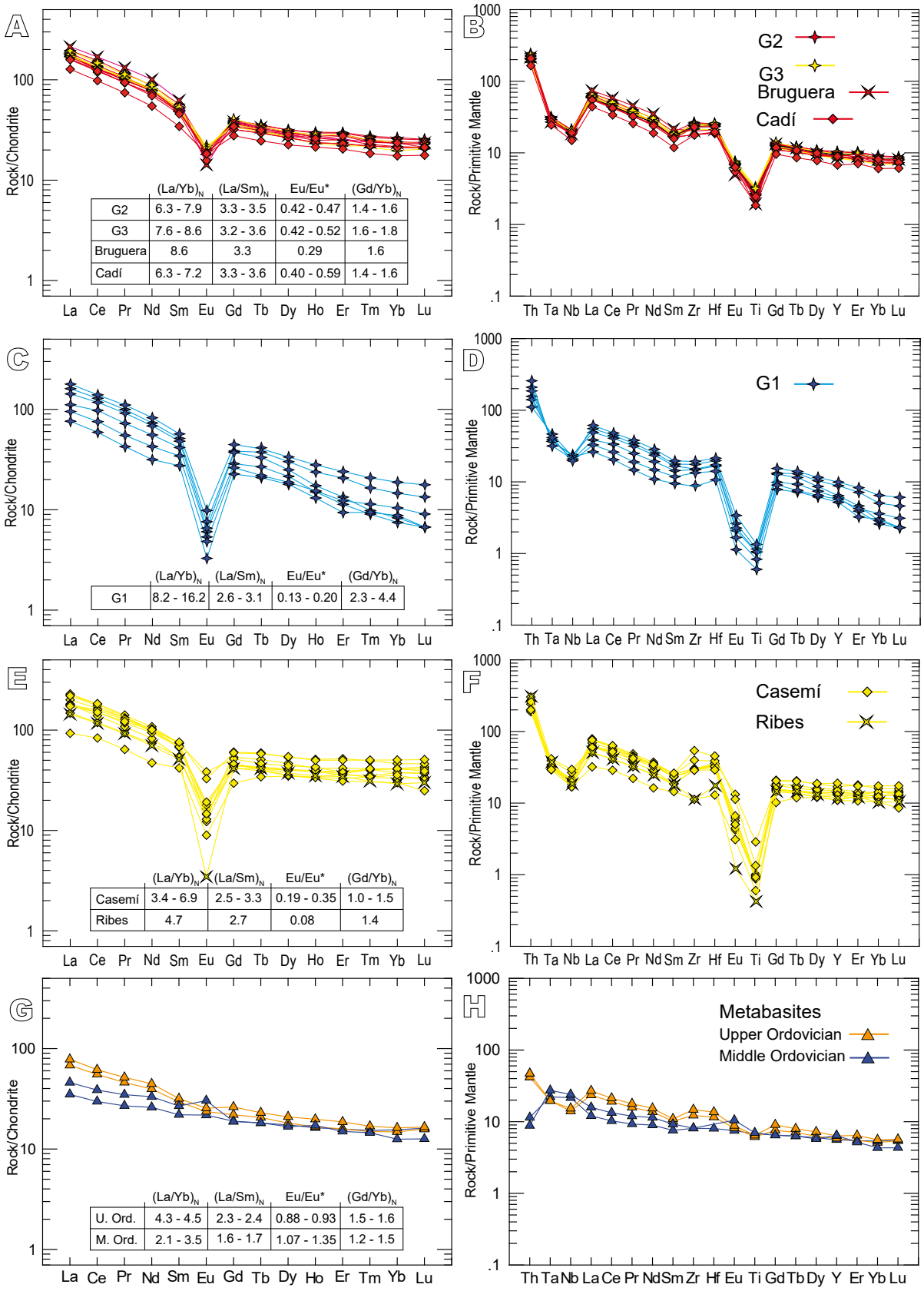

FIGURE 10. A, C, E, G) Chondrite-normalized (Sun and McDonough, 1989) REE diagrams; B, D, F, H) Primitive Mantle-normalized (Sun and McDonough, 1989) multi-element diagrams.

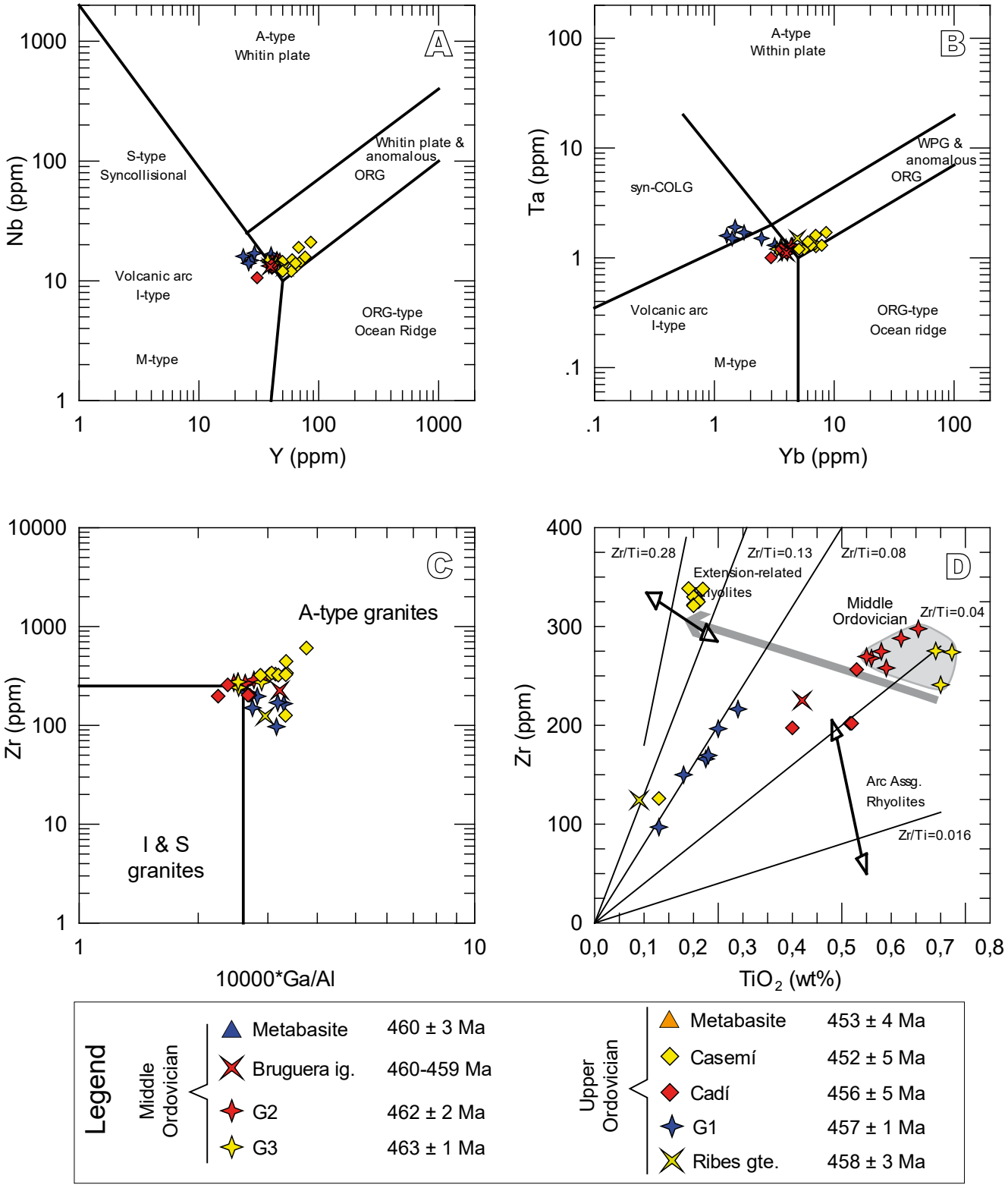

FIGURE 11. Tectonic discriminatory diagrams of the study samples. A) Nb vs.Y after Pearce *et al.* (1984); B) Yb vs.Ta after Pearce *et al.* (1984); C) Zr vs. 10^{4}*Ga/Al after Whalen *et al.* (1987); D) Zr vs. TiO_2 after Syme (1998).

(Casemí gneisses and Ribes granite) have a flat HREE pattern (Fig. 10F).

In the tectonic discriminatory diagrams of Pearce *et al.* (1984; Fig. 11), the G-1 orthogneisses plot either in the volcanic arc field (Fig. 11A) or in the syn-COLG (syn-collisional granites) field (Fig. 11B). The third group of rocks (Casemí gneisses and Ribes granite) plot in the within-plate granite field, because of their higher contents in Y and Yb (Fig. 11A-B). In the Zr-10000*Ga/Al diagram of Whalen *et al.* (1987), samples mainly plot in the A-type granites field (Fig. 11C). However, the gneisses of the first group (G-2, G-3 and Cadí), spread from S/I-type to A-type fields (Fig. 11C). In the Zr-TiO_2 binary diagram (Fig. 11D), the rocks of the Canigó massif show a temporal evolution from the Mid to the Late Ordovician. The Zr/Ti ratio increases from G-2 and G-3 gneisses, with a ratio of 0.04 typical of magmatic arcs, to the Casemí gneiss which has a ratio between 0.13 and 0.28, typical of extensional settings (Syme, 1998). The G-1 gneisses have a constant Zr/Ti ratio, close to 0.08.

The multi-element trace element patterns of the Ordovician magmatic rocks of the Canigó massif compared to the Upper Continental Crust (UCC) of Rudnick and Gao (2003) are shown in Figure 12. For the three groups of rocks, the most remarkable geochemical feature is the very strong negative Sr anomaly (Fig. 12). The first group of rocks (G-2, G-3 and Cadí gneisses and Bruguera ignimbrite) shows patterns very similar to those of the UCC (Fig. 12A). The main difference is the strong Sr negative anomaly, and slight enrichments in K, Rb, Ba, Th, Zr, Hf, Y and REE. In contrast, the G-1 gneiss samples show strong Sr, Ba and Ti negative anomalies and K and Th slight positive anomalies compared to the UCC (Fig. 12B). The rocks belonging to the third group (Casemí gneiss and Ribes granite) show strong negative anomalies in Sr, P and Ti, and positive anomalies in K, Rb, Th, Zr, Hf, Y and REE compared to the UCC (Fig. 12B). This silicic, peraluminous, potassic nature and its peraluminous mineralogy of the Canigó magmatism, together with the trace element pattern of the samples similar to the UUC, strongly suggest a predominantly crustal source for the magmatism. These geochemical features are common in S-type rocks (Chappell and White, 2001), an interpretation corroborated by the B-A diagram (Fig. 8C), where the general trend with increasing Fe+Mg+Ti content suggests they were derived from the melting of metaigneous and greywackes source rocks.

The Casemí gneiss have HREE flat pattern (Fig. 10E), which coupled with their high Y values, argues for partial melting with low amounts, or even complete absence, of garnet in the residuum.

Rodríguez *et al.* (2022) evaluated the ACF major element composition of the Ordovician felsic magmas (Ollo de Sapo Formation) of the Iberian Massif (Fig. 13A), to determine the possible protoliths. Most of the compositions fall within a triangle whose vertexes are the Kernel maximum of melts from fluid-absent and fluid-present experiments from biotite- and biotite+muscovite-bearing sources for P≤ 8kbar (García-Arias *et al.*, 2024). The arc-like signature is likely inherited from the general signature of the continental crust, as formerlyt suggested (Álvaro *et al.*, 2020; Casas *et al.*, 2024; Díez-Montes *et al.*, 2010; García-Arias *et al.*, 2018; Rodríguez *et al.*, 2022).

The studied rocks have low Sr/Y ratios (Fig. 13B). As the stability of garnet and plagioclase depends on pressure and temperature, this ratio is usually considered as a proxy to estimate melting pressure (Chiaradia, 2015; García-Arias *et al.*, 2018, 2024). The presence of plagioclase (Sr) and the absence of garnet (Y) in the source are indicators of low-pressure melting. This process fits the requirements of HT-LP melting conditions of the continental crust, as determined by Ti-in-zircon thermometry (Bea *et al.*, 2007) and is consistent with the flat HREE and very low Sr/Y signatures.

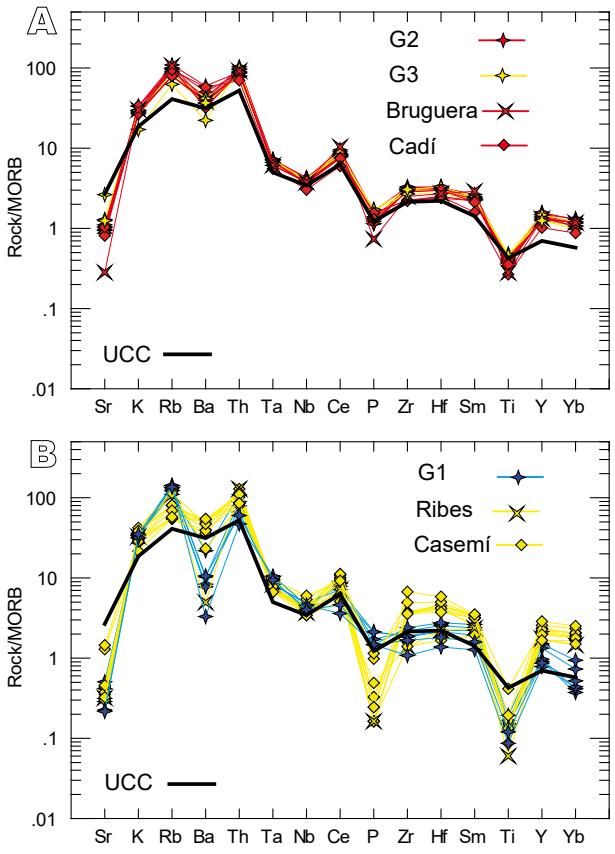

FIGURE 12. A, B) Multielemental diagram normalized to MORB after Pearce (1984). The Upper Continental Crust (UCC) of Rudnick and Gao (2003) is included for comparison.

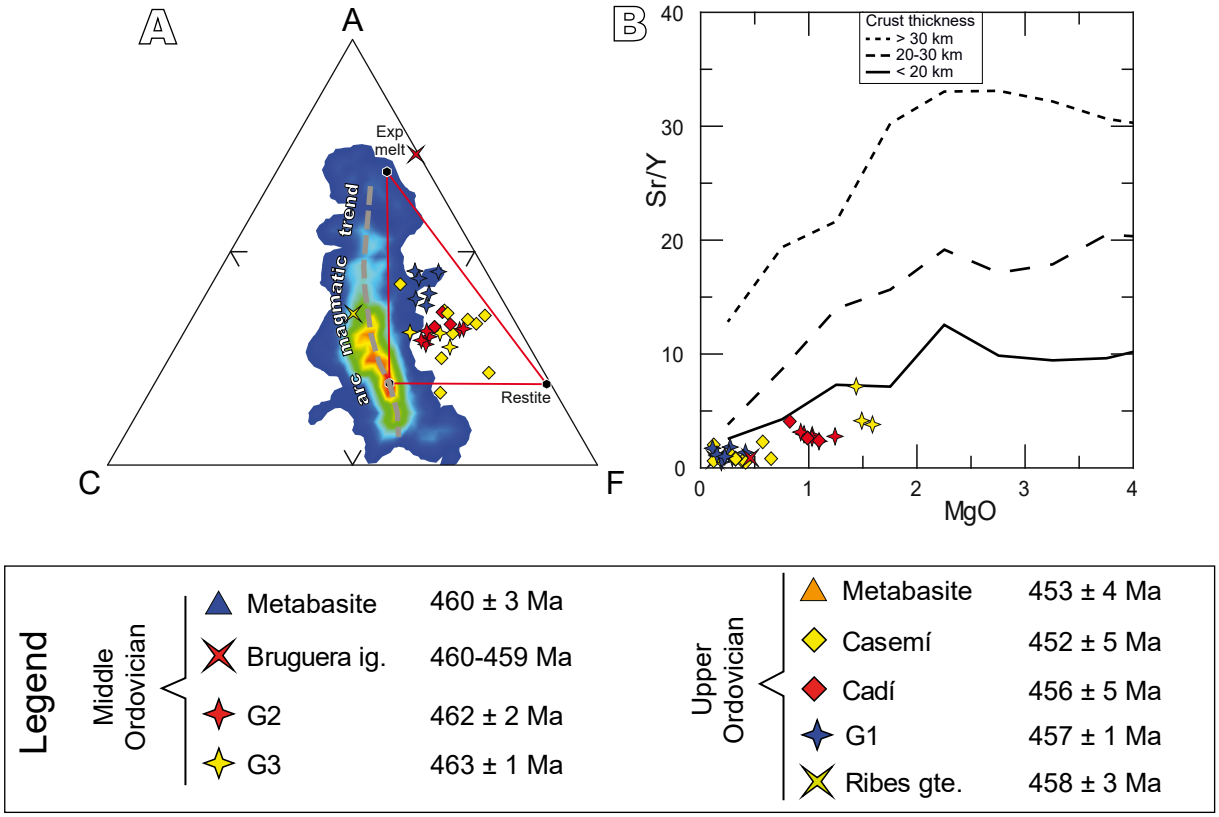

FIGURE 13. A) Eskola's ACF diagram showing compositional space relations of the Canigó felsic magmatic rocks. The experimental melt from the source of the Ollo de Sapo Formation at 800ºC and 6kbar (Castro *et al.*, 1999) is used instead of the kernel maximum of experimental melts. The kernel density distribution of Andean plutonic rocks from García-Arias *et al.* (2024). ACF plot according to the classical Eskola's diagram (A= molar Al_2O_3-Na_2O-K_2O; C= CaO; F= FeO^T+MgO+MnO). B) Sr/Y vs. MgO diagram after Chiaradia (2015).

Sm/Nd data from the Canigó samples (Table II of the Supplementary material) are shown in Figure 14, where the three groups of rocks can also be distiunguished. Groups 1 and 3 show more uniform $(^{143}Nd/^{144}Nd)_{455}$ ratios and εNd (455Ma) values than group 2. Group 1 samples, including those of the Cadi gneiss, have values between 0.511805 and 0.511849 with εNd between -3.6 to -4.43 (Fig. 14A-B; Table II of the Supplementary material). The single Bruguera ignimbrite sample is distinct from the rest of the group 1 samples and this may be due to chemical weathering, diagenesis and low-temperature alteration, which can result in significant changes of mineralogical and geochemical compositions compared to that of their source (*e.g.* McLennan *et al.*, 1993). The group formed by 3 samples, the Casemí gneiss and Ribes granite, have $^{143}Nd/^{144}Nd$ ratios ranging from 0.511940 to 0.511987, with εNd values between -1.3 and -2.2 for the Casemí gneiss and -2.5 for Ribes granite, according to Navidad *et al.* (2010). Group 2 samples, formed by the G-1 gneiss, have $^{143}Nd/^{144}Nd$ ratio between 0.511779 to 0.511876, with εNd ranging from -3.4 to -5.33 (Fig. 14A). All the samples of the Canigó massif display negative εNd values, ranging from -1.3 to -5.3 (Fig. 14A). These are higher than the $\varepsilon Nd_{(455)}$ values of the lower Paleozoic metasedimentary successions, whose εNd values vary from -5 to -10 (Martínez *et al.*, 2011), but are similar to the $\varepsilon Nd_{(580)}$ determined by Rojo-Pérez *et al.* (2023) for the Ediacaran metasedimentary rocks of the Cap de Creus massif (-3.8 to -5.4). Groups 1 and 3 felsic rocks and metabasites have Mesoproterozoic T_{DM} ages ranging from 1.10 to 1.56Ga, whereas T_{DM} ages of Group 2 gneiss vary from 1.54 to 2.75Ga (Fig. 14A, B). T_{DM} ages of ca. 1.5Ga are also predominant in the Ollo de Sapo magmatic rocks of the Central Iberian Zone (Bea *et al.*, 2010). According to Navidad *et al.* (2010), these T_{DM} ages are the result of the mixture of an old component (probably Palaeoproterozoic) with juvenile melts.

In the Pyrenean massifs, geochronological ages inherited from Pan-African (800Ma), Mesoproterozoic (1.0Ga), Orosirian (1.8 to 2.0Ga) and Archaean (2.5 to 3.1Ga) events have been reported in zircon crystals from Ordovician igneous rocks (Casas *et al.*, 2010; Castiñeiras *et al.*, 2008a; Cocherie *et al.*, 2005; Deloule *et al.*, 2002; Martí *et al.*, 2019; Martínez *et al.*, 2011; Navidad *et al.*, 2018; Table II of the Appendix). The inherited geochronological ages for the Canigó massif

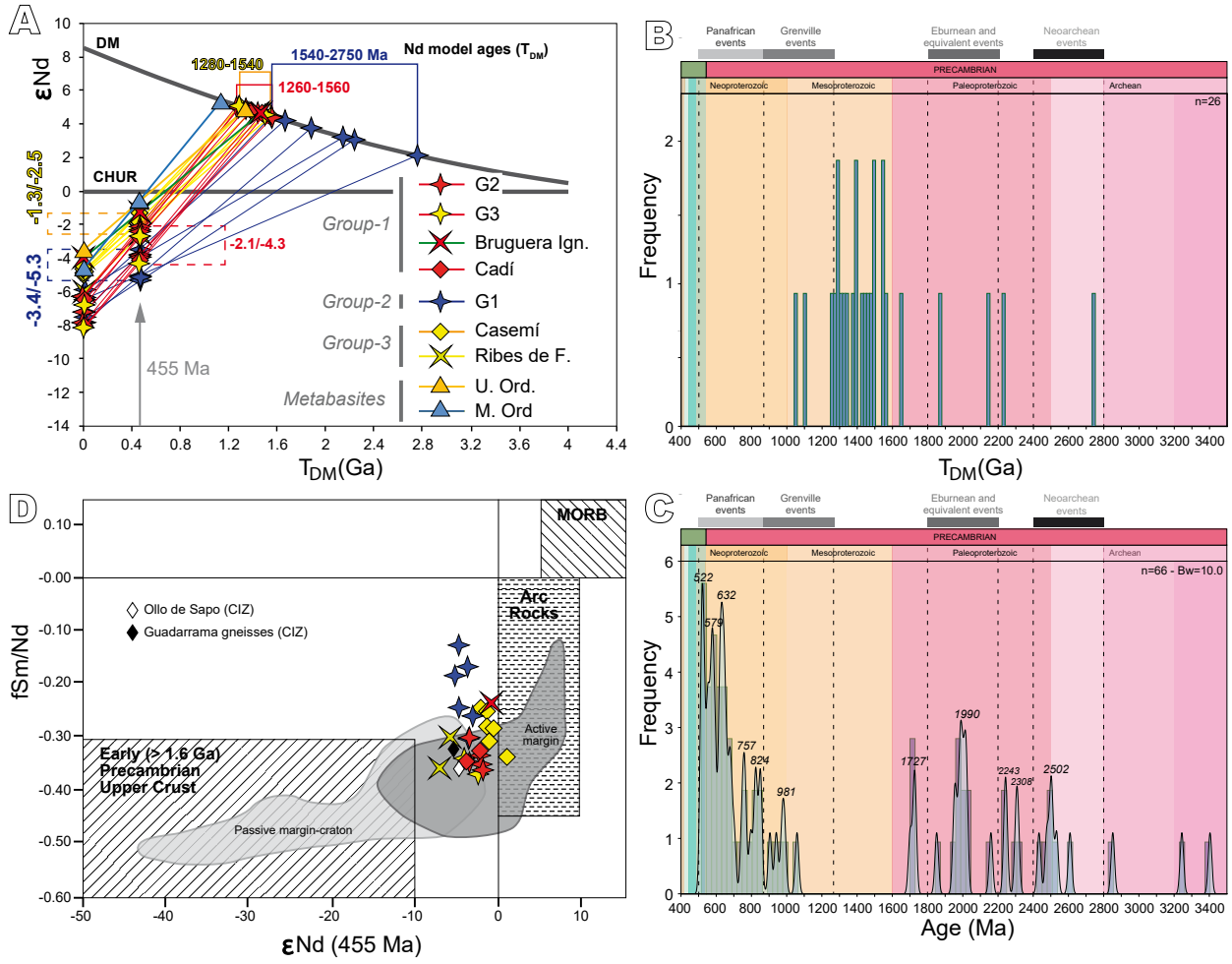

FIGURE 14. A) εNd(t) vs. age diagram (DePaolo, 1981; DePaolo and Wasserburg, 1976) for the Canigó gneiss. Data from Table I of the Supplementary material; B) Kernel density estimates diagram of T_{DM} ages of the Canigó plutonic felsic rocks and metabasites; C) Kernel density estimates diagram of all $^{206}Pb/^{238}U$ inherited zircon ages. Data from Table II of the Supplementary material; D) fSm/Nd vs. $\varepsilon Nd_{(455)}$ diagram for the analyzed samples showing fields used to discriminate tectonic setting (McLennan and Hemming, 1992). Data from the Ollo de Sapo and Guadarrama gneiss after Navidad and Castiñeiras (2011).

are represented in Figure 14C. Most samples host zircon populations with inherited ages ranging from Terreneuvian to Neoproterozoic, with maximum peaks of Terreneuvian to Cryogenian inherited ages (522 and 632Ma). This first group of inherited ages is considered to be the age of the source rock that generated the protoliths of the Ordovician Canigó gneisses. The second group of inherited ages are mainly Palaeoproterozoic, with subsidiary Archaean peaks. This second group is considered to reflect recycling of continental crust. A characteristic of these inherited zircon ages in the Ordovician magmatic rocks is the absence of Mesoproterozoic ages, as already noticed by Navidad *et al.* (2010). Therefore, the ages obtained from the zircon inheritance are different from the Nd model ages (T_{DM}) obtained for the Canigó rocks (Fig. 14B-C).

Groups 1 and 3 have homogeneous values of fSm/Nd and εNd (Fig. 14D), which suggest a common or similar crustal source for these groups. Samples from both groups tend to plot within the active margin field and the Casemí gneiss samples approach the arc field (McLennan and Hemming, 1992). The gneisses of group 1, including the Cadí gneisses, have a very narrow range of fSm/Nd values, and are very similar to the gneisses in the Central Iberian Zone of the Iberian Massif (Navidad and Castiñeiras, 2011), which suggests strong isotopic homogenization during the partial melting process. On the other hand, groups 2 and 3 show a wider range of fSm/Nd values, which suggests less homogenization of partial melting processes in the recycling of the continental crust.

In the Iberian Massif, Neoproterozoic metasedimentary rocks are characterized by εNd values ranging between -3 and -4, compatible with an active margin-continental arc setting or derivation from Pan African arc crust (Beetsma, 1995; Ugidos *et al.*, 2010). This interpretation is consistent

with the relatively high εNd and low T_{DM} (1.3-1.6Ga) values at the time of their deposition, which indicates a significant contribution of juvenile crust in the Neoproterozoic sedimentary rocks. These characteristics are shown by groups 1 and 3 of the Canigó massif, whereas group 2 (G-1 gneisses) are characterized by older T_{DM} values. In summary, this crustal component could reflect recycling of arc magmatism thereby yielding an arc-signature of metaigneous and greywacke rocks, as is evident in Figure 8C, where data project towards the field of greywacke and metaigneous rocks. As with whole-rock geochemical data, this signature was probably inherited by the melting of pre-existing Neoproterozoic-lower Palaeozoic calc-alkaline crust.

Metabasites

Middle Ordovician (Navidad *et al.*, 2018) and Upper Ordovician (Casas *et al.*, 2010; Navidad *et al.*, 2010) metabasites have been recognized in the Canigó massif and are. tholeiitic and calc-alkaline respectively (Fig. 8A-B, D): The older metabasite has 43wt.% SiO_2 and 9wt.% MgO, whereas the younger one has 50wt.% SiO_2 and 7.3wt.% MgO (Table I of the Supplementary material). Both bodies are partly altered, with Lost of Ignition (LOI) between 1.4 and 2.4wt.%.

The total REE concentrations are between 62 and 108ppm (Table I of the Supplementary material), values of $(La/Sm)_n/(Gd/Lu)_n$ are between 1.1 and 1.6, and Eu-anomalies are negligible. The chondrite-normalized REE patterns show a negative slope from La to Lu (Fig. 10G), indicating a moderate enrichment in LREE compared to HREE, with $(La/Lu)_n$ between 2.1 and 4.7. These patterns are similar to those of the felsic rocks (Fig. 10A, C, E) but with lower REE content and without an Eu anomaly. These values are also similar to typical Oceanic Island Basalts (OIB; see Humphreys and Niu, 2009; Shervais, 2022 and references therein).

In the Primitive Mantle-normalized multi-element diagram (Fig. 10H) the Middle Ordovician metabasite displays positive Nb and Ta anomaly and negative Th anomaly, whereas the Upper Ordovician metabasite displays a negative Nb and Ta anomaly, Th positive anomaly and slight enrichment in High Field Strength Elements (HFSE) such as Zr and Hf. The positive Nb anomaly is a clear indicator of an E-MORB source for the metabasite (Pearce, 2014). Again, these patterns are similar to typical OIB (Humphreys and Niu, 2009; Shervais, 2022 and references therein).

The Middle Ordovician metabasite has a Th/Yb ratio of 0.35, which indicates an enriched mantle (E-MORB)

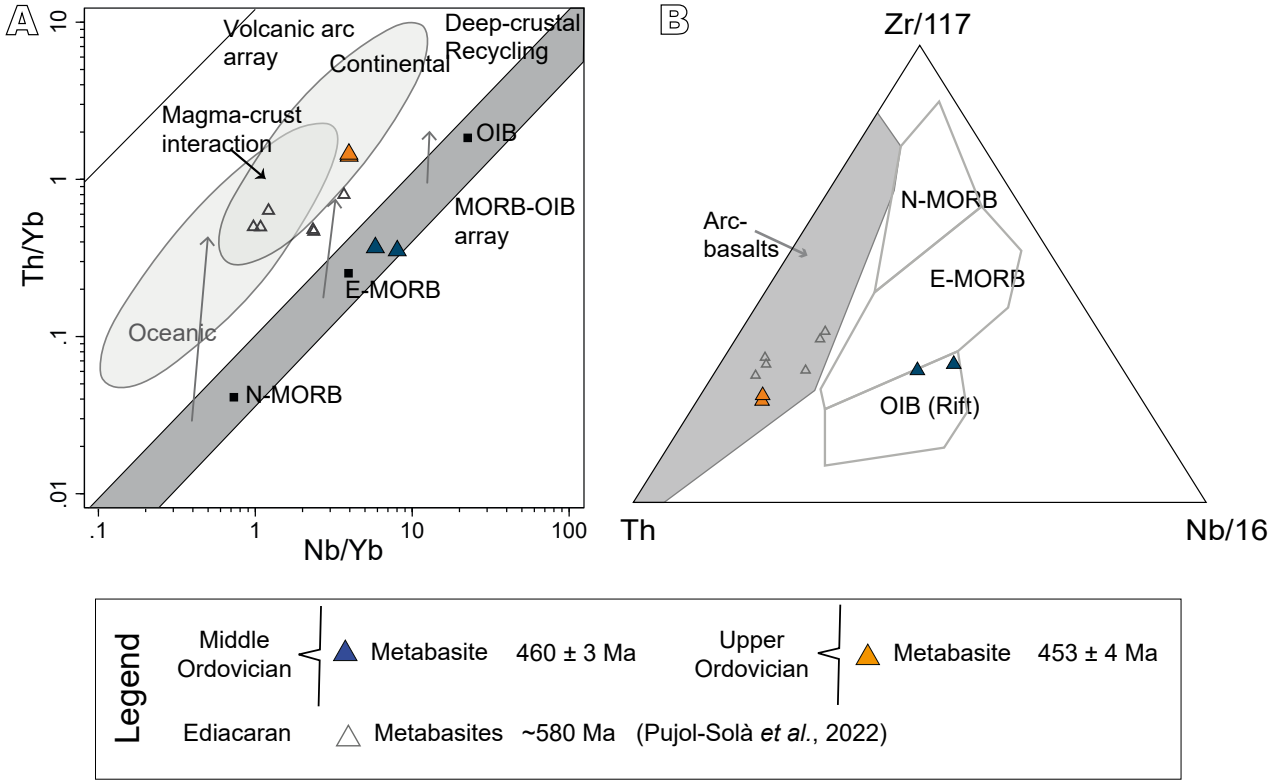

FIGURE 15. Tectonic setting of the Ordovician metabasites. A) Nb/Yb vs. Th/Yb (Pearce, 2014) including the MORB-IOB array and N-MORB and E-MORB of Sun and McDonough (1989); B) Th-Zr/117-Nb/16 ternary diagram from Wood (1980). Ediacaran metabasites (Pujol-Solà *et al.*, 2022) are included for comparison.

affinity (Fig. 15A), whereas the Th/Yb ratio is significantly higher for the Upper Ordovician metabasite (1.45), indicating that the samples are influenced by either contamination or assimilation of continental crust (Fig. 15A) (Pearce, 2014; Shervais, 2022 and references therein). The OIB signature for the Middle Ordovician metabasite is observed in the ternary diagram of Figure 15B, whereas the Upper Ordovician metabasite shows a more arc-like signature. Although these compositions are broadly similar to the Cadomian metabasites in the Pyrenees (Fig. 15; see Pujol-Solà *et al.*, 2022), the Ordovician samples have a more contaminated E-MORB source.

Sm-Nd isotopic data for these rocks were published by Navidad *et al.* (2018). The two samples display $^{143}Nd/^{144}Nd$ ratios ranging from 0.512011 to 0.512022, slightly negative εNd values (-0.41 and -0.58; Fig. 14A) and the calculated T_{DM} model ages are from 1147 to 1332 Ma, which is similar to the group 3 of felsic rocks (Fig. 14A-B) and slightly younger than the other groups. Navidad *et al.* (2018) interpreted the protolith of the Middle Ordovician metabasite to have been derived from either an enriched mantle or from a juvenile (mafic) crust enriched by assimilation of crustal elements. Based on the absence of genetic relationships, these authors interpreted the metabasite to have formed from a different mantle source than the felsic rocks. On the other hand, the Upper Ordovician metabasite was interpreted by Navidad *et al.* (2010, 2018) as a product of crustal contamination of mantle melts.

Thickness and geometry of the Canigó gneiss

The thickness and geometry of the several Canigó gneiss bodies can be deduced from geological maps and cross-sections through the massif. Guitard (1970) described a stratiform geometry for the whole gneiss body and documented an eastward decrease in its thickness in which maximum gneiss thickness (2,500-3,000m) occurs in the southwestern slope of the massif in comparison with 2,000m thickness in the northeastern slope and 1,200m on the eastern side.

Using detailed cross-sections throughout the massif (Casas, 1984), of the Núria-Queralbs area (Santanach, 1972b) and logs of the central part of the massif (Fig. 16), we can briefly discuss the thickness and geometry of the several gneiss type bodies.

G-2 gneiss is the main type of gneiss in the Canigó massif. Its thickness varies between 2000m in the southern slope to 1500m in the northern area, the base of the gneiss is not exposed in the southern area, and thus is considered as the minimum thickness. Its thickness clearly decreases toward the East, where its minimum estimated thickness inferred from geological maps is ca. 500m (Guitard, 1970).

The thickness of G-1 gneiss located on top of the G-2 gneiss ranges between 1000m, in the southern slope, to ca. 100m in the northern slope. In the Queralbs-Núria area, G-1 gneiss is 200m thick and is interlayered with Canaveilles Group metasedimentary successions (Santanach, 1972b). The top of the gneiss was emplaced along the base of the Canaveilles Group metasedimentary rocks, subparallel to the several marble layers of the Nyer Formation. Locally, the gneiss-metasediment contact cross-cuts some marble layers and the gneiss, several meters thick, is interlayered with the metasedimentary rocks (Fig. 7A-B).

In contrast, the bottom of the gneiss is more irregular and is typically interlayered with the Balaig Series mica-schists (Fig. 7C). G-1 and G-3 gneisses form isolated laccolithic bodies at the bottom of the main G-2 gneiss body, ranging in thickness from a few meters to 200m (Fig. 16). The Casemí gneiss tapers to the West and the East, forming a laccolithic-shaped body with a maximum thickness of ca. 500m, intercalated with the Balaig mica-schists (Fig. 16). The Cadí gneiss crops out below the Balaig mica-schists, in a small area near the centre of the massif, and thus, its thickness cannot be estimated.

According to the above descriptions and geochronological data, it appears that the main magmatic activity occurred in Mid Ordovician (Darriwilian) times, giving rise to the porphyritic granite protoliths of G-2 and G-3 gneiss, whereas Late Ordovician (Sandbian-Katian) magmatism gave rise to smaller and petrologically more varied magmatic bodies (G-1 and Casemi protoliths), emplaced at the bottom or at the top of the main G-2/G-3 gneissic body (Fig. 17). In this framework, the Cadí gneiss protolith can be interpreted as a late intrusion derived from the same magma chamber that yielded the main G-2 gneiss body (Fig. 17).

THE UPPER ORDOVICIAN UNCONFORMITY

Structural and cartographic evidence

After Llopis Lladó (1965) invoked "Caledonian movements", the first convincing description of the Upper Ordovician unconformity in the Pyrenees was made by Santanach (1972a) on the basis of geological mapping and structural data in the La Molina area, in the southern slope of the Canigó massif. Santanach (1972a) reported bedding orientations in the Upper Ordovician that were different from the underlying Cambrian-Ordovician series, and attributed this difference to a pre–Upper Ordovician tilting affecting only the Cambrian-Lower Ordovician series. This difference gave rise to a different geometry of the Variscan minor structures (main cleavage/bedding intersection lineation and fold axes) in

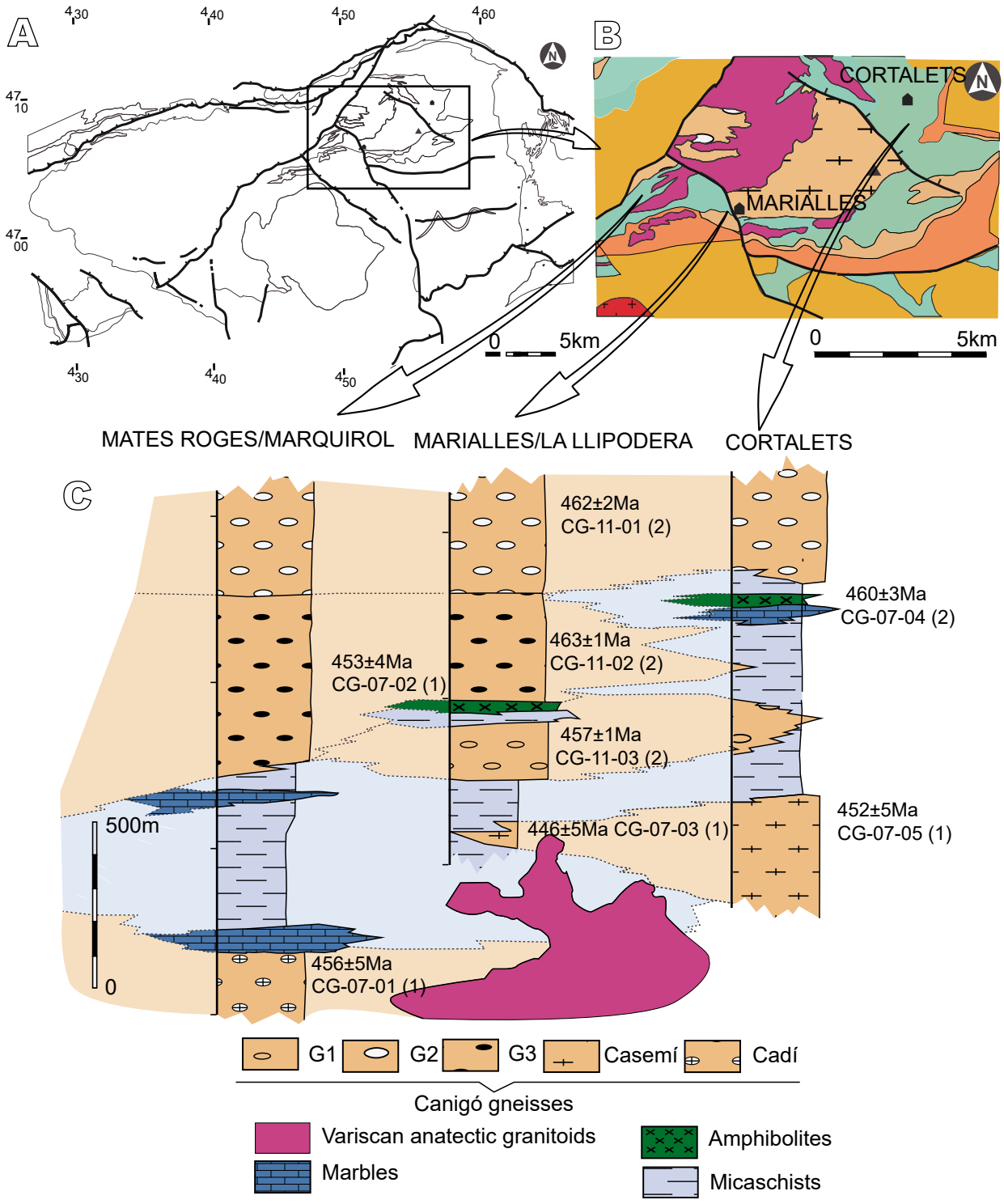

FIGURE 16. A) Sketch of the Canigó massif with the location of B; B) Geological map of the central part of the massif showing the location of the stratigraphic logs. Legend as in Figure 2; C) Synthetic stratigraphic logs of the central part of the Canigó massif. Geological data after Guitard (1970) and Casas (1984). Geochronological data of the protoliths of the gneiss after (1) Casas *et al.* (2010) and (2) Navidad *et al.* (2018).

both successions (Fig. 18). Moreover, geological mapping (Santanach, 1972a) showed that Upper Ordovician rocks unconformably overlie different formations of the pre-Upper succession.

It is now widely accepted that the Upper Ordovician succession unconformably overlies either the Ediacaran-Lower Ordovician Jujols or Canaveilles groups' in several areas of the Pyrenees (Den Brok, 1989; Casas and

Fernández, 2007; García-Sansegundo and Alonso, 1989; García-Sansegundo *et al.*, 2004; Kriegsman *et al.*, 1989; Puddu *et al.*, 2019). This unconformity is especially well exposed in the southern slope of the Canigó massif, in the La Molina and La Cerdanya areas where Cambrian-Ordovician rocks (Serdinya Formation) are onlapped by both the Sandbian Rabassa conglomerate and the Cava formations rocks, at angles ranging from a few degrees to 90°. This contact is planar to weakly undulated, and a locally irregular surface, and is considered to be a regional unconformity, ranging laterally from a paraconformity to an angular discordance. The current strike of the unconformity ranges from E-W to WNW-ESE (Casas and Fernández, 2007; González-Esvertit *et al.*, 2023; Puddu *et al.*, 2019).

Stratigraphic and geochronological constraints

As stated above, acritarchs recovered from the uppermost part of the Jujols Group (top of the Serdinya Formation) in the La Molina area yield a broad Furongian-Early Ordovician (ca. 475Ma) microphytoplancton assemblage (Casas and Palacios, 2012). Considering this age for the deposition of the uppermost part of the Jujols Group, and a Sandbian age (ca. 455Ma) for the base of the Upper Ordovician rocks (Hartevelt, 1970; Gil-Peña *et al.*, 2004), a minimum time gap of about 20m.y. is estimated for the Upper Ordovician unconformity in the Pyrenees. This time gap is supported by geochronological data, as a maximum depositional age of ca. 475Ma (Floian) for the uppermost part of the Jujols Group in the La Rabassa dome is implied by the U-Pb age for the youngest detrital zircon population (Margalef *et al.*, 2016). To the East, in the Albera massif, the uppermost part of a metasedimentary succession that can be correlated with the Jujols Group is

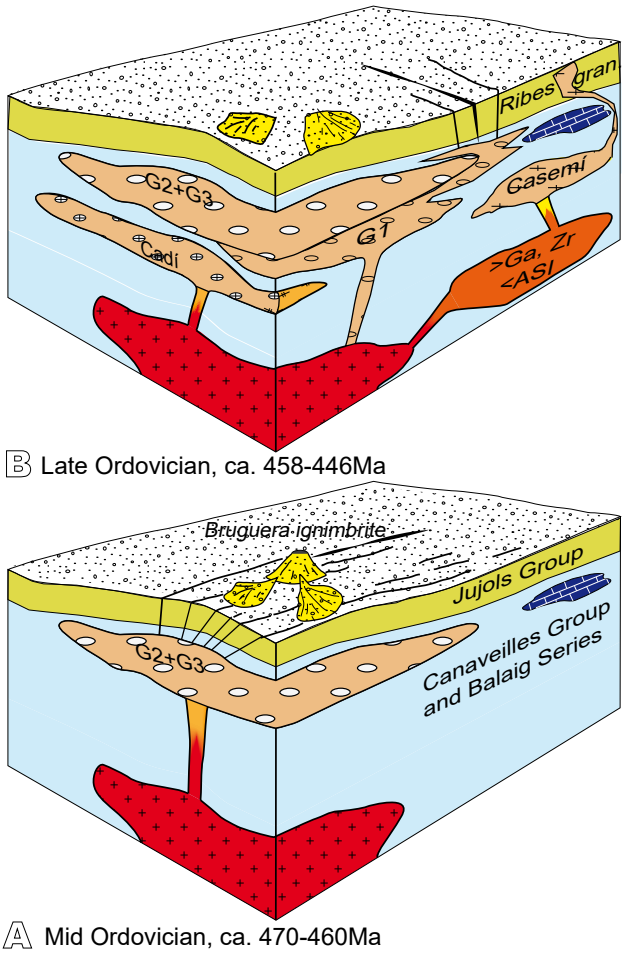

FIGURE 17. Sketch of two-phase emplacement of the Canigó magmatic rocks. Not to scale.

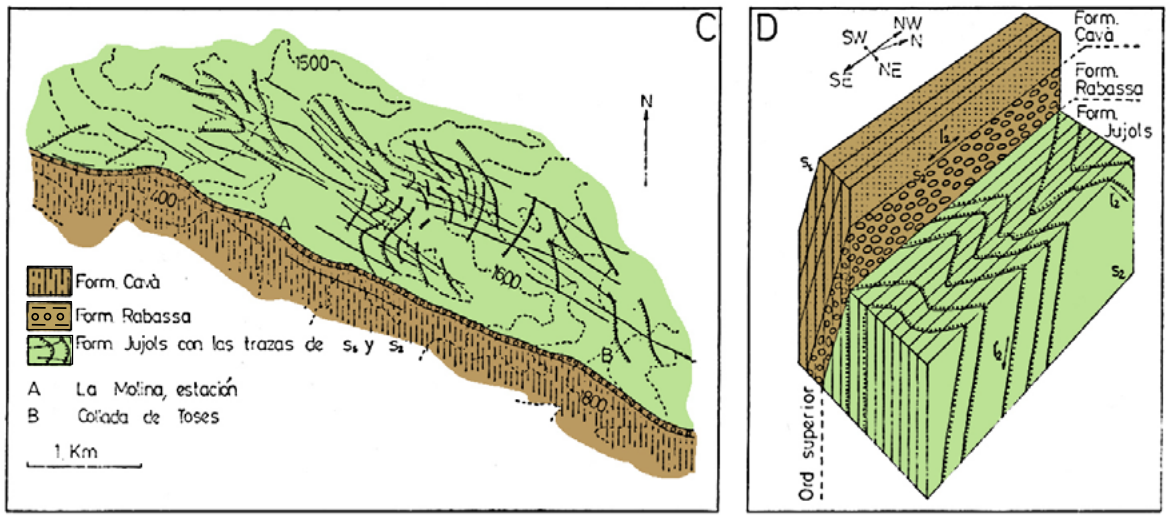

FIGURE 18. Sketch of the Upper Ordovician unconformity at the la Molina area after Santanach (1972a). C) Cartographic pattern of the Upper Ordovician unconformity in la Molina area and D) 3D block model showing the folds developed in Cambrian-Ordovician rocks that are not affecting the Upper Ordovician succession. Location in Figure 1.

crosscut by felsic 465-472Ma subvolcanic dykes, which constrain its minimum depositional age (Liesa *et al.*, 2011). In the La Rabassa dome, based on the U-Pb age of the detrital zircon population, Casas *et al.* (2024) proposed a maximum depositional age for the basal part of the Cava Formation of ca. 452Ma (Katian), suggesting a maximum time gap represented by the Upper Ordovician unconformity in this area of ca. 23m.y. This time gap increases from the La Rabassa dome, in the West, to the Ribes de Freser area, 50km to the East, where Upper Ordovician rocks crop out close to the top of the limestones of the Cambrian Series 2 Valcebollère Formation (Muñoz *et al.*, 1994; Vergés *et al.*, 1994), implying that a thickness of ca. 1500m of Cambrian-Ordovician rocks was eroded prior to the deposition of Upper Ordovician rocks (Fig. 19). In turn, 10km East of Ribes de Freser, near the town of Pardines, Upper Ordovician rocks overlie the Jujols Group rocks, whereas 15km further East, in the Molló area, Upper Ordovician rocks rest on top of limestones equivalent in age to the Cambrian Series 2 Valcebollère Formation (Fig. 19). In the northern slope of the massif, in the Conflent valley, Guitard *et al.* (1998) placed the Upper Ordovician rocks on top of the uppermost part of the Jujols Group succession. In contrast, in the eastern slope of the massif, in the Els Aspres region, Laumonier *et al.* (2015) placed the basal Upper Ordovician conglomerates on top of sandstones and shales that correlate with those of the Terreneuvian Err Formation, which is below the Vallcebollère limestones. If this proposed correlation is correct, the Upper Ordovician unconformity would attain its deepest erosional level in the Els Aspres area (Fig. 19).

This stratigraphic gap indicates a phase of uplift between the depoisition of Lower Ordovician and Upper Ordovician strata. This Early Ordovician to Sandbian-Katian time gap was maximum, reaching some 60-70m.y. in the Ribes de Freser, Molló and Els Aspres areas, compared to the West (Rabassa dome) and central part where the gap is about 20-23m.y. (Fig. 19). The regional variations in age of the Cambrian and Ordovician strata below the unconformity may result from the displacement along Mid(?)-Ordovician extensional faults affecting only the pre-Upper Ordovician strata (see below).

Detrital zircon data

Published detrital zircon age data are available from five samples of the La Rabasssa dome, from both sides of the Upper Ordovician unconformity, three samples in the uppermost part of the Jujols Group (RB-10-01, RB-10-02 and RB-10-03; Margalef *et al.*, 2016), one from the Bar Quartzite Formation (RB-10-04; Margalef *et al.*, 2016) and another from the basal levels of the Cava Formation, close to the unconformity (MOI-01; Casas *et al.*, 2024). Based on these data, two aspects can be highlighted: i) the detrital zircon populations below and above the Upper Ordovician unconformity in the Rabassa Dome are indistinguishable and ii) there is a general scarcity of Cambrian-Ordovician detrital zircon (Fig. 20). These five samples show similar age distributions dominated by a Neoproterozoic population (52-66%), followed in abundance by Mesoproterozoic zircon (12-16%), a variable representation of Palaeoproterozoic (4-15%) and Archaean zircon (4-7%), and with a minor percentage of Cambrian-Ordovician zircon (1-10%). The most prominent age cluster is at ca. 600–700Ma (Ediacaran-Cryogenian) with relatively minor clusters at 900Ma (Tonian), 1000–1050Ma (Stenian), 1800–2000Ma (Orosirian) and 2600Ma (Neoarchean) (Fig. 20).

The Neoproterozoic zircon population in the Ordovician Pyrenean samples is the most prominent one, although less abundant than in the Ediacaran samples of the Pyrenees and neighbouring areas, as Montagne Noire, where it is about 80% (Padel *et al.*, 2017). Most authors consider a long transport for these Neoproterozoic zircon grains, originating probably in the Pan African magmatic events fom the Trans-Saharan Belt, the Saharan Metacraton and/or the Arabian Nubian Shield (Casas and Murphy, 2018; Casas *et al.*, 2024; Chichorro *et al.*, 2022; Hart *et al.*, 2016; Margalef *et al.*, 2016; Padel *et al.*, 2017, 2022, among others). The subrounded to rounded morphology of these zircon grains (Casas *et al.*, 2024) and the age interval for the Cadomian magmatic activity recognized in the Pyrenees (ca. 570-530Ma; Álvaro *et al.*, in press), are compatible with this craton-related origin for the Ediacaran-Cryogenian zircon population hosted in the marine Lower Ordovician Jujols Group rocks. However, a long-distance origin is unrealistic for the alluvial and fluvial Upper Ordovician strata, that exhibit a similar detrital zircon population. As suggested by Casas *et al.* (2024) this similarity can reflect the denudation of the directly underlying Jujols Group rocks, and deposition in the accommodation space provided by the hangingwall blocks of the extensional faults, implying a local origin of the Upper Ordovician siliciclastic rocks. The euhedral morphology of the youngest zircon grains (Casas *et al.*, 2024) is also consistent with a local origin for the Upper Ordovician sedimentary rocks.

On the other hand, the scarcity of Palaeozoic detrital zircon (Fig. 20) reflects a minor contribution from Cambrian and Ordovician magmatic events. This could be due to the scarcity or absence of Lower and Middle Ordovician volcanic rocks and/or the localized extent of the Upper Ordovician volcanic ones in neighbouring areas. In addition, the Ordovician plutonic rocks (protoliths of the different types of Canigó gneiss, for instance), were emplaced at depths not reached by Ordovician erosion. In the Canigó massif, Middle to Upper Ordovician plutonic rocks were emplaced beneath the uppermost part of the

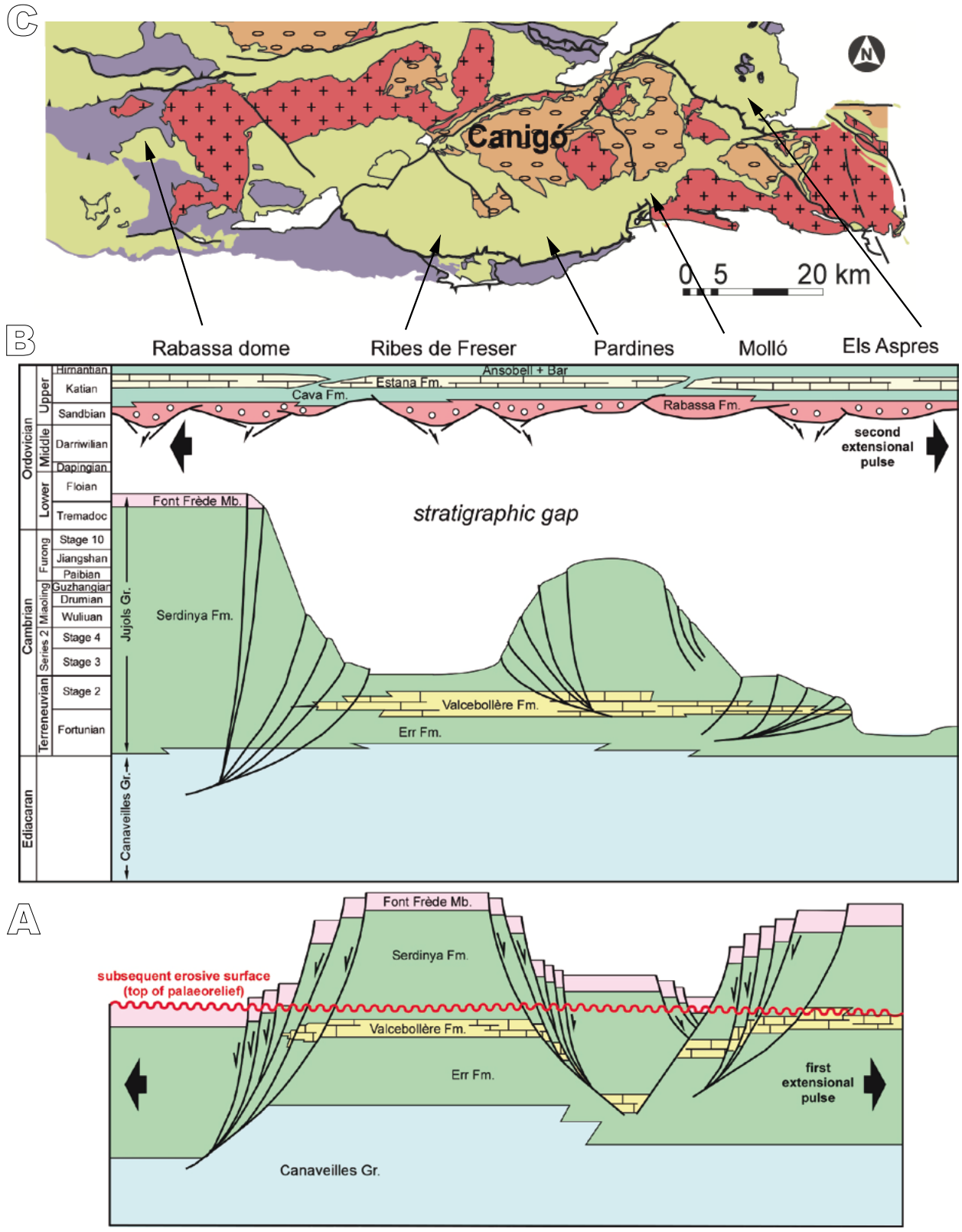

FIGURE 19. A) Tentative palaeogeographic W-E transect of the southern and eastern slope of the Canigó massif illustrating a first extensional pulse that post-date the Sardic generalized uplift event and develop a horst-and-graben geometry. B) Upper Ediacaran-Ordovician stratigraphic chart of the Canigó massif showing the geometrical relationships between pre- and post-Sardic sedimentary rocks, illustrating the second extensional pulse responsible for the channel-shaped geometries of the Rabassa Conglomerate formation, and the ranges of the diachronous stratigraphic gaps throughout the whole basin. C) Geological map of the eastern Pyrenees with setting of the selected logs. Legend as in Figure 1.

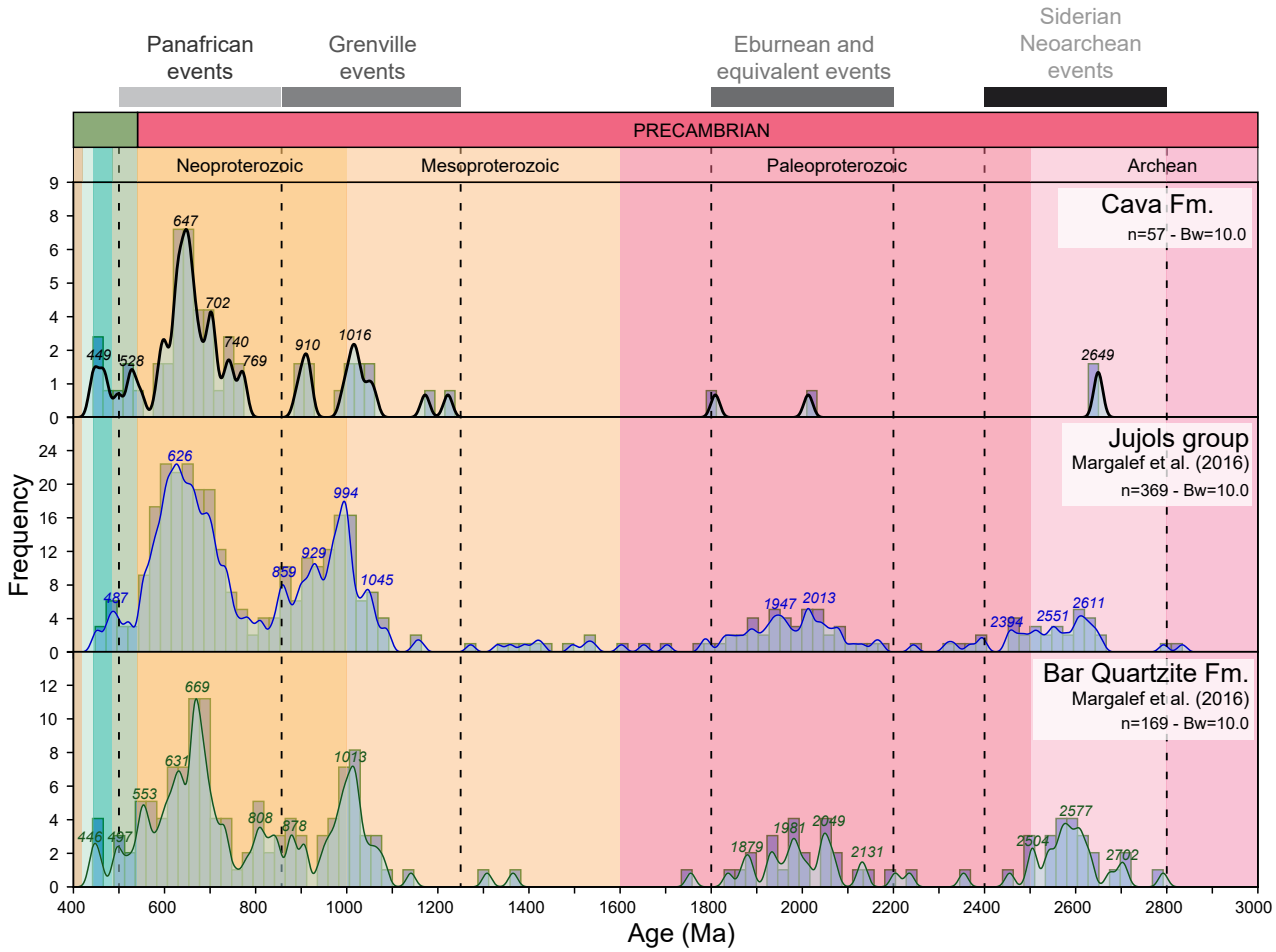

FIGURE 20. Kernel density estimates plots showing the peak ages for the samples located below (Jujols Group, RB-10-01, RB-10-02 and RB-10-03 samples) and above (Cava Fm., MOI-01 sample, and Bar Quartzite Fm., RB-10-04 sample) the Upper Ordovician unconformity. Abbreviations: Bw= band width; n= number of samples. Figure constructed using the HistogramsApp (Rodriguez-Corcho and actions-user, 2021; Rodriguez-Corcho *et al.*, 2020). After Casas *et al.* (2024) modified.

Canaveilles Group succession (Fig. 3), which is roughly 1500m below the maximum level reached by the Ordovician erosion in most areas (Fig. 19).

ORDOVICIAN TECTONICS

The Early-Mid Ordovician folding episode

Santanach (1972a) documented the different bedding orientations for the Upper Ordovician and underlying Cambrian-Ordovician series. Similarly, Casas (2010), Casas *et al.* (2012) and Puddu *et al.* (2019) showed that the orientations of bedding of the Cambrian–Lower Ordovician succession are more variable, and range from subvertical to subhorizontal, whereas the Upper Ordovician strata exhibit a more regular W-E to NW-SE strike and dip mostly towards the South. Casas (2010), Casas *et al.* (2012) and Puddu *et al.* (2019) proposed that the wider dispersion of the bedding in Cambrian–Ordovician strata is due to the superposition of several fold systems, one of them Early–Mid? Ordovician in age, affecting only the Cambrian-Lower Ordovician succession with later folding related to Variscan tectonics.

In the La Cerdanya area, Puddu *et al.* (2019) estimated a wavelength of 10 to 100m-scale for the Ordovician folds, with initially subhorizontal NE-SW oriented fold axes, a short limb oriented NE-SW that was steeply dipping to subvertical, and a long limb that was subhorizontal or gently dipping towards either the SE or NW. However, the effect of superposed Variscan folds and the lack of exposure of key horizons precludes assessing whether Ordovician folds had a NW or SE vergence. Casas *et al.* (2012) documenred Ordovician folds with a NW-SE orientation in the La Molina area. These different attitudes suggest that two distinct Ordovician fold systems may co-exist, although further work is necessary to evaluate this possibility. In the Els

Aspres massif, Laumonier *et al.* (2015) described WNW-ESE oriented South-verging pre-Variscan folds of ca. 2km wavelength, that could correlate with those observed in the La Molina area.

However, the interpretation of the origin of this folding event is not straightforward, as neither deformational mesostructures nor metamorphism accompanied these folds in the Pyrenees. Casas (2010) and Casas *et al.* (2012) proposed that these structures formed in a transient Mid Ordovician orogenic pulse. However, Puddu *et al.* (2019) argued against a contractional origin for the Ordovician folds in the Pyrenees and proposed that they are related to upward-propagation extensional faults. According to these authors, the folds formed in the hangingwall blocks of subvertical or steeply dipping extensional faults that may have not reached the topographic surface and so are blind faults within the pre–Upper Ordovician succession. In this scenario, the Upper Ordovician unconformity ranges from a paraconformity in the gently dipping long limb of the Ordovician folds or in the footwall of the faults, to an angular unconformity in the hinge zone or in the vertical limbs of the Ordovician folds close to the hangingwall faults (Fig. 21). Erosion of a palaeorelief defined by the hangingwall blocks of these extensional faults may explain the different level attained by the pre-Upper Ordovician erosion, which can achieve ca. 1500m, providing a maximum vertical throw for these faults (Fig. 19).

The Late Ordovician fracture episode

In the Canigó massif, extensional tectonics developed synchronously with the deposition of the lower part of the Upper Ordovician succession, as attested by extensional faults cutting the pre–Upper Ordovician succession, the Upper Ordovician unconformity and the lower part of the Upper Ordovician succession (Rabassa Conglomerate and Cava formations) in the Cerdanya area (Casas, 2010; Puddu *et al.*, 2019). These Late Ordovician synsedimentary extensional faults are subvertical, NNE–SSW-trending and led to the contemporaneous opening of grabens and half-grabens infilled with the alluvial, fluvial and volcano-sedimentary deposits of the Upper Ordovician Rabassa Conglomerate and Cava formations (Fig. 22). According to Puddu *et al.* (2019), maximum throws of the faults vary between 200 and 750m and the displacement of some of these faults diminishes progressively up-section and vanishes in the Upper Ordovician rocks, especially in the lower part of the Cava Formation. These relationships indicate a Sandbian-Katian age for the fault movement, as the faults became inactive before the deposition of the overlying Estana strata. Faults are planar, either non-rotational or with a dominant value of 18º of rotation affecting the beds in the hangingwall and ca. 20° fault rotation, indicating a minor amount of E-W extension (Puddu *et al.*, 2019).

In the El Conflent area, in the Evol valley and near Újols town, a set of hectometre-kilometre-sized steep faults cuts the Upper Ordovician succession, the Upper Ordovician unconformity and the Cambro-Ordovician metasedimentary successions (Guitard *et al.*, 1992). Faults gave rise to hectometre-kilometre displacements, are oriented mainly N-S and, as in the La Cerdanya area, and their hangingwall block is the eastern block in most cases. The faults separate regions with marked thickness variations in the Upper Ordovician rocks and peter out in the upper part of the succession below the Silurian rocks (Casas, 2010: fig. 6).

However, these N-S to NW-SE oriented extensional faults cannot explain the marked stratigraphic differences between the Ribes de Freser, Bruguera and El Baell units (Figs. 3; 4). A set of roughly E-W oriented normal faults can limit these units and have controlled the active volcanism (Casas, 2010), as well as the sedimentation of up 500m of limestones and marly limestones of the El Baell Formation (Puddu *et al.*, 2018). Based on the correlation of the El Baell and Estana formations proposed by Puddu *et al.* (2018), a Katian age can be proposed for the time of displacement along these E-W faults. These E-W-oriented faults could have coexisted with the aforementioned N-S normal faults. The former faults were probably inverted

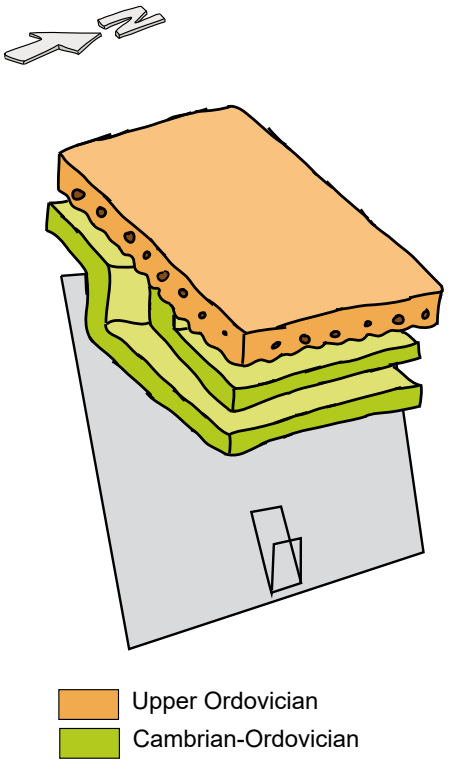

FIGURE 21. Sketch of the Upper Ordovician unconformity overlying Cambrian–Ordovician subvertical or subhorizontal beds close to upward propagating extensional faults.

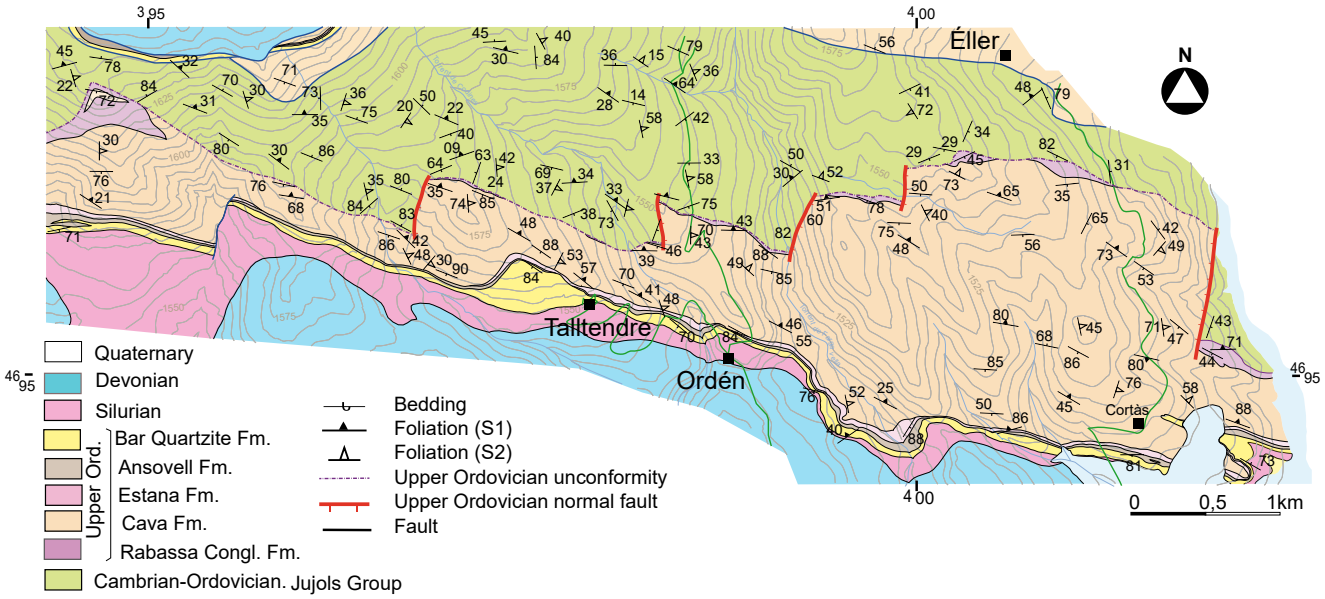

FIGURE 22. Geological map of the Talltendre area, north of Bellver de Cerdanya. Modified after Puddu *et al.* (2019). Location on Figure 1. Geographical coordinates are provided in UTM.

during subsequent Variscan and/or Alpine tectonics, whereas evidence of Ordovician displacement along the latter faults, because of their unfavourable N-S orientation, is preserved.

More indirect evidence for this Late Ordovician faulting event is provided by marked variations in the thickness of the Upper Ordovician successions reported by several authors (Hartevelt, 1970; Llopis Lladó, 1965; Speksnijder, 1986). Hartevelt (1970) documented sharp variations from 200m to more than 850m in the thickness of the Cava Formation and in the East of la Seu d'Urgell. Casas and Fernández (2008) proposed that the thicknesses of the Rabassa Conglomerate Formation and that of the Cava Formation attained more than 800m, before sharply diminishing to some tens of meters within a few kilometres. In this area, the maximum observed thickness occurs together with the maximum grain size of the conglomerates, where pebbles exceeding 50cm in diameter occur (Casas and Fernández, 2008).

DISCUSSION

Time and development of the Ordovician tectonic events in the Canigó massif

Ordovician tectonic events in the Canigó massif developed from ca. 475 to 446Ma (Fig. 23). At ca. 475Ma marine sedimentation ceased after the deposition of the quartzarenites of the uppermost part of the Serdinya Formation. Continental sedimentation started in Sandbian times, at ca. 455Ma, with the sedimentation of the Rabassa Conglomerates and the lower part of Cava Formation (early Katian), suggesting late Early Ordovician (Floian) to early Katian (roughly Mid Ordovician) uplift. Marine conditions restarted in the early-mid Katian with the sedimentation of the rest of the Cava Formation and the remaining Upper Ordovician succession. The Mid Ordovician uplift promoted forced sea-level regression and subaerial exposure, which caused an unconformity encompassing a gap interval of ca. 20m.y. during the Late Ordovician, and was locally linked to the erosion of ca. 1500m of the underlying Cambrian-Ordovician rocks.

In this area, magmatism started at ca. 470-465Ma and continued until ca. 446Ma, along 15-20m.y. (Fig. 23). The magmatic activity started slightly later than the uplift and seems continuous, although two peaks of marked activity can be recognized. The first peak occurred ca. 470-460Ma with the emplacement of the main monzogranitic to granodioritic bodies, up to 2000m thick and with laccolith morphology. This event produced protoliths of G-2 and G-3 gneisses, the Bruguera ignimbrites and the Cortalets metre-scale thick body metabasite (Fig. 17). The second peak is bracketed between ca. 458 to 446Ma, and yielded a varied suite of magmatic rocks, less voluminous and with different composition, ranging from granitic (G-1 and Casemí gneisses and Ribes granophyre), to monzogranitic-granodioritic (Cadí gneiss) and dioritic (metre-scale thick Marialles diorite) in composition (Fig. 17).

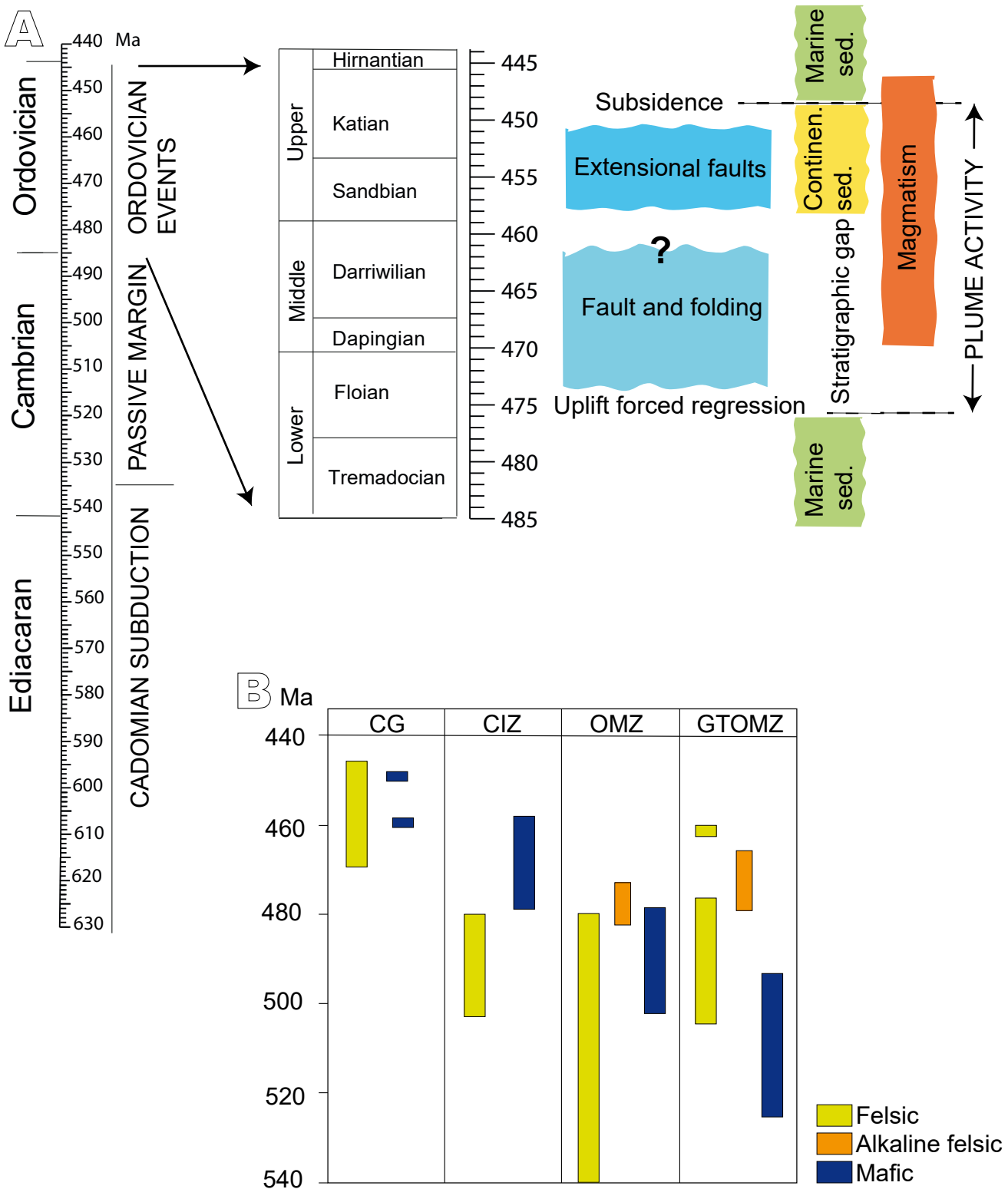

FIGURE 23. A) Summary and time of development of the Ordovician events in the Canigó massif; B) Age variation of the Cambrian-Ordovician felsic and mafic magmatism in the Canigó massif (CG), Central-Iberian Zone (CIZ), Galicia-Tras-os-Montes Zone (GTOMZ) and Ossa-Morena Zone (OMZ). Modified after Orejana *et al.* (2016).

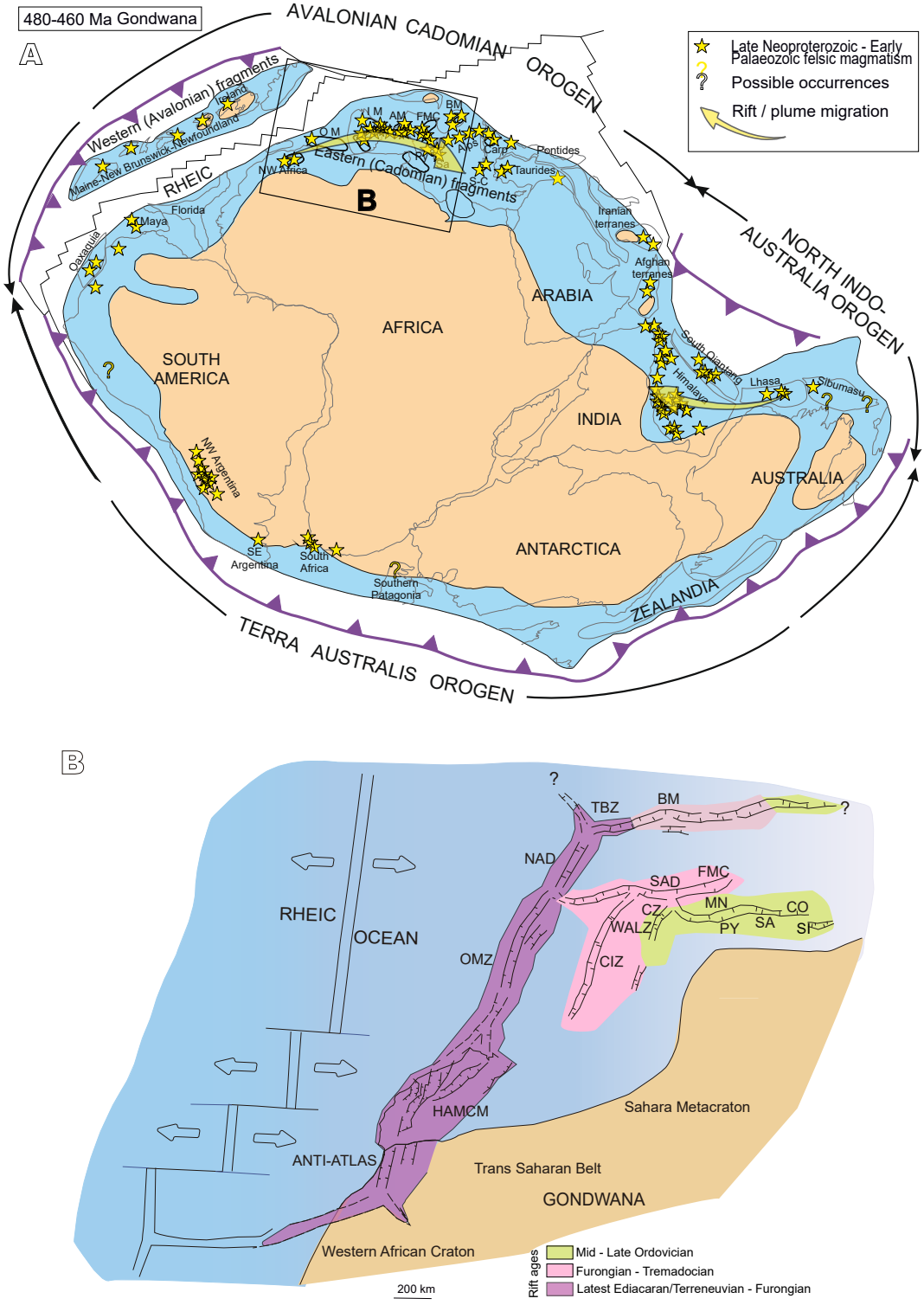

FIGURE 24. A) Early Ordovician map of Gondwana showing the location of the peri-Gondwanan Neoproterozoic – Early Palaeozoic felsic magmatism, modified after García-Arias *et al.* (2024). Map based on Cocks and Torsvik (2021), modified by Murphy *et al.* (2024). Note that Ganderia, Meguma and Avalonian terranes have been grouped under western (Avalonian) fragments. In Eastern (Cadomian) fragments: AM= Armorican Massif; BM= Bohemian Massif; Carp= Carpathians; FMC= French Massif Central; IM= Iberian Massif; OM= Ossa Morena; Py= Pyrenees; Sa= Sardinia; S-C= Sicily-Calabria. B) Rift migration in the Eastern (Cadomian) peri-Gondwanan fragments. Based on Álvaro *et al.* (2014, 2020, 2024a), Orejana *et al.* (2016), Cambeses *et al.* (2017), Casas and Murphy (2018) and Casas *et al.* (2023). Abbreviations: BM= Bohemian Massif; CIZ= Central Iberian Zone; CO= Corsica; CZ= Cantabrian Zone; FMC= French Massif Central, HAMCM= High Atlas Moroccan Coastal Meseta; MN= Montagne Noire; NAD= North Armorican Domain, OMZ= Ossa-Morena Zone; SAD= South Armorican Domain; Py= Pyrenees; SA= Sardinia; TBZ= Tepla Barrandian Zone; WALZ= Western Asturian Leonese Zone.

Extensional faulting developed in two episodes. The age of the first episode is not precisely constrained, as fault-related folds affect the Serdinya Formation and are sealed by the Sandbian Rabassa conglomerates. Thus its age is constrained from late Early Ordovician (Floian) to Mid Ordovician (pre-Sandbian), contemporaneous with the uplift of this area. Folds are probably related to two systems of upward-propagating extensional faults, oriented NE-SW and WNW-ESE. The second faulting episode developed in Sandbian-Katian times, giving rise to N-S and probably E-W oriented extensional faults. Although a correlation between the two extensional fracture episodes and the two main peaks of magmatic activity is possible, (Fig. 23A) more precise data on the age of the first fracture episode are needed to support this possibility.

The Ordovician events in the northwestern Gondwana margin

In the rest of the Pyrenees, voluminous orthogneissic bodies derived from Ordovician intrusive protoliths are also well represented in the Aston and Hospitalet massifs and in the Albera dome (Fig. 1). In the Aston and Hospitalet massifs, the Riete orthogneiss yielded 470±6Ma and 472±2Ma (Dapingian and Floian protolith ages, respectively; Denèle *et al.*, 2009), although a 467±2Ma age (Darriwilian-Dapingian), more similar to that of the Canigó G-2 and G-3 gneiss, was obtained in the Aston massif by Mezger and Gerdes (2016). The Albera augen orthogneiss, very similar to the Canigó G-2 type, provided a 470.4±3.1Ma age (Dapingian-Floian; Liesa *et al.*, 2011). In this massif, rhyolitic rocks have yielded ages similar to those of the main gneissic body (465.0±4.3 and 472.0±3Ma; Liesa *et al.*, 2011). West of the study area, in the La Pallaresa dome and the La Massana anticline, some metre-scale rhyolitic to dacitic subvolcanic sills yielding 453.6±1.5Ma (Clariana *et al.*, 2018) and 457±1.5Ma (Casas *et al.*, 2024) (Sandbian-Katian ages) are interbedded within pre-Upper Ordovician strata located close to the base of the Upper Ordovician succession. This Upper Ordovician felsic volcanism was probably widespread in other western Pyrenean massifs, such as the Pierrefitte dome (Calvet *et al.*, 1988), although geochronological data are needed to confirm the Ordovician age attributed to the rhyolitic sills and basalts of this massif.

South of the Pyrenees, Upper Ordovician felsic metavolcanic rocks occur in the Catalan Coastal Range, interbedded with conglomerates equivalent to those of the La Rabassa Formation, at the base of the succession (Gavarres massif, Els Metges volcanics, 455.2±1.8Ma; Navidad *et al.*, 2010), or within the succession (Guilleries massif, St. Martí volcanics, 452±4Ma; Martínez *et al.*, 2011).

In Sardinia, the Ordovician felsic magmatism started earlier than in the Canigó massif and the felsic volcanism is not restricted in age to the Sandbian-Katian as in the Pyrenees or the Catalan Coastal Range. Instead, it ranged from ca. 462Ma to 458Ma (Darriwilian to Katian) in the southernmost area (Cruciani *et al.*, 2018; Pavanetto *et al.*, 2012), and according to the available geochronological data, from ca. 491Ma to ca. 447Ma (Furongian to Katian) in the External Nappe Zones (Cruciani *et al.*, 2012, 2013; Garbarino *et al.*, 2005; Giacomini *et al.*, 2006; Oggiano *et al.*, 2010). In the Internal Nappe Zone, volcanism is mainly ca. 486-479Ma in age (Tremadocian) (Oggiano *et al.*, 2010). Secondly, plutonic Ordovician felsic rocks are subordinate in volume, and are Katian in age in the South of Sardinia (ca. 449Ma; Ludwig and Turi, 1989) and range from ca. 474Ma to ca. 456Ma (Floian to Sandbian) in the northern Internal Nappe Zones (Helbing and Tiepolo, 2005; Giacomini *et al.*, 2006). In this internal area, Ordovician-derived metabasites (453±14Ma and 460±5Ma; Palmeri *et al.*, 2004; Giacomini *et al.*, 2005; respectively) were metamorphosed to eclogite facies during Variscan high-grade metamorphism. However, the most striking similarity is the Sardic unconformity, well exposed in the Iglesiente area, associated with an intra-Ordovician stratigraphic gap in the autochthonous Palaeozoic basement of the Iglesiente-Sulcis area (southwestern Sardinia).

Teichmüller (1931) and Stille (1939) were the first to recognize an intra-Ordovician stratigraphic hiatus that separates the Cambrian–Lower Ordovician Nebida, Gonnesa and Iglesias groups (Pillola *et al.*, 1998) from the overlying coarse-grained ("puddinga") Monte Argentu metasedimentary rocks (Laske *et al.*, 1994; Leone *et al.*, 1991, 2002). A chronostratigraphically constrained minimum gap of about 17 or 18m.y. includes the Floian and Dapingian (Barca and Cherchi, 2004; Barca *et al.*, 1987; Cocco *et al.*, 2022; Pillola *et al.*, 1998), which is a very similar time span to that of the Upper Ordovician unconformity in the Canigó massif (Fig. 19). In addition, the erosive surface incised the substrate to a depth of 1200m to reach the Cambrian Series 2 rocks (Cocco *et al.*, 2022), a situation comparable with that of the Canigó massif, where pre-Upper Ordovician erosion reaches ca. 1500m. This hiatus is related to neither metamorphism nor deformation, though some 1 to 100m-scale E–W folds without cleavage and faults have been documented in the Gonnesa Anticline and the Iglesias Syncline, unconformably overlain by Upper Ordovician strata (Cocco and Funedda, 2012, 2019; Cocco *et al.*, 2018; Pasci *et al.*, 2008). As a result, the Upper Ordovician succession in SE Sardinia overlies Cambrian–Ordovician beds with different attitudes, *i.e.* similar relationships to that described above from the Eastern Pyrenees. The occurrence of faults and the environment of half-grabens have been proposed by Brusca and Dessau (1968) and Martini *et al.* (1991), who associate them with

a post-unconformity deposit (Monte Argentu Formation) in SW Sardinia, the lower part of this formation was deposited in alluvial to fluvial environments (Loi and Dabard, 1997; Loi *et al.*, 1992; Martini *et al.*, 1991). A similar gap was reported by Calvino (1972) in the Sarrabus-Gerrei units of the external nappe zone, in the eastern area.

North of the study area, in the Mouthoumet massif (Fig. 1), there is evidence of 455±1Ma felsic metavolcanics (Sandbian, Casas *et al.*, 2024) emplaced unconformably above a Lower Ordovician succession (Álvaro *et al.*, 2016). Mouthoumet metavolcanics were emplaced coevally with the protoliths of the orthogneisses in the Montagne Noire Axial Zone in the southern slope of the French Central Massif (456±3Ma and 450±6Ma; Roger *et al.*, 2004; 455.2 ± 2.2Ma; Pitra *et al.*, 2012). In the French Central Massif, Melleton *et al.* (2010) described protolith ages ranging from ca. 451Ma to 475Ma for the gneiss involved in the main tectonic units, implying a time span of Ordovician magmatism in this region (Floan to Katian) was similar to that in the Pyrenees. In the southern French Central Massif Lotout *et al.* (2017) reported ages ca. 468-470Ma (Dapingian), and in the eastern area Chelle-Michou *et al.* (2017), Faure *et al.* (2017) and Couzinié *et al.* (2022) described ca. 486Ma to 477Ma ages (Tremadocian and Floian) for the gneiss protoliths, confirming the widespread development of Ordovician magmatism in the French Central Massif.

In the Armorican Massif, ages ca 494–472Ma (Toledanian Furongian-Early Ordovician) were obtained for the volcanic rocks of the "Porphyroid Nappe" in the units of the Southern Armorican Domain (Ballèvre *et al.*, 2012; El Korh *et al.*, 2012; Pouclet *et al.*, 2017). These rocks share the same texture and mineral compositions as the "porphyroids" from the French Massif Central and their age of emplacement is coincident with that of their French Massif Central equivalents (Thiéblemont *et al.*, 2017). In contrast, the Late Ordovician magmatic pulse (ca. 455 to 450Ma) has not been documented in the Armorican Massif.

A similar situation arises in the Bohemian Massif, where a well-expressed Cambrian-Ordovician magmatism (ca. 496 to 470Ma) is recognized in the Saxo-Thuringian (Kröner and Willner, 1998; Linnemann *et al.*, 2000; Mingram *et al.*, 2004; Tichomirowa *et al.*, 2001; Tichomirowa *et al.*, 2012) and Moldanubian zones (Friedl *et al.*, 2004; Soejono *et al.*, 2019; Teipel *et al.*, 2004; von Quadt, 1997; Žák *et al.* 2023).

In the Iberian Massif, the "Ollo de Sapo" represents a mainly felsic magmatic event developed in the Central Iberian Zone from ca. 495Ma to ca. 470Ma, with a magmatic peak at ca. 482–477Ma. Magmatism is located mainly in the core of a 650km long, concave to the East, Ollo de Sapo antiform, in the Guadarrama and Tormes domes and in the contact between the Central Iberian and Ossa Morena Zones (Urra Formation) (Álvaro *et al.*, 2020; Bea *et al.*, 2006, 2007; Castiñeiras *et al.*, 2008b; Díaz-Alvarado *et al.*, 2016; Díez-Montes *et al.*, 2010; García-Arias *et al.*, 2018; López-Sánchez *et al.*, 2015; Montero *et al.*, 2007, 2009; Navidad and Castiñeiras, 2011; Rodríguez *et al.*, 2022; Talavera *et al.*, 2013; Valverde-Vaquero and Dunning, 2000; Villaseca *et al.*, 2016; Zeck *et al.*, 2007). Although this Furongian-Lower Ordovician magmatism is mainly felsic, subordinate mafic bodies with tholeiitic affinity, ranging in age from ca. 473 to 453Ma, have been described in the Guadarrama dome (Orejana *et al.*, 2016, 2017; Villaseca *et al.*, 2015).

In the Ossa Morena Zone (Iberian Massif) the magmatism started earlier, in the Terreneuvian, ca. 530Ma, close in age to the termination of subduction-related Cadomian magmatism (Álvaro *et al.*, 2014; Cambeses *et al.*, 2017; Expósito, 2005; Sánchez-García *et al.*, 2003, 2008; Simancas *et al.*, 2004). This magmatism continued until ca. 500Ma (Cambeses *et al.*, 2017; Chichorro, 2006; Chichorro *et al.*, 2008; Cordani *et al.*, 2006; Ochsner, 1993; Ordóñez, 1998; Pereira *et al.*, 2006, 2011, 2012; Romeo *et al.*, 2006; Sánchez-García *et al.*, 2008, 2014) with two peaks related to an early (530–520Ma) and a main rifting event (510Ma; Sánchez-García *et al.*, 2008, 2010; Sarrionandia *et al.*, 2012; Quesada, 2006). In the Teplá-Barrandian Zone (Bohemian Massif), pervasive lower Cambrian magmatism also developed between 524 and 510Ma (Dörr *et al.*, 1998, 2002; Zulauf *et al.*, 1997).

In the Central Iberian Zone (Iberian Massif), "Ollo de Sapo" magmatism is penecontemporaneous with the development of the so-called Toledanian unconformity, representing a sedimentary gap of ca. 22m.y. This gap is related to the onlap of Lower Ordovician (upper Tremadocian–Floian) rocks above Ediacaran-Miaolingian rocks forming an inherited palaeorelief defined by tilted blocks. According to Álvaro *et al.* (2021, 2024) and Casas *et al.* (2023), this unconformity can be correlated with the 'Furongian gap' reported in the Ossa-Morena Zone (Sánchez-García *et al.*, 2019) and the Anti-Atlas (Álvaro and Vizcaïno, 2018), the 'Norman gap' of the Central and North Armorican domains (Le Corre *et al.*, 1991), the 'Upper Cambrian' gap in Saxo-Thuringian (Linnemann *et al.*, 2000) and the 'Cambrian-Ordovician transition gap' in Bohemia (Bruthansová *et al.*, 2007).

In the Peloritani mountains (Sicily and Calabria, southern Italy), intermediate to felsic ca. 461Ma to ca 451Ma magmatism (Darriwilian-Katian; Trombetta *et al.*, 2004) is recorded in the basement rocks involved in the Alpine thrusts. In other Variscan basement rocks involved in the Alpine Mediterranean orogens, Ordovician magmatism is also well represented, such as in the basement of several units of the Alps (ca. 487 to 445Ma; Arboit *et al.*, 2019;

Maino *et al.*, 2019; Nosenzo *et al.*, 2024; Scheiber *et al.*, 2013; Schulz *et al.*, 2004) or in the Carpathians (ca. 482 to 459Ma; Balintoni *et al.*, 2010; Putis *et al.*, 2008).

Further East, in Turkey, Early and Late Ordovician igneous rocks are reported in Anatolia (ca. 446Ma; Özbey *et al.*, 2013), Istranca massif (ca. 453Ma; Yılmaz Şahin *et al.*, 2024), Sakarya zone (ca. 488 to 471Ma; Uğurcan and Ustaömer, 2024) and late Furongian-Lower Ordovician granites in Iran (ca. 490 and 483Ma; Karimi *et al.*, 2024; Shirdashtzadeh *et al.*, 2018). Also in Iran, in the Alborz Mountains, Álvaro *et al.* (2022) described Upper Ordovician basaltic lava flows with intraplate tectonic affinity, compatible with Ocean Island Basalt (OIB)-like mantle sources, linked to Sandbian to early Katian uplift pulse.

Early Palaeozoic (mostly Furongian-Mid Ordovician) magmatic events can be also recognized as far as the NE Gondwana margin in the Himalaya, Lhasa, Southern Qiangtang, Baoshan, Tengchong, Sibumasu, Helmand and Karakorum terranes (Dan *et al.*, 2022). These authors described a belt of granitic rocks formed between ca. 510Ma and 460Ma, with two major pulses at ca. 500 and 480Ma. Interestingly, Dan *et al.* (2022) reported a regional scale sedimentary hiatus between Furongian and Lower/Middle Ordovician strata in the Himalaya and peri-Gondwanan terranes. This hiatus is recorded by an angular unconformity or by a disconformity in the Himalaya, Lhasa, and Baoshan terranes.

According to the recent review of García-Arias *et al.* (2024), this early Palaeozoic magmatism is also recognized in other areas of the Gondwana margin, such as SW South Africa, NE Patagonia, NW Argentina, Colombia, SE Mexico and Guatemala or in adjacent peri-Gondwanan terranes as Avalonia-Meguma-Ganderia (Fig. 24A). For the description of these areas not encompassed in our contribution, we refer to the work of García-Arias *et al.* (2024), which includes petrographic, geochemical and geochronological descriptions together with a tectonic model for these different areas. These authors point out that all these areas formed an early Palaeozoic magmatic belt of several thousands of kilometres, along the Gondwana periphery (Fig. 24A). The similarities and extension of this magmatism led several authors to propose that it may form several silicic Large Igneous Provinces (LIPs) (*e.g.* Dan *et al.*, 2022; Díez-Montes *et al.*, 2010) and García-Arias *et al.* (2024) discussed if, given these similarities, this magmatism comprise a big single LIP.

The quest for a geodynamic scenario: the plume model and the Cambrian-Ordovician rifting

Following Puddu *et al.* (2019), Dan *et al.* (2022) and Murphy *et al.* (2024), we propose that the upwelling of a mantle plume beneath the continental lithosphere of the Pyrenees and surrounding areas would explain all the Ordovician events recorded in the Canigó massif. The impinging of a plume under this region of Gondwana, at ca. 475Ma, could have instigated lithospheric doming uplift that may explain the Mid Ordovician forced sea-level regression, subaerial exposure, erosion and the development of the Upper Ordovician unconformity. In this scenario, voluminous peraluminous felsic magmatism developed between ca. 470 to 446Ma, starting after the uplift, as described in several LIPs (Condie, 2001; Saunders *et al.*, 2007) (Fig. 23A). Magmatism originated under HT-LP melting conditions, which requires input of sufficient heat to melt the Neoproterozoic crustal rocks (granitoids and derived sedimentary rocks), from which they inherited a calc-alkaline signature. Decompression triggered partial melting of the head of the plume at the asthenosphere/lithosphere boundary causing ascending mafic magmas that may have facilitated advection of sufficient heat to trigger crustal melting at mid to lower-crustal levels (~15km; García-Arias *et al.*, 2018; Casas *et al.*, 2023). Felsic magmas were then emplaced at lower-crustal levels. The scarcity of coeval metabasites may be explained if large volumes of intracrustal silicic melts acted as a rheological barrier, preventing the rise of mafic magmas to the surface (Hupert and Sparks, 1988; Bindeman and Valley, 2003; Bea *et al.*, 2007). The E-MORB character of the Middle Ordovician metabasite fits well with this setting.

Plume activity would have been active during ca. 20m.y, between ca. 475 and 446Ma, from Floian to early-mid Katian times. In early-mid Katian times, plume activity finished in this portion of Gondwana, as signalled by the subsidence that restarted the marine conditions, and the end of the magmatic and tectonic activity (Fig. 23A). Coeval development of extensional faults may have originated from the stretching of the external part of the lithosphere, although other explanations (*e.g.* collapse of the uplift due to magma chamber deflation?) or a combination of several mechanisms cannot be ruled out. The potential correlation of the development of two extensional fracture episodes with the two main magmatic peaks requires that the timing of the first fracture episode to be more thoroughly investigated.

In a regional context, the existence of an Ordovician plume event has been previously invoked to understand other significant Ordovician processes, such as the lack of magnetic reversals (the Tremadocian-Darriwilian Moyero Long Reversed Superchron; Courtillot and Olson, 2007; Pavlov and Gallet, 2005), enhanced biological activity and extensive black shale deposits (Barnes 2004; Condie, 2001, 2004), decline in seawater $^{87}Sr/^{86}Sr$ ratios (Ernst and Buchan, 2003; Qing *et al.*, 1998), severe perturbations in atmospheric pCO_2 with feedbacks causing both warming (Boda event) and cooling (Hirnantian glaciation) events

(Ernst and Buchan, 2003; Lefebvre *et al.*, 2010), upwelling of ferruginous waters (Matheson *et al.*, 2022; Matheson *et al.*, 2020) or the formation of pronounced magnetic anomalies (Casas *et al.*, 2023), among others. Positive carbon isotope excursions have been also related to an increase in nutrient delivery associated with basaltic weathering during Mid Ordovician (Adiatma *et al.*, 2024; Swanson-Hysell and Macdonald, 2017).

Early Palaeozoic rifting affecting the northwestern Gondwana margin developed after the cessation of the Pan African and Cadomian subduction, originated by oblique ridge/trench collision (Linnemann *et al.*, 2008; Murphy and Nance, 1989; Nance *et al.*, 2002) or a subduction of the mid-ocean ridge beneath the continental upper plate (Sánchez-García *et al.*, 2003, 2008, 2010) (Fig. 24A). This early Palaeozoic rifting event leading to the export of the western (Avalonian) terranes of the former Avalonian–Cadomian belt from the Gondwanan margin, whereas the eastern (Cadomian) segments, were separated from Avalonian terranes by a mid-ocean ridge within the embryonic Rheic Ocean. This rift is thought to have developed along an inherited Neoproterozoic suture, and facilitated complete separation of Avalonian terranes and the birth of the Rheic Ocean (Murphy *et al.*, 2006). This ridge may have continued northwards and connected with a hypothetical ridge, trending NW-SE (Casas *et al.*, 2023; Syahputra *et al.*, 2022; Žák *et al.*, 2023) or NE-SW (Cambeses *et al.*, 2017; Linnemann *et al.*, 2008), depending on the reconstructions used (Fig. 24A). Reconstruction of the eastern (Cadomian) fragments of northern Gondwana is not straightforward, due to the severe Variscan and Alpine overprinting. Nevertheless, several reconstructions of the early Palaeozoic massifs forming the NW Gondwana margin agree in placing Anti-Atlas, High Atlas and Moroccan Coastal Meseta, Ossa-Morena Zone and North Armorican Domain in an outboard (westernmost) part of the margin, Northeast of the West African Craton (WAC), between the WAC and the Trans Saharan Belt (see discussion in Cambeses *et al.*, 2017 and Casas and Murphy, 2018, among others). The Central Iberian Zone, the rest of the Armorican Massif, the French Massif Central and the rest of the Bohemian Massif would be clustered in a relatively central position, North of Saharan Metacraton, and the West Asturian-Leonese and Cantabrian Zones, Pyrenees, Sardinia, Corsica and Sicily were likely located in an easternmost position, closer to Gondwana margin (Álvaro *et al.*, 2021; Casas and Murphy, 2018; Casas *et al.*, 2023; Cambeses *et al.*, 2017; Quesada, 1991; Robardet, 2002; Robardet and Gutiérrez Marco, 2004) (Fig. 24B).

In this eastern (Cadomian) sector, Álvaro *et al.* (2024a) proposed a scenario of diachronous Southwest-to-Northeast opening of several rift branches of the Atlas–Ossa–Morena–North Armorican Rift, with restricted or no signals of true oceanization. Oceanization probably developed further to the NW, between the Moroccan Coastal Meseta and the rest of the Avalonian fragments (Fig. 24B) (Álvaro *et al.*, 2014; Pouclet *et al.*, 2007). In the Anti-Atlas, in the southerwesternmost area of this eastern Cadomian sector, rifting began close to the Ediacaran-Cambrian boundary interval (Álvaro *et al.*, 2018, 2024a) and ended in the Furongian with the onset of a break-up unconformity (Álvaro and Vizcaïno, 2018). In the Ossa Morena Zone, rifting started in Terreneuvian times (Álvaro *et al.*, 2014) and ended in another Furongian break-up unconformity (Venta del Ciervo unconformity; Sánchez-García *et al.*, 2019), although some magmatic activity continued until the Tremadocian-Floian (Cambeses *et al.*, 2017; Sánchez-García *et al.*, 2019), indicating a NW-SE propagation in present-day coordinates. Several branches, connected to the main rift axis, propagated through the western Gondwana landmass (Fig. 24B). In these branches, the rift migrated from West-to-East, as indicated by the younger age of magmatism and the Furongian-Lower Ordovician unconformities to the East (Cambeses *et al.*, 2017; Casas and Murphy, 2018; García-Arias *et al.*, 2024). One of these rift arms split in two, involving on one side the Central Iberian Zone, and on the other one the South Armorican Domain and the French Massif Central with the development of the Furongian-basal Tremadocian Ollo de Sapo magmatic even in both branches (Fig. 24B). In turn, the northern arm split in two, and propagated to the South and to the East, originating the Mid-Late Ordovician magmatism and the formation of the Sardic unconformity mainly recorded in the Pyrenees (Canigó massif), Sardinia and the Occitan Domain (Montagne Noire and Mouthoumet massifs) (Fig. 24B) (Casas *et al.*, 2023). This eastward migration is accompanied by a progressive decrease in the rifting intensity, as signaled by the decrease in the duration and intensity of the magmatism and in the amount of subsidence. In this scenario, Ordovician events recorded in the Canigó massif (Fig. 23; 24) would represent the declining manifestations of this rifting.

If the Cambrian-Ordovician unconformities and magmatism are considered plume proxies, such plume activity would have affected several areas fringing NW Gondwana, such as the Anti-Atlas to Moroccan Coastal ranges, the Iberian, Armorican, French Central or the Bohemian massifs. This geographical dispersion suggests that a cluster of Cambrian-Ordovician plumes, rather than a single one, may have developed. When considering the different ages of the Cambrian-Ordovician magmatism and the Cambrian-Ordovician unconformities in these massifs, it appears that plume activity began in latest Ediacaran to Terreneuvian times in the Anti-Atlas, Ossa-Morena (Iberian Massif), North Armorica and Teplà Barrandian (Bohemian Massif) zones, was active during Furongian-

Early Ordovician in the Central Iberian Zone, Armorican, French Central and Bohemian massifs, and from Mid Ordovician until early-mid Katian times in the Occitan Domain, Pyrenees, Sardinia and surrounding areas, that is, a SW-to-NE migration, parallel to that of the rifting activity (Fig. 24B).

Plume activity, coeval with rift development, may provide an overarching interpretation for the different kinds of mantle involvement in Cambrian-Ordovician magmatism. Such activity may have caused i) severe thermal modification of the lithosphere, probably caused by an underlying thermal anomaly in the Ossa-Morena Zone (Sánchez-García *et al.*, 2008, 2010, 2019); ii) rapid crustal melting produced by the advection of heat provided by mafic magmas underplating the lower crust under extensional conditions in the Central Iberian Zone (Bea *et al.*, 2007; Díez-Montes *et al.*, 2010; Montero *et al.*, 2009); iii) extensive decompression melting which yielded basaltic magma emplacement in the Bohemian Massif (Žák *et al.*, 2023) or iv) progressive crustal thinning and the uplift of lithospheric mantle geotherms which induced anatexis of a juvenile crust, hot spot activity or abnormally hot mantle radiating from a mantle plume, in the Pyrenees (Marini 1988; Navidad *et al.*, 2018; Pin and Marini, 1993; respectively).

It should be noted that in NE Gondwana and in the adjacent peri-Gondwanan terranes, Dan *et al.* (2022) attributed Cambrian–Ordovician magmatism to the upwelling of a mantle plume in an intraplate setting, which can also explain the uplift forming the regional Cambrian–Ordovician unconformity. In this NE margin of Gondwana, García-Arias *et al.* (2024) propose an East-to-West propagation and opening of the Proto-Tethys Ocean, based on the variation in age of the magmatism (from 520 to 490Ma) in the Lhasa terrane to 490-460Ma in the western Himalaya. That propagation, similar to what happened in the study area in NW Gondwana, suggests an inward migration of plume activity towards the centre of Gondwana (Fig. 24A).

Geodynamic models suggest that mantle plumes preferentially emanate from the edges of subducted slabs along the core-mantle boundary (Murphy *et al.*, 2024; Tan *et al.*, 2002, 2011). In our case, subducted slabs reflecting Pan-African collisions would have underlain the core of Gondwana after its assembly (Murphy *et al.*, 2021), providing an explanation for rifting and plume development that would have affected much of the Gondwana margin (García-Arias *et al.*, 2024). Coeval development of rift and plume activity suggests that Cambrian–Ordovician plume-related magmatism may fit with the LIP-Producer or LIP-Trigger categories proposed by Koptev and Cloetingh (2024).

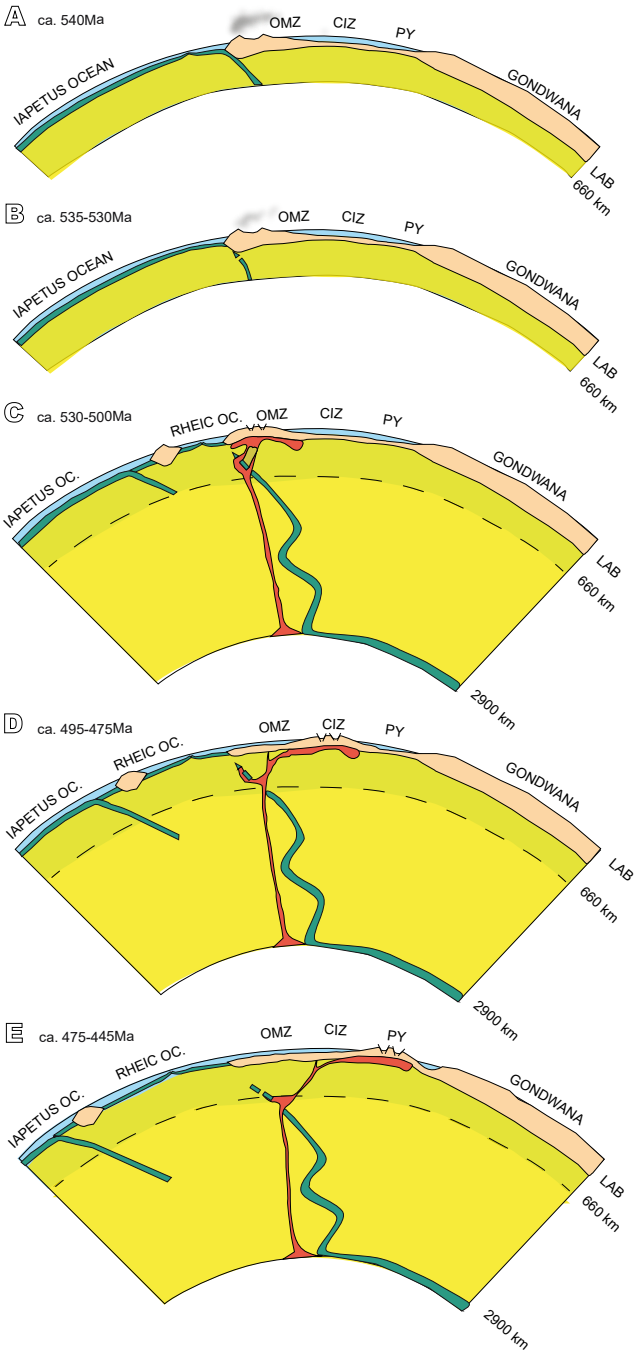

FIGURE 25. Sketch showing the eastward migration of the plume activity, toward the centre of Gondwana, between Fortunian to late Katian times. A) Latest stages of the Cadomian subduction; B) End of the subduction caused by oblique trench subduction or ridge-trench collision; C) Beginning of the plume activity under NW Gondwana, coeval to Avalonia migration and birth of the Rheic Ocean; D) Plume activity migrates under CIZ; D) Plume actrivity migrates and vanishes under Pyrenees and neigbhouroing areas. Abbreviations: LAB= Lithosphere-Astenosphere boundary; CIZ= Central Iberian Zone; OMZ= Ossa-Morena Zone and PY= Pyrenees.

We propose that the first phase of magmatism reflects the arrival of a mantle plume under a thick lithosphere (recently formed Pan African and Cadomian continental

magmatic arcs, as in the Anti-Atlas and Ossa-Morena Zone) (Fig. 25A) exploiting the development of a slab window or slab break-off event that caused the cessation of the Cadomian arc magmatism (Fig. 25B-C). After that, the plume migrated, or was attracted, to areas of relatively thin and hot lithosphere, represented by the former back-arc areas of the Cadomian subduction (Central Iberian Zone and Pyrenes; Álvaro *et al.*, 2024b; Rojo-Pérez *et al.*, 2023), the trailing margin of which was transformed into a passive margin located inwards Gondwana (Fig. 25D-E). Plume migration may be accounted by flow along the lithosphere/asthenosphere boundary of material delivered from the plume source towards these thinner lithospheric areas (Koptev and Cloetingh, 2024).

CONCLUSIONS

In the Canigó massif, voluminous felsic magmatism, 15-20my. In duration, occurred between Mid to Late Ordovician, coeval with basalt with E-MORB affinity and with a Mid Ordovician uplift and erosion that produced the Upper Ordovician (Sardic) unconformity. Synchronous extensional faults built propagation cleavage-free folds that only affected pre-Upper Ordovician succession. Finally, early Late-Ordovician synsedimentary normal faults produced significant thickness variations in the Upper Ordovician successions. These inter-relationships between sedimentation, erosion, tectonics and magmatism in addition to the volume, age and composition of the igneous rocks themselves, are interpreted as evidence for the upwelling of a Mid-Late Ordovician mantle plume beneath the continental lithosphere of the Pyrenees and surrounding areas.

It is proposed that this plume belongs to a cluster of plumes impacting the Gondwana periphery between Cambrian and Late Ordovician times which in some instances caused stretching of this margin, and may have led to the birth and development of the Rheic and other intervening oceans.

Finally, this study is an example of the crucial role of field-based data when discussing several geodynamic scenarios, such as those proposed to explain the early Palaeozoic Gondwana evolution in this pivotal time interval of Earth's evolution.

ACKNOWLEDGMENTS

It is a pleasure to honour the pioneer geologists, whose fieldwork in the 50's, 60's and early 70's of the last century, often under hard conditions, provided the basis for the knowledge of the Pyrenean geology. Among them, G. Guitard occupies a preeminent position. After their work, we can take advantage of modern analytical techniques to shed some light on old problems.

This publication is a contribution to grants PID2021-122467NB-C22 and PID2021-125585NB-I00 funded by MICIU/AEI/ 10.13039/501100011033 and by ERDF/EU. JMC acknowledge the support of the James Chair for Pure and Applied Sciences, St. Francis Xavier University (Antigonish, NS). JBM acknowledges the continuing support of NSERC, Canada. NPS acknowledges a Juan de la Cierva grant from the University of Granada. We also thank Z. Belaústegui for his help with some pictures and L. Rincón for the editorial handling. Detailed and constructive revisions by J.R. Martínez Catalán and F.J. Fernández are greatly appreciated.

G. Guitard in a field trip in the Cap de Creus massif (May 1980, picture by J.M. Casas).

REFERENCES

Adiatma, Y.D., Saltzman, M.R., Griffith, E.M., 2024. Calcium isotope constraints on a Middle Ordovician carbon isotope excursion. Earth and Planetary Science Letters, 641, 118805. DOI: https://doi.org/10.1016/j.epsl.2024.118805

Alías, G., Casas, J.M., Cirés, J., Liesa, M., 2000. The large-scale structure of the Canigó Massif (Eastern Pyrenees) implications for the Hercynian tectonics. A Coruña (Spain), 15th International Conference on Basement Tectonics.

Álvaro, J.J., Vizcaïno, D., 2018. The Furongian break-up (rift-drift) unconformity in the Anti-Atlas, Morocco. Journal of Iberian Geology, 44, 567-587.

Álvaro, J.J., Bellido, F., Gasquet, D., Pereira, M.F., Quesada, C., Sánchez-García, T., 2014. Diachronism in the late Neoproterozoic–Cambrian arc-rift transition of North Gondwana: A comparison of Morocco and the Iberian Ossa-Morena Zone. Journal of African Earth Sciences, 98, 113-132.

Álvaro, J.J., Colmenar, J., Monceret, E., Pouclet, A., Vizcaïno, D., 2016. Late Ordovician (post-Sardic) rifting branches in the North-Gondwanan Montagne Noire and Mouthoumet massifs of southern France. Tectonophysics, 681, 111-123.

Álvaro, J.J., Casas, J.M., Quesada, C., 2018. Early Palaeozoic geodynamics in NW Gondwana. Journal of Iberian Geology, 44, 551-565.

Álvaro, J.J., Sánchez-García, T., Puddu, C., Casas, J.M., Díez-Montes, A., Liesa, M., Oggiano, G., 2020. Comparative geochemical study on Furongian–earliest Ordovician (Toledanian) and Ordovician (Sardic) felsic magmatic events in south-western Europe: underplating of hot mafic magmas linked to the opening of the Rheic Ocean. Solid Earth, 11, 2377-2409.

Álvaro, J.J., Casas, J.M., Quesada, C., 2021, Reconstructing the pre-Variscan puzzle of cambro-ordovician basement rocks in the southwestern European margin of Gondwana. In: Murphy, J.B., Strachan, R.A., Quesada, C. (eds.). Pannotia to Pangaea: Neoproterozoic and paleozoic orogenic cycles in the Circum-Atlantic region. London, The Geological society, 503 (Special Publications), 531-562.

Álvaro, J.J., Ghobadi Pour, M., Sánchez-García, T., Hairapetian, V., Kebria-Ee Zadeh, M.R., And Popov, L., 2022. Stratigraphic and volcanic signatures of Miaolingian to Ordovician rift pulses in the eastern Alborz Mountains, northern Iran. Journal of Asian Earth Sciences, 233, 105240. DOI: https://doi.org/10.1016/j.jseaes.2022.105240

Álvaro, J.J., Sánchez-García, T., Casas, J.M., 2024a. The Cambrian Atlas – Ossa-Morena – Northarmorican Rift, West Gondwana: along- and off-axis, stratigraphic and volcano-tectonic patterns. In: Nance, R.D., Strachan, R.A., Quesada, C., Lin, S. (eds.). Supercontinents, Orogenesis and Magmatism. London, The Geological Society, 542 (Special Publications), 465-505. DOI: https://doi.org/10.1144/SP542-2023-24

Álvaro, J.J., Lorenzo, S., Martínez-Benítez, B., Pieren, A.P., 2024b. Late Ediacaran carbonate production and REE+Y signatures tracing redox conditions in a Cadomian retroarc basin, Central Iberian Zone, Spain. Geologica Acta, 22.5, 1-21, I.

Álvaro, J.J., Casas, J.M., Clausen, S., Padel, M., Sánchez-García, T., Pujol-Solà, N, Proenza, J., in press. Cadomian cycle in the Pyrenees. In: Álvaro, J.J., Quesada, C., Oliveira, J.T. (eds.). The Geology of Iberia: a Geodynamic Approach. Regional Geology Reviews series, Heidelberg, Springer, 1(3).

Arboit, F., Chew, D., Visoná, D., Massironi, M., Sciascia, F., Benedetti, G., Rodani, S., 2019. The geodynamic evolution of the Italian South Alpine basement from the Ediacaran to the Carboniferous: Was the South Alpine terrane part of the peri-Gondwana arc-forming terranes? Gondwana Research, 65, 17-30.

Arenas, R., Díez Fernández, R., Sánchez Martínez, S., Gerdes, A., Fernández-Suárez, J., Albert, R., 2014. Two-stage collision: exploring the birth of Pangea in the Variscan terranes. Gondwana Research, 25, 756-763.

Autran, A., Guitard, G., 1969. Mise en évidence de nappes hercyniennes de style penninique dans la série métamorphique du massif du Roc de France (Pyrénées orientales): Liaison avec la nappe du Canigou. Paris, Comptes Rendus de l'Académie des Sciences, 269, 2479-2499.

Autran, A., Fonteilles, M., Guitard, G., 1966. Discordance du Paléozoïque inférieur métamorphique sur un socle gneissique anté-hercynien dans le massif des Albères (Pyrénées orientales). Paris, Comptes Rendus de l'Académie des Sciences, 263, (D), 317-320.

Ayora, C., 1980. Les concentrationes metàl□liques de la Vall de Ribes. PhD. Thesis. Barcelona University, 182pp.

Ayora, C., Casas, J.M., 1986. Strabound As-Au mineralization in pre-Caradocian rocks form the Vall de Ribes, Eastern Pyrenees, Spain. Mineralium Deposita, 21, 278-287.

Balintoni, I., Balica, C., Ducea, M.N., Hann, H.P., Şabliovschi, V., 2010. The anatomy of a Gondwanan terrane: The Neoproterozoic–Ordovician basement of the pre-Alpine Sebeş–Lotru composite terrane (South Carpathians, Romania). Gondwana Research, 17, 561-572.

Ballèvre, M., Fourcade S., Capdevila, R., Peucat, J.J., Cocherie, A., Mark Fanning, C., 2012. Geochronology and geochemistry of Ordovician felsic volcanism in the Southern Armorican Massif (Variscan belt, France): Implications for the breakup of Gondwana. Gondwana Research, 21, 1019-1036.

Barbey, P., Cheilletz, A., Laumonier, B., 2001. The Canigou orthogneisses (Eastern Pyrenees, France, Spain): an Early Ordovician rapakivi granite laccolith and its contact aureole. Paris, Comptes Rendus de l'Académie des Sciences, 332, 129-136.

Barca, S., Cherchi, A., 2004. Regional geological setting. In: Barca, S., Cherchi, A. (eds.). Sardinian Palaeozoic Basement and its Meso–Cainozoic Cover (Italy). Italy, 32nd International Geological Congress, Field Trip Guide Book, P39(5), 3-8.

Barca, S., Cocozza, T., Del Rio, M., Pillola, G.L., Pittau Demalia, P., 1987. Datation de l'Ordovicien inférieur par Dyctionema flabelliforme et Acritarhes dans la partie supérieure de la formation «Cambrienne» de Cabitza (SW de la Sardaigne, Italie): conséquences géodynamiques. Paris, Comptes Rendus de l'Académie des Sciences, 305, 1109-1113.

Barnes, C., 2004. Was there an Ordovician superplume event? In: Webby, B.D., Paris, F., Droser, M., Percival, I. (eds.). The Great Ordovician Biodiversification Event. New York, Columbia University Press, 77-80.

Bea, F., Montero, P., Talavera, C., Zinger, T., 2006. A revised Ordovician age for the Miranda do Douro orthogneiss, Portugal. Zircon U-Pb ion-microprobe and LA-ICPMS dating. Geologica Acta, 4(3), 395-401.

Bea, F., Montero, P., González Lodeiro, F., Talavera, C., 2007. Zircon inheritance reveals exceptionally fast crustal magma generation processes in Central Iberia during the Cambro–Ordovician. Journal of Petrology, 48, 2327-2339.

Bea, F., Montero, P., Talavera, C., Anbar, M.A., Scarrow, J.H., Molina, J.F., Moreno, J.A., 2010. The palaeogeographic position of Central Iberia in Gondwana during the Ordovician: evidence from zircon chronology and Nd isotopes. Terra Nova, 22, 341-346.

Beetsma, J.J., 1995. The late Proterozoic/Paleozoic and Hercynian crustal evolution of the Iberian Massif, N Portugal as traced by geochemistry and Sr-Nd-Pb isotope systematics of pre-Hercynian terrigenous sediments and Hercynian granitoids. PhD. Thesis. Amsterdam, Vrije University, 223pp.

Belaústegui, Z., Puddu, C., Casas, J.M., 2016. New ichnological data from the lower Paleozoic pf the Central Pyrenees: presence of Artrophycus Brogniartii (Harlam, 1832) in the Upper Ordovician Cava Formation. IX Congreso Geológico de España, Geo-Temas, 16(1), 271-274.

Bindeman, I.N., Valley, J.W., 2003. Rapid generation of both high- and low-$\delta^{18}O$, large-volume silicic magmas at the timber mountain/oasis Valley caldera complex, Nevada. Geological Society of America Bulletin, 115, 581-595.

Brusca, C., Dessau, G., 1968. I giacimenti piombo-zinciferi di S. Giovanni (Iglesias) nel quadro della geologia del Cambrico sardo. L'Industria Mineraria, 19, 533-556.

Bruthansová, J., Fatka, O., Budil, P., Král, J., 2007. 200 years of trilobite research in the Czech Republic. In: Mikulic, D.G., Landing, E., Kluessendorf, J. (eds.). Fabulous Fossils – 300 Years of Worldwide Research on Trilobites. New York Museum Bulletin, 507, 51-79.

Calvet, P., Lapierre, H., Charvet, J., 1988. Diversité du volcanisme ordovicien dans la région de Pierrefitte (Hautes-Pyrénées): rhyolites calco-alcalines et basalts alcalins. Paris, Comptes Rendus de l'Académie des Sciences, série 2, 307, 805-812.

Calvino, F., 1972. Note illustrative della Carta Geologica d'Italia, Foglio 227-Muravera. Roma, Servizio Geologico d'Italia, 60pp.

Cambeses, A., Scarrow, J.H., Montero, P., Lázaro, C., Bea, F., 2017. Palaeogeography and crustal evolution of the Ossa–Morena Zone, southwest Iberia, and the North Gondwana margin during the Cambro-Ordovician: a review of isotopic evidence. International Geology Review, 59, 94-130. DOI: http://dx.doi.org/10.1080/00206814.2016.1219279

Casas, J.M., 1984. Estudi de la deformació ens els gneiss del massís del Canigó. PhD. Thesis. Barcelona, Barcelona University, 284pp.

Casas, J.M., 2010. Ordovician deformations in the Pyrenees: new insights into the significance of pre–Variscan ('sardic') tectonics. Geological Magazine, 147, 674-689.

Casas, J.M., Fernández, O., 2007. On the Upper Ordovician unconformity in the Pyrenees: New evidence from the La Cerdanya area. Geologica Acta, 5(2), 193-198.

Casas, J.M., Fernández, O., 2008. Late Ordovician extensional tectonics in the Eastern Pyreenes. Geo-Temas, 10, 213.

Casas, J.M., Murphy, B., 2018. Unfolding the arc: The use of pre-orogenic constraints to assess the evolution of the Variscan belt in Western Europe. Tectonophysics, 736, 47-61.

Casas, J.M., Palacios, T., 2012. First biostratigraphical constraints on the pre–Upper Ordovician sequences of the Pyrenees based on organic-walled microfossils. Comptes Rendus Géoscience, 344, 50-56.

Casas, J.M., Castiñeiras, P., Navidad,, M., Liesa M., Carreras, J., 2010. New insights into the Late Ordovician magmatism in the Eastern Pyrenees: U–Pb SHRIMP zircon data from the Canigó massif. Gondwana Research, 17, 317-324.

Casas, J.M., Queralt, P., Mencos, J., Gratacós, O., 2012. Distribution of linear mesostructures in oblique folded surfaces: unravelling superposed Ordovician and Variscan folds in the Pyrenees. Journal of Structural Geology, 44, 141-150. DOI: https://doi.org/10.1016/j.jsg.2012.08.013

Casas, J.M., Navidad, M., Castiñeiras, P., Liesa, M., Aguilar, C., Carreras, J., Hofmann, M., Gärtner, A., Linnemann, U., 2015. The Late Neoproterozoic magmatism in the Ediacaran series of the Eastern Pyrenees: new ages and isotope geochemistry. International Journal of Earth Sciences, 104, 909-925. DOI: https://doi.org/10.1007/S00531-014-1127-1

Casas, J.M., Murphy, J.B., Díez-Montes, A., Sánchez-García, T., de Poulpiquet, J., Álvaro, J.J., Guimerà, J., 2023. Does the Ollo de Sapo magmatic event support Furongian-Tremadocian mantle plume activity fringing NW Gondwana? International Geology Review, 66, 1956-1970. DOI: https://doi.org/10.1080/00206814.2023.2263787

Casas, J.M., Sánchez-García, T., Díez-Montes, A., Clariana, P., Margalef, A., Valverde-Vaquero, P., Beranoaguirre, A., Román-Alpiste, M.J, Pujol-Solà, N., Álvaro, J.J., 2024. Extent and significance of the Upper Ordovician felsic volcanism in the Pyrenees and Mouthoumet massifs, SW Europe. In: Nance, R.D., Strachan, R.A., Quesada, C., Lin, S. (eds.). Supercontinents, Orogenesis and Magmatism. London, The Geological Society, 542 (Special Publications), 433-463. DOI: https://doi.org/10.1144/SP542-2022-358

Castiñeiras, P., Navidad, M., Liesa, M., Carreras, J., Casas, J.M., 2008a. U-Pb zircon ages (SHRIMP) for Cadomian and Lower Ordovician magmatism in the Eastern Pyrenees: new insights in the pre-Variscan evolution of the northern Gondwana margin. Tectonophysics, 461, 228-239.

Castiñeiras, P., Villaseca, C., Barbero, L., Martín-Romera, C., 2008b. SHRIMP U–Pb zircon dating of anatexis in high-grade migmatite complexes of Central Spain: implications in the Hercynian evolution of Central Iberia. International Journal of Earth Sciences, 97, 35-50. DOI: 10.1007/s00531-006-0167-6

Castro, A., Patiño Douce, A.E., Corretgé, L.G., De La Rosa, J.D., El-Biad, M., El-Hmidi, H., 1999. Origin of peraluminous granites and granodiorites, Iberian Massif, Spain: an experimental test of granite petrogenesis. Contributions to Mineralogy and Petrology, 135, 225-276.

Castro, A., García-Casco, A., Fernández, C., Corretgé, L.G., Moreno-Ventas, I., Gerya, T., Löw, I., 2009. Ordovician ferrosilicic magmas: experimental evidence for ultrahigh temperaturas affecting a metagreywacke source. Gondwana Research, 16, 622-632.

Cavet, P. 1957. Le Paléozoïque de la zone axiale des Pyrénées orientales françaises entre le Roussillon et l'Andorre. Bulletin du Service de la Carte géologique de France, 55, 303-518.

Chappell, B.W., White, J.R., 2001. Two contrasting granite types: 25 years later. Australian Journal of Earth Sciences, 48, 489-499.

Chelle-Michou, C., Laurent, O., Moyen, J.F., Block, S., Paquette, J.L., Couziné, S., Gardien, V., Vanderhaeghe, O., Villaros, A., Zeh, A., 2017. Pre–Cadomian to late–Variscan odyssey of the eastern Massif Central, France: Formation of the West European crust in a nutshell. Gondwana Research, 46, 170-190.

Chiaradia, M., 2015. Crustal thickness control on Sr/Y signatures of recent arc magmas: an Earth scale perspective. Scientific Reports, 5, 8115. DOI: 10.1038/srep08115

Chichorro, M., 2006. Estrutura do Sudoeste da Zona de Ossa-Morena: Área de Santiago de Escoural — Cabrela (Zona de Cisalhamento de Montemor-o-Novo, Maciço de Évora). PhD. Thesis. Portugal, Universidade de Évora, 502pp.

Chichorro, M., Pereira, M.F., Díaz-Azpiroz, M., Williams, I.S., Fernández, C., Pin, Ch., Silva, J.B., 2008. Cambrian ensialic rift-related magmatism in the Ossa-Morena Zone (E´vora–Aracena metamorphic belt, SW Iberian Massif): Sm–Nd isotopes and SHRIMP zircon U–Th–Pb geochronology. Tectonophysics, 461, 91-113.

Chichorro, M., Solá, A.R., Bento dos Santos, T., Amaral, J.L., Crispim, L., 2022. Cadomian/Pan-African consolidation of the Iberian Massif assessed by its detrital and inherited zircon populations: is the c. 610 Ma age peak a persistent Cadomian magmatic inheritance or the key to unravel its Pan-African basement? Geologica Acta, 20.15, 1-29. DOI: https://doi.org/10.1344/GeologicaActa2022.20.15

Clariana, P., Valverde-Vaquero, P., Rubio-Ordóñez, A., Beranoaguirre, A., García-Sansegundo, J., 2018. Pre-Variscan tectonic events and Late Ordovician magmatism in the Central Pyrenees: U–Pb age and Hf in zircon isotopic signature from subvolcanic sills in the Pallaresa massif. Journal of Iberian Geology, 44, 589-601.

Cocco, F., Funedda, A., 2012. The Variscan basement of the Riu Ollastu area (Sarrabus, SE Sardinia, Italy). Geology of France and Surrounding Areas, 1, 89-91.

Cocco, F, Funedda, A., 2019. The Sardic phase: field evidence of Ordovician tectonics in SE Sardinia, Italy. Geological Magazine, 156, 25-38. DOI: https://doi.org/10.1017/S0016756817000723

Cocco, F., Oggiano, G., Funedda, A., Loi, A., Casini, L., 2018. Stratigraphic, magmatic and structural features of Ordovician tectonics in Sardinia (Italy): a review. Journal of Iberian Geology, 44, 619-639. DOI: https://doi.org/10.1007/s41513-018-0075-1

Cocco, F., Loi, A., Funedda, A., Casini, L., Ghienne, J.F., Pillola, G.L., Vidal, M., Meloni, M.A., Oggiano, G., 2022. Ordovician tectonics of the South European Variscan Realm: new insights from Sardinia. International Journal of Earth Sciences, 112, 321-344. DOI: https://doi.org/10.1007/s00531-022-02250-w

Cocherie, A., Baudin, Th., Autran, A., Guerra, C., Fanning, C.M., Laumonier, B., 2005. U-Pb zircon (ID-TIMS and SHRIMP) evidence for the early Ordovician intrusion of metagranites in the late Proterozoic Canaveilles Group of the Pyrenees and the Montagne Noire (France). Bulletin de la Société géologique de France, 176, 269-282.

Condie, K.C., 2001. Mantle Plumes and Their Record in Earth History. Cambridge, Cambridge University Press, 306pp.

Condie, K.C., 2004. Supercontinents and superplume events: distinguishing signals in the geologic record. Physics of the Earth and Planetary Interiors, 146, 319-332.

Cordani, U.G., Nutman, A.P., Andrade, A.S., Santos, J.F., Azevedo, M.R., Mendes, M.H., Pinto, M.S., 2006. New U–Pb SHRIMP ages for pré-variscan orthogneisses from Portugal and their bearing on the evolution of the Ossa-Morena Tectonic Zone. Anais da Academia Brasileira de Ciências, 78, 133-149.

Cocks, L.R., Torsvik, T.H., 2021. Ordovician palaeogeography and climate change. Gondwana Research, 100, 53-72.

Courtillot, V., Olson, P., 2007. Mantle plumes link magnetic superchrons to Phanerozoic mass depletion events. Earth and Planetary Science Letters, 260, 495-504.

Couzinié, S., Bouilhol, P., Laurent, O., Grocolas, T., Montel, J.M., 2022. Cambro–Ordovician ferrosilicic magmatism along the northern Gondwana margin: constraints from the Cézarenque–Joyeuse gneiss complex (French Massif Central). Bulletin de la Société géologique de France, 193(15), 1-23.

Cruciani, G., Franceschelli., M., Musumeci, G., Spano, M.E., Tiepolo, M., 2012. Late Ordovician magmatism in the Monte Grighini Unit of the Nappe Zone, central-western Sardinia: insights from U–Pb zircon age. Geólogie de la France, 1, 94-95.

Cruciani, G., Franceschelli, M., Musumeci, G., Spano, M.E., Tiepolo, M., 2013. U–Pb zircon dating and nature of metavolcanics and metarkoses from the Monte Grighini Unit: new insights on Late Ordovician magmatism in the Variscan belt in Sardinia, Italy. International Journal of Earth Sciences, 102, 2077-2096.

Cruciani, G., Franceschelli, M., Puxeddu, M., Tiepolo, M., 2018. Metavolcanics from Capo Malfatano, SW Sardinia, Italy: New insight on the age and nature of Ordovician volcanism in the Variscan foreland zone. Geological Journal, 53, 1573-1585.

Dan, W., Murphy, J.B., Tang, G.J., Zhang, X.Z., White, W.M., Wang, Q., 2022, Cambrian–Ordovician magmatic flare-up in NE Gondwana: A silicic large igneous province? Geological Society of America Bulletin, 135, 1618-1632. DOI: https://doi.org/10.1130/B36331.1

Debon, F., Le Fort, P., 1983. A chemical-mineralogical classification of common plutonic rocks and associations. Transactions of the Royal Society of Edinburgh. Earth Sciences, 73, 135-149.

Delaperrière, E., Raspaut, J.P., 1995. Un âge ordovicien de l'orthogneis de La Preste par le méthode d'évaporation directed du plomb sur monozircon remet en question l'existence d'un socle précambrien dans le Massif du Canigou (Pyrénées Orientales, France). Paris, Comptes Rendus de l'Académie des Sciences, série 2, 320, 1179-1185.

Delaperrière, E., Soliva, J., 1992. Détermination d'un âge Ordovicien supérieur-Silurien des gneiss de Casemi (Massif du Caigou, Pyrénées Orientales) par la méthode d'évaporation du plomb sur monozircon. Paris, Comptes Rendus de l'Académie des Sciences, Série 2, 314, 345-350.

Deloule, E., Alexandrov, P., Cheilletz, A., Laumonier, B., Barbey, P., 2002. In-situ U–Pb zircon ages for Early Ordovician magmatism in the eastern Pyrenees, France: the Canigou orthogneisses. International Journal of Earth Sciences, 91, 398-405.

Den Brok, S.W.J., 1989. Evidence for pre–Variscan deformation in the Lys Caillaouas area, Central Pyrenees, France. Geologie en Mijnbouw, 68, 377-380.

Denèle, Y., Barbey, P., Deloule, E., Pelleter, E., Olivier, Ph., Gleizes, G., 2009. Middle Ordovician U-Pb age of the Aston and Hospitalet orthogneissic laccoliths: their role in the Variscan evolution of the Pyrenees. Bulletin de la Societé géologique de France, 180, 209-216.

DePaolo, D.J., 1981. Neodymiun isotopes in the Colorado Front Range and crust-mantle evolution in the Proterozoic. Nature, 291, 193-196. DOI: https://doi.org/10.1038/291193a0

DePaolo, D.J., Wasserburg, G.J., 1976. Nd isotopic variations and petrogenetic models. Geophysical Research Letters, 3, 249-252.

Díaz-Alvarado, J., Fernández, C., Chichorro, M., Castro, A., Pereira, M.F., 2016. Tracing the Cambro-Ordovician ferrosilicic to calc-alkaline magmatic association in Iberia by in situ U–Pb SHRIMP zircon geochronology (Gredos massif, Spanish Central System batholith). Tectonophysics, 681, 95-110.

Díez-Montes, A., Martínez Catalán, J.R.,Bellido Mulas, F., 2010. Role of the Ollo de Sapo massive felsic volcanism of NW Iberia in the Early Ordovician dynamics of northern Gondwana. Gondwana Research, 17, 363-376.

Dörr, W., Fiala J., Vejnar Z.Å., Zulauf G., 1998. U–Pb zircon ages and structural development of metagranitoids of the Teplá crystalline complex: evidence for pervasive Cambrian plutonism within the Bohemian massif (Czech Republic). Geologische Rundschau, 87, 135-149.

Dörr, W., Zulauf, G., Fiala, J., Franke, W., Vejnar, Z., 2002. Neoproterozoic to Early Cambrian history of an active plate margin in the Teplá–Barrandian—a correlation of U–Pb isotopic dilution-TIMS ages (Bohemia, Czech Republic). Tectonophysics, 352, 65-85.

El Korh, A., Schmidt, S.Th., Ballèvre, M., Ulianov, A., Bruguier, O., 2012. Discovery of an albite gneiss from the Ile de Groix (Armorican Massif, France): geochemistry and LA-ICP-MS U–Pb geochronology of its Ordovician protolith. International Journal of Earth Sciences, 101, 1169-1190. DOI: 10.1007/s00531-011-0732-5

Ernst, R.E., Buchan, K.L., 2003. Recognizing Mantle Plumes in the Geological Record. Annual Review of Earth and Planetary Sciences, 31, 469-523. DOI: 10.1146/annurev.earth.31.100901.145

Expósito, I., 2005. Evolución estructural de la mitad septentrional de la Zona de Ossa-Morena y su relación con el límite Zona de Ossa Morena/Zona Centroibèroica. Ediciós do Castro. Laboratorio Xeolóxico de Laxe. Area de Xeología e Minería do Seminario do Estudios Galegos. Serie Nova Terra, 27, 286pp.

Faure, M., Li, X.H., Lin, W., 2017. The northwest-directed "Bretonian phase" in the French Variscan Belt (Massif Central and Massif Armoricain): A consequence of the Early Carboniferous Gondwana–Laurussia collision. Comptes Rendus Geoscience, 349, 126-136.

Fontboté, J.M. 1949. Nuevos datos geológicos sobre la cuenca allta del Ter. Anales del Instituto de Estudios Gerundenses, 4, 1-57.

Fontboté, J.M., Guitard, G., 1958. Aperçus sur la tectonique cassante de la zone axiale dels Pyrénées orinentales entre les bassins de la Cerdagne et de l'Ampurdan-Roussillon. Bulletin de la Societé géologique de France, 8, 884-890.

Fonteilles, M., Guitard, G., 1972. Nappe de socle et socle authoctone dans les Pyrésnées, lorts de l'orogenèse hercynienne. Paris , Comptes Rendus de l'Académie des Sciences, série D, 274, 3504-3507.

Fonteilles, M., Guitard, G., 1977. Influence des noyaux de socle precambrien sur le mémorphisme et la structure profonde de l'orogen hercynien des Pyrénées orientales. Comparison avec les régions voisines. La chaÎne varisque d'Europe Moyenne et occidentale. Rennes, Colloque International of the Cente National Récherche Scientifique (CNRS), 243, 81-87.

Fonteilles, M., Guitard, G., 1988. Precambrian basement in the Variscan belt of the Pyrenees. In: Zoubek, V. (ed.). Precambrian in Younger Fold Belts. London, Wiley, 553-573.

Friedl, G., Finger, F., Paquette, J.-L., von Quadt, A., McNaughton, N.J., Fletcher, I.R., 2004. Pre-Variscan geological events in the Austrian part of the Bohemian Massif deduced from U–Pb zircon ages. International Journal of Earth Sciences, 93, 802-823.

Frost, B.R., Frost, C.D., 2008. A geochemical classification for feldspathic igneous Rocks. Journal of, Petrology, 49, 1955-1969.

Frost, B.R., Barnes, C.G., Collins, W.J., Arculus, R.J., Ellis, D.J., Frost, C.D., 2001. A geochemical classification for granitic rocks. Journal of Petrology, 42, 2033-2048.

Gámez, J.A., de Gibert, J.M., Casas, J.M., 2012. First ichnological data from the pre-Upper Ordovician rocks of the Pyrenees. Geo-Temas, 13.

Garbarino, C., Naitzla, S., Rizzo, R., Tocco, S., Barca, S., Farci, A., Serri, R., 2005. New evidence of pre-Hercynian volcanics from Southern Sulcis (Southwestern Sardinia). Bolletino della Società Geologica Italiana, 124, 69-85.

García-Arias, M., Díez-Montes, A., Villaseca, C., Blanco-Quintero, I.F., 2018. The Cambro-Ordovician Ollo de Sapo magmatism in the Iberian Massif and its Variscan evolution: A review. Earth-Science Reviews, 176, 345-372.

García-Arias, M., Morales Cámera, M., Dahlquist, J.A., Gao, P., Couzinié, S., Díez-Montes, A., 2024. The tectonic significance of peri-Gondwanan Late Neoproterozoic-Early Paleozoic felsic peraluminous magmatism. Earth-Science Reviews, 104803. DOI: https://doi.org/10.1016/j.earscirev.2024.104803

García-Sansegundo, J., Alonso, J.L., 1989. Stratigraphy and structure of the southeastern Garona Dome. Geodininamica Acta, 3, 127-134.

García-Sansegundo, J., Gavaldà, J., Alonso, J.L., 2004. Preuves de la discordance de l'Ordovicien supérieur dans la zone axiale des Pyrénées: exemple de dôme de la Garonne (Espagne, France). Comptes Rendus Géoscience, 336, 1035-1040.

Giacomini, F., Bomparola, R.M., Ghezzo, C., 2005. Petrology and geochronology of metabasites with eclogite facies relics from NE Sardinia: constraints for the Palaeozoic evolution of Southern Europe. Lithos, 82, 221–248.

Giacomini, F., Bomparola, R.M., Ghezzo, C., Gulbransen, H., 2006. The geodynamic evolution of the Southern European

Variscides: constraints from the U/Pb geochronology and geochemistry of the lower Palaeozoic magmatic-sedimentary sequences of Sardinia (Italy). Contributions to Mineralogy and Petrology, 152, 19-42.

Gil-Peña, I., Barnolas, A., Villas, E., Sanz-López, J., 2004. El Ordovícico Superior de la Zona Axial. In: Vera, J.A. (ed.). Geología de España. Madrid, Sociedad Geológica de España-Instituto Geológco y Minero de España (SGE-IGME), 247-249.

González-Esvertit, E., Molins-Vigatà, J., Canals, A., Casas, J.M., 2023. The geology of the Gréixer area (La Cerdanya, Eastern Pyrenees): Sardic, Variscan, and Alpine imprints. Trabajos de Geología, 37, 81-95.

Guitard, G., 1953. La structure du massif du Canigou. Bulletin de la Societé géologique de France, 3, 907-924.

Guitard, G., 1955. Sur l'évolution des gneiss des Pyrénées. Bulletin de la Societé géologique de France, 5, 441-469.

Guitard, G., 1958. Gneiss acides d'origine rhyolitique dans le massif du Canigou (Pyrénées-Orientales). Comptes Rendus sommaires de la Société géologique de France, 23-27.

Guitard, G., 1963a. Sur la présence de feldspaths à structure "rapakivi" et à inclusions en zone dans les gneiss oeillés du massif de Canigou-Carança (Pyrénées orientales). Comptes Rendus sommaires de la Société géologique de France, 82-83.

Guitard, G., 1963b. Sur l'importance des orthogneiss dérivant du métamorphisme d'anciens granites parmi les gneiss oeillés du Canigou (Pyrénées orientales). Comptes Rendus sommaires de la Société géologique de France, 130-132.

Guitard, G., 1967. Phases de plissement dans les terrains métamorphiques de la zone axiale pyrénéenne du Canigou, durant l'orogenèse hercynienne. Paris, Comptes Rendus de l'Académie des Sciences, série D, 256, 1357-1360.

Guitard, G., 1970. Le métamorphisme hercynien mésozonal et les gneiss oeillés du massif du Canigou (Pyrénées-Orientales). Mémoire Bureau Recherches Géologiques et Minières, 63, 353pp.

Guitard, G., 1976. Quelques aspects des relations entre tectonique et métamorphisme. Bulletin du Bulletin des Récherches Géologiques et Minières (BRGM) (deuxième série) Section, I(4), 321-340.

Guitard, G., Geyssant, J., Laumonier, B., Autran, A., Fonteilles, M., Dalmayrach, B., Vidal, J.C., Bandet, Y., 1992. Carte géologique de la France à 1:50.000 Prades (1095). Orléans, Service Géologique National, Bulletin des Récherches Géologiques et Minières (BRGM), 198pp.

Guitard, G., Autran, A, Fonteilles, M., 1996. Le substratum précambrien du Paléozoïque. In: Barnolas A., Chiron J.C. (eds.) Synthèse géologique et géophysique des Pyrénées. Bulletin des Récherches Géologiques et Minières-Instituto Tecnológico y Geominero de España (BRGM-ITGE), Cycle Hercynien, 1, 137-155.

Guitard, G., Laumonier, B., Autran, A., Bandet, Y., Berger, G.M., 1998. Notice explicative, Carte géologique de France. France (1/50 000), feuille Prades (1095). Orléans, Service Géologique National, Bulletin des Récherches Géologiques et Minières (BRGM), 198pp.

Gutiérrez-Alonso, G., Fernández-Suárez, J., Weil, A.B., Murphy, J.B., Nance, R.D., Corfu, F., Johnston, S.T., 2008. Self-subduction of the Pangaean global plate. Nature Geoscience, 1, 549-553. DOI: http://dx.doi.org/10.1038/ngeo250

Hart, N.R., Stockli, D.F., Hayman, N.W., 2016. Provenance evolution during progressive rifting and hyperextension using bedrock and detrital zircon U–Pb geochronology, Mauléon Basin, western Pyrenees. Geosphere, 12, 1166-1186. DOI: https://doi.org/10.1130/GES01273.1

Hartevelt, J.J.A., 1970. Geology of the upper Segre and Valira valleys, Central Pyrenees, Andorra/Spain. Leidse Geologische Mededelingen, 45, 167-236.

Helbing, H., Tiepolo, M., 2005. Age determination of Ordovician magmatism in NE Sardinia and its bearing on Variscan basement evolution. London, Journal of the Geological Society, 162, 689-700.

Humphreys, E.R., Niu, Y., 2009. On the composition of ocean island basalts (OIB): The effects of lithospheric thickness variation and mantle metasomatism. Lithos, 112(1-2), 118-136. DOI: 10.1016/j.lithos.2009.04.038

Hupert, H.E., Sparks, R.S.J., 1988. The generation of granitic magmas by intrusion of basalt into continental crust. Journal of Petrology, 29, 599-624. DOI: doi.org/10.1093/petrology/29.3.599

Jaffrezo, M. (coord.), 1977. Pyrénées orientales Corbières. Masson, London, Guides géologiques régionaux, 191pp.

Jäger, E., Zwart, H.J., 1968. Rb-Sr age determinations of some gneiss and granites of the Aston-Hospitalet massif (Pyrenees). Geologie en Mijnbow, 47, 349-357.

Karimi, H., Topuz, G., Ratschbacher, L., Shen, C., Li, J., 2024. Geochemistry and geochronology of the Neyshabur meta-volcanic rocks, Binalood mountains, NE Iran: witnesses of Paleo-Tethys rifting and closure. International Journal of Earth Sciences, 113, 285-302. DOI: https://doi.org/10.1007/s00531-023-02371-w

Koptev, A., Cloetingh, S., 2024. Role of Large Igneous Provinces in continental break-up varying from "Shirker" to "Producer". Communications Earth & Environment, 5, 27. DOI: https://doi.org/10.1038/s43247-023-01191-9.

Kriegsman, L.M., Aerden, D.G.A.M., Bakker, R.J., den Brok, S.W.J., Schutjens, P.M.T.M., 1989. Variscan tectonometamorphic evolution of the eastern Lys-Caillaouas massif, Central Pyrenees – evidence for late orogenic extension prior to peak metamorphism. Geologie en Mijnbouw, 68, 323-333.

Kröner, A., Willner, A.P., 1998. Time of formation and peak of Variscan HP-HT metamorphism of quartz-feldspar rocks in the central Erzgebirge, Saxony, Germany. Contributions to Mineralogy and Petrology, 132, 1-20.

Laske, R., Bechstadt, T., Boni, M., 1994. The post-Sardic Ordovician series. In: Bechstadt, T., Boni, M. (eds.). Sedimentological, stratigraphical and ore deposits field guide of the autochtonous cambro-ordovician of southwestern Sardinia. Roma, Memorie Descrittive della Carta Geologica D'Italia, Servizio Geologico d'Italia, 48, 115-146.

Laumonier, B., Calvet, M., Wiazemsky, M., Barbey, P., Marignac, C., Lambert,J., Lenoble, J.L., 2015. Avec la collaboration de Autran, A., Cocherie, A., Baudin, T., Llac, F. Notice explicative, Carte géologique de France (1/50000), feuille Céret (1096). Orléans, Bulletin de la Societé Geólogique de France (BRGM), 164pp.

Le Bas, M.J., LeMaitre, R.W., Streckeisen, A., Zanettin, B., 1986. A chemical classification of volcanic rocks based on the total alkali silica diagram. Journal of Petrology, 27, 745-750.

Le Corre, C., Auvray, B., Ballèvre, M., Robardet, M., 1991. Le Massif Armoricain. Sciences Géologiques, Bulletin, 44, 31-103.

Lefebvre, V., Servais, T., François, L., Averbuch, O., 2010. Did a Katian large igneous province trigger the Late Ordovician glaciation? A hypothesis tested with a carbon cycle model. Palaeogeography, Palaeoclimatology, Palaeoecology, 296, 310-319.

Lefebvre, B., Álvaro, J.J., Casas, J.M., Ghienne, J.F., Herbosch, A., Loi, A., Monceret, E., Verniers, J., Vidal, M., Vizcaïno, D., Servais, T., 2023. The Ordovician of France and neighbouring areas of Belgium and Germany. In: Harper, D.A.T., Lefebvre, B., Percival, I.G., Servais, T. (eds.). A Global Synthesis of the Ordovician System: Part 1. London, The Geological Society, 532 (Special Publications), 375-408. DOI: https://doi.org/10.1144/SP532-2022-268

Leone, F., Hammann, W., Laske, R. Serpagli, E., Villas, E., 1991. Lithostratigraphic units and biostratigraphy of the post-sardic Ordovician sequence in south-west Sardinia. Bollettino della Società Paleontologica Italiana, 30, 201-235.

Leone, F., Ferretti, A., Hammann, W., Loi, A., Pillola, G.L., Serpagli, E., 2002. A general view of the post-Sardic Ordovician sequence from SW Sardinia. Rendicontti de la Società Paleontologica Italiana, 1, 51-68.

Liesa, M., 1988. El metamorfisme del vessant sud del Massís del Roc de Frausa (Pirineus Orientals). Doctoral Thesis. Barcelona, Universitat de Barcelona, unpublished, 233pp.

Liesa, M., Carreras, J., Castiñeiras, P., Casas, J.M., Navidad, M., Vilà, M., 2011. U–Pb zircon age of Ordovician magmatism in the Albera Massif (Eastern Pyrenees). Geologica Acta, 9(1), 93-101.

Linnemann, U., Gehmlich, M., Tichomirowa, M., Buschmann, B., Nasdala, L., Jonas, P., Lützner, H., Bombach, K., 2000. From Cadomian subduction to Early Palaeozoic rifting: the evolution of Saxo-Thuringia at the margin of Gondwana in the light of single zircon geochronology and basin development (Central European Variscides, Germany). In: Franke, W., Haak, V., Oncken, O., Tanner, D. (eds.). Orogenic Processes: Quantification and Modelling in the Variscan Belt. London, The Geological Society, 179 (Special Publications), 131-153.

Linnemann, U., Pereira, F.M., Jeffries, T.E., Drost, K., Gerdes, A., 2008. The Cadomian Orogeny and the opening of the Rheic Ocean: The diacrony of geotectonic processes constrained by LA-ICP-MS U-Pb zircon dating (Ossa-Morena and Saxo-Thuringian Zones, Iberian and Bohemian Massifs). Tectonophysics, 461, 21-43. DOI: 10.1016/j.tecto.2008.05.002

Llopis Lladó, N., 1965. Sur le Paléozoïque inférieur de l'Andorre. Bulletin de la Société géologique de France, 7, 652-659.

Loi, A., Dabard, M.P., 1997. Zircon typology and geochemistry in the palaeogeographic reconstruction of the Late Ordovician of Sardinia (Italy). Sedimentary Geology, 112, 263-279. DOI: https:// doi. org/ 10. 1016/S0037- 0738(97) 00038-9

Loi, A., Barca, S., Chauvel, J.J., Dabard, M.P., Leone, F., 1992. Analyse de la sédimentation post-phase sarde les dépôts initiaux à placers du SE de la Sardaigne. Paris, Comptes Rendus de la Société géologique de France, série 2, 315, 1357-1364.

López-Sánchez, M.A., Iriondo, A., Marcos, A., Martínez, F.J., 2015. A U–Pb zircon age (4795±Ma) from the uppermost layers of the Ollo de Sapo Formation near Viveiro (NW Spain): implications for the duration of rifting-related Cambro-Ordovician volcanism in Iberia. Geological Magazine, 152, 341-350. DOI: 10.1017/S0016756814000272

Lotout, C., Pitra, P., Poujol, M., Van Den Driessche, J., 2017. Ordovician magmatism in the Lévézou massif (French Massif Central): tectonic and geodynamic implications: International Journal of Earth Sciences, 106, 501-515. DOI: 10.1007/00531-016-1387-z

Ludwig, K.R., Turi, B., 1989. Paleozoic age of the Capo Spartivento Orthogneiss, Sardinia, Kitaly. Chemical Geology, 79, 147-153.

Maino, M., Gaggero, L., Langone, A., Seno, S., Fanning, M., 2019. Cambro-Silurian magmatisms at the northern Gondwana margin (Penninic basement of the Ligurian Alps). Geoscience Frontiers, 10(1), 315-330. DOI: https://doi.org/10.1016/j.gsf.2018.01.003

Margalef, A., Castiñeiras, P., Casas, J.M., Navidad, M., Liesa, M., Linnemann, U., Hofmann, M., Gärtner, A., 2016. Detrital zircons from the Ordovician rocks of the Pyrenees: Geochronological constraints and provenance. Tectonophysics, 681, 124-134.

Marini, F., 1988. "Phase" sarde et distension ordovicienne du domaine sud-varisque, effets de point chaud? Une hypothèse fondée sur les données nouvelles du volcanisme albigeois. Paris, Comptes Rendus de l'Académie des Sciences, série 2, 306, 443-450.

Martí, J., Muñoz, J.A., Vaquer, R., 1986. Les roches volcaniques de l'Ordovicien supérieur de la région de Ribes de Freser-Rocabruna (Pyrénées catalanes): caractères et signification. Paris, Comptes Rendus Académie des Sciences, 302, 1237-1242.

Martí, J., Solari, L., Casas, J.M., Chichorro, M., 2019. New geochronological data on the Upper Ordovician volcanism in the Eastern Pyrenees (NE Iberia): stratigraphic and geodynamic implications. Geological Magazine, 156, 1783-1792. DOI: https://doi.org/10.1017/S0016756819000116

Martí, J., Casas, J.M., Muñoz, J.A., 2024. Reconstructing a Super-Eruption From the Upper Ordovician Period in the Eastern Pyrenees, Spain. Lithosphere, 2, lithosphere_2024_100. DOI: https://doi.org/10.2113/2024/lithosphere_2024_100.

Martínez, F., Iriondo, A., Dietsch, C., Aleinikoff, J.N., Peucat, J.J., Cirès, J., Reche, J., Capdevila, R., 2011. U–Pb SHRIMP–RG

zircon ages and Nd signature of lower Paleozoic rifting-related magmatism in the Variscan basement of the Eastern Pyrenees. Lithos, 127, 10-23.

Martini, I.P., Tongiorgi, M., Oggiano, G., Cocozza, T., 1991. Ordovician alluvial fan to marine shelf transition in SW Sardinia, Western Mediterranean Sea: tectonically ("Sardic phase") influenced clastic sedimentation. Sedimentary Geology, 72, 97-115. DOI: https://doi.org/10.1016/0037-0738(91)90125-W

Maurel, O., Brunel, M., Monié, P., 2002. Exhumation cénozoïque des massifs du Canigou et de Mont-Louis (Pyrénées Orientales, France). Comptes Rendus Geoscience, 334, 941-948.

Matheson, E.J., Pufahl, P.K., Voinot, A., Murphy, J.B., Fitzgerald, D.M., 2022. The ironstone record of protracted Paleozoic ocean oxygenation and transient deep-ocean anoxia. Earth and Planetary Science Letters, 574, 117715. DOI: https://doi.org/10.1016/j.epsl.2022.117715

McLennan, S.M., Hemming, S., 1992. Samarium-neodymium elemental and isotopic systematic in sedimentary rocks. Geochimica et Cosmochimica Acta, 561, 2015-2050.

McLennan, S.M., Hemming, S., McDaniel, D.K., Hanson, G.N., 1993. Geochemical approaches to sedimentation, provenance, and tectonics. In: Johnsson, M.J., Basu. A. (eds.). Geological Society of America Special Papers. Geological Society of America, 21-40. DOI: https://doi.org/10.1130/SPE284-p21

Melleton, J., Cocherie, A., Faure, M., Rossi, P., 2010. Precambrian protoliths and Early Paleozoic magmatism in the French Massif Central: U–Pb data and the North Gondwana connection in the west European Variscan belt. Gondwana Research, 17, 13-25.

Mezger, J., Gerdes, A., 2016. Early Variscan (Visean) granites in the core of central Pyrenean gneiss domes: implications from laser ablation U–Pb and Th–Pb studies. Gondwana Research, 29, 181-198.

Mingram, B., Kröner, A., Hegner, E., Krentz, O., 2004, Zircon ages, geochemistry, and Nd isotopic systematics of pre–Variscan orthogneisses from the Erzgebirge, Saxony (Germany), and geodynamic interpretation. International Journal of Earth Sciences, 93, 706-727.

Montero, P., Bea, F., González-Lodeiro, F., Talavera, C., Whitehouse, M.J., 2007. Zircon ages of the metavolcanic rocks and metagranites of the Ollo de Sapo Domain in central Spain: implications for the Neoproterozoic to Early Palaeozoic evolution of Iberia. Geological Magazine, 144, 963-976.

Montero, P., Talavera, C., Bea, F., Lodeiro, F.G., Whitehouse, M.J., 2009. Zircon geochronology of the Ollo de Sapo Formation and the age of the Cambro–Ordovician rifting in Iberia. Journal of Geology, 117, 174-191.

Morre-Biot, N., Robert, J.F., 1976. Sur la découverte d'un complexe ignimbritique stéphanien dans la région de Ribes de Freser (Province de Gérone, Espagne). Paris, Comptes Rendus de l'Académie des Sciences, 282, 1933-1935.

Muñoz, J.A., 1985. Estructura alpina i herciniana a la vora sud de la zona axial del Pirineu oriental. PhD Thesis. Barcelona, University of Barcelona, 185pp.

Muñoz, J.A., 1992. Evolution of a continental collision belt: ECORS Pyrenees crustal balanced cross-section. In: McClay, K.R. (ed.). Thrust Tectonics. London, Chapman and Hall, 235-246.

Muñoz, J.A., Vergés, J., Martínez-Rius, A., Fleta, J., Cirés, J., Casas, J.M., Sàbat, F., 1994. Mapa geológico de España a escala 1:50.000, hoja de Ripoll (no. 256). Madrid, Intstituto Tecnológico y Geominero de España (ITGE).

Muñoz, J.A., 2019. Alpine orogeny: Deformation and structure in the northern Iberian margin (Pyrenees s.l.). In: Quesada, C., Oliveira, J. (eds.). The geology of Iberia: A geodynamic approach. Heidelberg, Springer, 3 (Chapter 9), Regional Geology Reviews series, 433-451.

Murphy, J.B., Nance R.D., 1989. A model for the evolution of the Avalonian-Cadomian belt. Geology, 17, 735-738. DOI: https://doi.org/10.1130/0091-7613(1989)017<0735:MFTEOT>2.3.CO;2

Murphy, J.B., Gutierrez-Alonso, G., Nance, R.D., Fernandez-Suarez, J., Keppie, J.D., Quesada, C., Strachan, R.A., Dostal, J., 2006. Origin of the Rheic Ocean: rifting along a Neoproterozoic suture? Geology, 34, 325-328.

Murphy, J.B., Nance, D.R., Cawood, P.A., Collins, W.J., Dan, W., Doucet, L.S., Heron, P.J., Li, Z.-X., Mitchell, R.N., Pisarevsky, S., Pufahl, P.K., Quesada, C., Spencer, C.J., Strachan, R.A., Wu, L., 2021. Pannotia: In defence of its existence and geodynamic significance. In: Murphy, J.B., Strachan, R.A., Quesada, C. (eds.). Pannotia to Pangaea: Neoproterozoic and Paleozoic orogenic cycles in the circum-Atlantic region. London, Geological society, 503 (Special Publications), 13-39. DOI: 10.1144/SP503-2020-96

Murphy, J.B., Nance, R.D., Johnston, S.T., Casas, J.M., Cawood, P.A., Matheson, E.J.,. Pufahl, P.K, Dan,, W., Álvaro J.J., Heron, Ph.J., Strachan, R.A., 2024. Speculations on the Paleozoic legacy of Gondwana amalgamation. Gondwana Research, 129, 107-131. DOI: https://doi.org/10.1016/j.gr.2023.12.002

Nance, R.D., Murphy, J.B., Keppie, J.D., 2002. A Cordilleran model for the evolution of Avalonia. Tectonophysics, 352, 11-32.

Nance, R.D., Gutiérrez-Alonso, G., Keppie, J.D., Linnemann, U., Murphy, J.B., Quesada, C., Strachan, R.A., Woodcock, N.H., 2010. Evolution of the Rheic Ocean. Gondwana Research, 17, 194-222.

Navidad, M., Castiñeiras, P., 2011. Early Ordovician magmatism in the northern Central Iberian Zone (Iberian Massif): new U-Pb (SHRIMP) ages and isotopic Sr-Nd data. In: Gutiérrez-Marco, C., Rábano, I., García-Bellido, D. (eds.). Ordovician of the World. Madrid, Instituto Geológico y Minero de España, Cuadernos del Museo Geominero, 14, 391-398. ISBN 978-84-7840-857-3

Navidad, M., Castiñeiras, P., Casas, J.M., Liesa, M., Fernández Suárez, J., Barnolas, A., Carreras, J., Gil-Peña, I., 2010. Geochemical characterization and isotopic age of Caradocian magmatism in the northeastern Iberian Peninsula: Insights into the Late Ordovician evolution of the northern Gondwana margin. Gondwana Research, 17, 325-337.

Navidad, M., Castiñeiras, P., Casas, J.M., Liesa, M., Belousova, E., Proenza, J., Aiglsperger, T., 2018. Ordovician magmatism in the Eastern Pyrenees: implications for the geodynamic evolution of northern Gondwana. Lithos, 314-315, 479-496.

Nesbitt, H.W., Young, G.M.,1982. Early Proterozoic climates and plate motions inferred from major element chemistry of lutites. Nature, 299, 715-717.

Nosenzo, F., Manzotti, P., Krona, M., Ballèvre, M., Poujol, M., 2024. Tectonic architecture of the northern Dora-Maira Massif (Western Alps, Italy): field and geochronological data. Swiss Journal of Geosciences, 117(6), 1-33. DOI: https://doi.org/10.1186/s00015-024-00459-2

Ochsner, A., 1993. U–Pb Geochronology of the Upper Proterozoic–Lower Paleozoic geodynamic evolution in the Ossa-Morena Zone (SW Ibéria): constraints on the timing of the cadomian orogeny. PhD. Thesis. Zurich, Geology, Swiss Federal Institute of Technology Zurich, Eidgenössische Technische Hochschule (ETH), 249pp.

Oggiano, G., Gaggero, L., Funedda, A., Buzzi, L., Tiepolo, M., 2010. Multiple early Paleozoic volcanic events at the northern Gondwana margin: U–Pb age evidence from the Southern Variscan branch (Sardinia, Italy). Gondwana Research, 17, 44-58.

Ordóñez, B., 1998. Geochronological studies of the Pre-Mesozoic basement of the Iberian Massif: The Ossa Morena Zone and the Allochthonous Complexes within the Central Iberian Zone. PhD. Thesis. Zurich, Geology, Swiss Federal Institute of Technology Zurich, Eidgenössische Technische Hochschule (ETH), 207pp.

Orejana, D., Villaseca, C., Merino Martínez, E., 2016. Age and geological setting of the basic Ordovician magmatism from the Spanish Central System. Geo-Temas, 16(1), 415-418.

Orejana, D., Villaseca, C., Merino Martínez, E., 2017. Basic Ordovician magmatism of the Spanish Central System: Constraints on the source and geodynamic setting. Lithos, 284-285, 608-624. DOI: http://dx.doi.org/10.1016/j.lithos.2017.05.012

Özbey, Z., Ustaömer, T., Robertson, A.H.F., Ustaömer, P.A., 2013. Tectonic significance of Late Ordovician granitic magmatism and clastic sedimentation on the northern margin of Gondwana (Tavşanlı Zone, NW Turkey). London, Journal of the Geological Society, 170, 159-173.

Padel, M., Álvaro, J.J., Clausen, S., Guillot, F., Poujol, M., Chichorro, M., Monceret, E.., Pereira, M.F., Vizcaïno, D., 2017. U–Pb laser ablation ICPMS zircon dating across the Ediacaran–Cambrian transition of the Montagne Noire, southern France. Comptes Rendus Geosciences, 349, 380-390. DOI: https://doi.org/10.1016/j.crte.2016.11.002

Padel, M., Clausen, S., Álvaro, J.J., Casas, J.M., 2018a. Review of the Ediacaran–Lower Ordovician (pre-Sardic) stratigraphic framework of the Eastern Pyrenees, southwestern Europe. Geologica Acta, 16(4), 339-355. DOI: https://doi.org/10.1344/GeologicaActa201 8.16.4.1

Padel, M., Álvaro, J.J., Casas, J.M., Clausen, S., Poujol, M., Sánchez-García, T., 2018b. Cadomian volcanosedimentary complexes across the Ediacaran–Cambrian transition of the Eastern Pyrenees, southwestern Europe. International Journal of Earth Sciences, 107, 1579-1601. DOI: https://doi.org/10.1007/S00531-017-1559-5

Padel, M., Clausen, S., Guillot, F., Poujol, M., Álvaro, J.J., 2022. Shifts in the Ediacaran to Lower Ordovician sedimentary zircon provenances of Northwest Gondwana: the Pyrenean files. Geologica Acta, 20.14, 1-18. DOI: https://doi.org/10.1344/GeologicaActa2022.20.14

Palmeri, R., Fanning, M., Franceschelli, M., Memmi, I., Ricci, C.A., 2004. SHRIMP dating of zircons in eclogite from the Variscan basement in northeastern Sardinia (Italy). Monatshefte, Neues Jahrbuch für Mineralogie, 6, 275-288.

Pasci, S., Pertusati, P.C., Salvadori, I., Murtas, A., 2008. I rilevamenti CARG del Foglio geologico 555 'Iglesias'e le nuove implicazioni strutturali sulla tettonica della 'Fase Sarda.' Rendiconti Online Della Società Geologica Italiana Abstracts, 3, 614-615.

Pavanetto, P., Funedda, A., Northrup, C.J., Schmitz, M., Crowley, J., Loi, A., 2012. Structure and U–Pb zircon geochronology in the Variscan foreland of SW Sardinia, Italy. Geological Journal, 47, 426-445.

Pavlov, V., Gallet, Y., 2005. A third superchron during the Early Paleozoic. Episodes, 28, 1-7.

Pearce, J.A., 2014. Immobile element fingerprinting of ophiolites. Elements, 10(2), 101-108. DOI: https://doi.org/10.2113/gselements.10.2.101

Pearce, J.A., Harris, B.W., Tindle, A.G., 1984. Trace element discrimination diagrams for the tectonic interpretation of granitic rocks. Journal of Petrology, 25, 956-983.

Pereira, M.F., Chichorro, M., Linnemann, U., Eguiluz, L., Silva, J.B., 2006. Inherited arc signature in Ediacaran and Early Cambrian basins of the Ossa-Morena Zone (Iberian Massif, Portugal): paleogeographic link with European and North African Cadomian correlatives. Precambrian Reserach, 144, 297-315.

Pereira, M.F., Chichorro, M., Solá, A.R., Silva, J.B., Sánchez-García, T., Bellido, F., 2011. Tracing the Cadomian magmatism with detrital/inherited zircon ages by in-situ U–Pb SHRIMP geochronology (Ossa-Morena Zone, SW Iberian Massif). Lithos, 123, 204-217.

Pereira, M.F., Solá, A.R., Chichorro, M., Lopes, L., Geres, A., Silva, J.B., 2012. North-Gondwana assembly, break-up and paleogeography: U–Pb isotope evidence from detrital and igneous zircons of Ediacaran and Cambrian rocks of SW Iberia. Gondwana Research, 22, 866-881.

Pereira, M.F., Fernández, C., Rodríguez, C., Castro, A., 2022. Ordovician tectonics and crustal evolution at the Gondwana margin (Central Iberian Zone). Journal of the Geological Society, 179, jgs2021-168. DOI: https://doi.org/10.1144/jgs2021-168

Pereira, S., Colmenar, J., Silvério, G., 2024. Discovery of the first Ordovician trilobite from Andorra. Geo-Temas, 20, 916.

Pillola, G.L., Leone, F., Loi, A., 1998. The Cambrian and Early Ordovician of SW Sardinia. Giornale di Geologia, 60, 25-38.

Pin, C., Marini, F., 1993. Early Ordovician continental break-up in Variscan Europe: Nd-Sr isotope and trace element evidence from bimodal igneous associations of the Southern Massif Central, France. Lithos, 29, 177-196.

Pitra, P., Poujol, M., Den Driessche, J.V., Poilvet, J.C., Paquette, J.L., 2012. Early Permian extensional shearing of an Ordovician granite: The Saint-Eutrope "C/S-like" orthogneiss (Montagne Noire, French Massif Central). Comptes Rendus Geoscience, 344, 377-384.

Pouclet, A., Aarab, A., Fekkak, A., Benharref, M., 2007. Geodynamic evolution of the north-western Paleo-Gondwanan margin in the Moroccan Atlas at the Precambrian-Cambrian boundary. In: Linnemann, U., Nance, R.D., Kraft, P., Zulauf, G. (eds.). The Evolution of the Rheic Ocean: From Avalonian-Cadomian Active Margin to Alleghanian-Variscan Collision. Geological Society of America, 423 (Special Papers), 27-60.

Pouclet, A., Álvaro, J.J., Bardintzeff, J.M., Gil Imaz, A., Monceret, E,, Vizcaïno, D., 2017. Cambrian–Early Ordovician volcanism across the South Armorican and Occitan Domains of the Variscan Belt in France: Continental break-up and rifting of the northern Gondwana margin. Geoscience Frontiers, 8, 25-64.

Puddu, C., Casas, J.M., 2011. New insights into the stratigraphy and structure of the Upper Ordovician rocks of the la Cerdanya area (Pyrenees). In: Gutiérrez-Marco, J.C., Rábano, I., García-Bellido, D. (eds.). Ordovician of the World. Cuadernos del Museo Geominero, 14, 441-445.

Puddu, C., Álvaro, J.J., Casas J.M., 2018. The Sardic unconformity and the Upper Ordovician successions of the Ribes de Freser area, Eastern Pyrenees. Journal of Iberian Geology, 44, 603-617. DOI: https://doi.org/10.1007/s41513-018-0084-0

Puddu, C., Álvaro, J.J., Carrera, N., Casas, J.M., 2019. Deciphering the Sardic (Ordovician) and Variscan deformations in the Eastern Pyrenees. London, Journal of the Geological Society, 176, 1191-1206.

Pufahl, P.K., Squires, A.D., Murphy, J.B., Quesada, C., Lokier, S.W., Álvaro, J.J., Hatch, J., 2020. Ordovician ironstone of the Iberian margin: Coastal upwelling, ocean anoxia and Palaeozoic biodiversity. The Depositional Record, 6, 581-604.

Pujol-Solà, N., Casas, J.M,, Proenza, J.A., Blanco-Quintero, I.F., Druguet, E., Liesa, M., Román-Alpiste, M.J., Álvaro, J.J., 2022. Cadomian metabasites of the Eastern Pyrenees revisited. Geologica Acta, 20.17, 1-26. DOI: 10.1344/GeologicaActa2022.20.17

Putis, M., Sergeev, S., Ondrejka, M., Larionov, A., Siman, P., Spišiak, J., Uher, P., Paderin, I., 2008 Cambrian-Ordovician metaigneous rocks associated with Cadomian fragments in the West-Carpathian basement dated by SHRIMP on zircons: a record from the Gondwana active margin setting. Geologica Carpathica, 59, 3-18.

Qing, H., Barnes, C.R., Buhl, D., Veizer, J., 1998. The strontium isotopic composition of Ordovician and Silurian brachiopods and conodonts: relationships to geological events and implications for coeval seawater. Geochimica et Cosmochimica Acta, 62, 1721-1733.

Quesada, C., 1991. Geological constraints on the Paleozoic tectonic evolution of tectonostratigraphic terranes in the Iberian Massif. Tectonophysics, 185, 225-245.

Quesada, C., 2006. The Ossa Morena Zone of the Iberian Massif: a tectonostratigraphic approach to its evolution. Zeitschrift der Deutschen Gesellschaft für Geowissenschaften, 157, 585-595.

Robardet, M., 2002. Alternative approach to the Variscan Belt in southwestern Europe: Preorogenic paleobiogeographical constraints. In: Martínez Catalán, J.R., Hatcher, R.D., Arenas, R., Díaz García, F, (eds.). Variscan-Appalachian dynamics: The building of the late Paleozoic basement. Boulder (Colorado), Geological Society of America, 364 (Special paper), 1-15.

Robardet, M., Gutiérrez-Marco, J.C., 2004. The Ordovician, Silurian and Devonian sedimentary rocks of the Ossa-Morena Zone (SW Iberian Peninsula, Spain). Journal of Iberian Geology, 30, 73-92.

Robert, J.F., 1980. Étude géologique et métallogénique du val de Ribas sur le versant espagnol des Pyrénées catalanes. PhD. Thesis. Université Franche-Comté, 294pp.

Robert, J.F., Thiebaut, J., 1976. Découverte d'un volcanisme acide dans le Caradoc de la région de Ribes de Feser (Prov. de Gerone). Paris, Comptes Rendus Académie Sciences, 282, 2050-2079.

Rodríguez, C., Castro, A., Gómez-Frutos, D., Gutiérrez-Alonso, G., Pereira, F.M., Fernández, C., 2022. The unique Cambro-Ordovician silicic large igneous province of NW Gondwana: Catastrophic melting of a thinned crust. Gondwana Research, 106, 164-173. DOI: 10.1016/j.gr.2022.01.011

Rodriguez-Corcho, A.F., actions-user, 2021. andresrcorcho/CGD_HistogramsApp: HistogramsApp_1.3 (Version 1.3): Zenodo. Last accessed: July 2025. Website: https://zenodo.org/records/4593488 DOI: https://doi.org/10.5281/zenodo.4593488

Rodriguez-Corcho, A.F., Rojas-Agramonte, Y., Barrera-Gonzalez, J.A., Marroquin-Gomez, M.P., Bonilla-Correa, S., Izquierdo-Camacho, D., Delgado-Balaguera, S.M., Cartwright-Buitrago, D., Muñoz-Granados, M.D., Carantón-Mateus, W.G., Corrales-García, A., Laverde-Martinez, A.F., Cuervo-Gómez, A., Rodriguez-Ruiz, M.A., Marin-Jaramillo, J.P., Salazar-Cuellar, N., Esquivel-Arenales, L.C., Daroca, M.E., Carvajal, A.S., Perea-Pescadora, A.M., Solano-Acosta, J.D., Diaz, S., Guillen, A., Bayona, G., Cardona-Molina, A., Eglington, B., Montes, C., 2020. The Colombian geochronological database (CGD). International Geology Review, 64(12), 1635-1669. DOI: https://doi.org/10.1080/00206814.2021.1954556

Roger, F., Respaut, J.P., Brunel, M., Matte, P., Paquette, J.L., 2004. Première datation U–Pb des orthogneiss oeillés de la zone axiale de la Montagne Noire (Sud du Massif central): nouveaux témoins du magmatisme ordovicien dans la chaîne Varisque. Comptes Rendus Geoscience, 336, 19-28. DOI: https://doi.org/10.1016/j.crte.2003.10.014

Rojo-Pérez, E., Druguet, E., Casas, J.M., Proenza, J.A, Fuenlabrada, J.M., Sánchez Martínez, S., García-Casco, A.,

Arenas, R., 2023. Geochemistry of metasedimentary rocks from the Eastern Pyrenees (Iberian Peninsula): Implications for correlation of Ediacaran terranes along the Gondwanan margin. Precambrian Research, 397, 107186. DOI: https://doi.org/10.1016/j.precamres.2023.107186

Romeo, I., Lunar, R., Capote, R., Quesada, C., Piña, R., Dunning, G.R., Ortega, L., 2006. U/Pb age constraints on Variscan magmatism and Ni–Cu-PGE metallogeny in the Ossa–Morena Zone (SW Iberia). Journal Geological Society, 163, 837-846.

Rubio-Ordóñez, A., Valverde-Vaquero, P., Corretge, L.G., Cuesta, A., Gallastegui, G., Fernández-González, M., Gerdes, A., 2012. An Early Ordovician tonalitic-granodioritic belt along the Schistose-Greywacke Domain of the Central Iberian Zone (Iberian Massif, Variscan Belt). Geological Magazine, 149, 927-939.

Rudnick, R.L., Gao, S., 2014. Composition of the Continental Crust. In: Holland, H.D., Turekian, K.K. (eds.). Treatise on Geochemistry. Elsevier, Second Edition, 1-51. ISBN: 9780080983004 DOI: https://doi.org/10.1016/B978-0-08-095975-7.00301-6

Sánchez-García, T., Bellindo, F., Quesada, C., 2003. Geodynamic setting and geochemical signatures of Cambrian–Ordovician rift-related igneous rocks (Ossa-Morena Zone, SW Iberia). Tectonophysics, 365, 233-255.

Sánchez-García, T., Quesada, C., Bellido, F., Dunning, G., González de Tanago, J., 2008. Two-step magma flooding of the upper crust during rifting: the Early Paleozoic of the Ossa-Morena zone (SW Iberia). Tectonophysics, 461, 72-90.

Sánchez-García, T., Bellido, F., Pereira, M.F., Chichorro, M., Quesada, C., Pin, Ch., Silva, J.B., 2010. Rift-related volcanism predating the birth of the Rheic Ocean (Ossa-Morena zone, SW Iberia). Gondwana Research, 17, 392-407.

Sánchez-García, T., Pereira, M.F., Bellido, F., Chichorro, M., Silva, J.B., Valverde-Vaquero, P., Pin, Ch., Solá, A.R., 2014. Early Cambrian granitoids of North Gondwana margin in the transition from a convergent setting to intra-continental rifting (Ossa-Morena Zone, SW Iberia). International Journal of Earth Sciences (Geologische Rundschau), 103, 1203-1218. DOI: 10.1007/s00531-013-0939-8

Sánchez-García, T., Chichorro, M., Solá, R., Álvaro, J.J., Díez-Montes, A., Bellido, F., Ribeiro, M.L., Quesada, C., Lopes, J.C., Silva, I.F.D., Clavijo, E.G., Barreiro, J.G., López-Carmona, A., 2019. The Cambrian–Early Ordovician Rift Stage in the Gondwanan Units of the Iberian Massif. In: Quesada, C., Oliveira, J.T. (eds.). The Geology of Iberia: A Geodynamic Approach. Heidelberg, Regional Geology Reviews, Springer, 2, 27-74.

Santanach, P.F., 1972a. Sobre una discordancia en el Paleozoico inferior de los Pirineos orientales. Acta Geológica Hispánica, 7(5), 129-132.

Santanach, P.F., 1972b. Estudio tectónico del Paleozoico inferior del Pirineo entre la Cerdaña y el río Ter. Acta Geológica Hispánica, 7(2), 44-49.

Sánz-López, J., Sarmiento, G.N., 1995. Asociaciones de conodontos del Ashgill y Llandovery en horizontes carbonatados del Valle del Freser (Girona). Tremp, XI Jornadas de Paleontología, 157-160.

Sarmiento, G.N., Gutiérrez-Marco, J.C., Rodríguez-Cañero, R., Algarra, A.M., Navas-Parejo, P., 2011. A brief summary of Ordovician conodont faunas from the Iberian Peninsula. In: Gutiérrez-Marco, J.C., Rábano, I., García-Bellido, D. (eds.). Ordovician of the World. Madrid, Instituto Geológico y Minero de España, Cuadernos del Museo Geominero, 14, 505-514.

Sarrionandia, F., Carracedo Sánchez, M. Eguiluz, L., Ábalos, B., Rodríguez, J., Pin, C., Gil Ibarguchi, J.I., 2012. Cambrian rift-related magmatism in the Ossa-Morena Zone (Iberian Massif): Geochemical and geophysical evidence of Gondwana break-up. Tectonophysics, 570-571, 135-150.

Saunders, A.D., Jones, S.M., Morgan, L.A., Pierce, K.L., Widdowson, M., Xu, Y.G., 2007. Regional uplift associated with continental large igneous provinces: The roles of mantle plumes and the lithosphere. Chemical Geology, 241, 282-318.

Schaltegger, U., Schmitt, A.K., Horstwood, M.S.A., 2015. U–Th–Pb zircon geochronology by ID-TIMS, SIMS, and laser ablation ICP-MS: Recipes, interpretations, and opportunities. Chemical Geology, 402, 89-110. DOI: https://doi.org/10.1016/j.chemgeo.2015.02.028

Scheiber, T., Berndt, J., Heredia, B.D., Mezger, K., Pfiffner, O.A., 2013. Episodic and long lasting Paleozoic felsic magmatism in the pre-Alpine basement of the Suretta nappe (eastern Swiss Alps). International Journal of Earth Sciences (Geologische Rundschau), 102, 2097-2115.

Schulz, B., Bombach, K., Pawlig, S., Brätz, H., 2004. Neoproterozoic to Early-Palaeozoic magmatic evolution in the Gondwana-derived Austroalpine basement to the south of the Tauern Window (Eastern Alps). International Journal of Earth Sciences (Geologische Rundschau), 93, 824-843.

Sebastián, A., Martínez, F.J., Gil Ibarguchi, J.I., 1982. Petrología y geoquímica de los gneises de Queralbs-Núria (Provincia de Gerona). Boletín Geológico y Minero, 93(6), 508-523.

Shervais, J.W., 2022. The petrogenesis of modern and ophiolitic lavas reconsidered: Ti-V and Nb-Th. Geoscience Frontiers, 13(2), 101319. DOI: https://doi.org/10.1016/J.GSF.2021.101319

Shirdashtzadeh, N., Torabi, G., Schaefer, B., 2018. A magmatic record of Neoproterozoic to Paleozoic convergence between Gondwana and Laurasia in the northwest margin of the Central-East Iranian Microcontinent. Journal of Asian Earth Science Earth Science, 166, 35-47.

Simancas, J.F., Expósito, I., Azor, A., Martínez Poyatos, D., González Lodeiro, F., 2004. From the Cadomian orogenesis to the Early Paleozoic Variscan rifting in Southwest Iberia. Journal of Iberian Geology, 30, 53-71.

Soejono, I., Matchek, M., Sláma, J., Janoušek, V., Kohút, M., 2019. Cambro-Ordovician anatexis and magmatic recycling at the thinned Gondwana margin: new constraints from the Kouřim Unit, Bohemian Massif. Journal Geological Society, 177, 325-341.

Speksnijder, A., 1986. Geological analysis of Paleozoic large-scale faulting in the south-central Pyrenees. Geologica Ultraiectina, 43, 1-211.

Stille, H., 1939. Bemerkungen betreffend die "Sardische" Faultung und den Ausdruck "Ophiolithisch". Zeitschrift der Deutschen Geologischen Gesellschaft, 91, 771-773.

Štorch, P., Roqué Bernal, J., Gutiérrez-Marco, J.C., 2019. A graptolite-rich Ordovician–Silurian boundary section in the south-central Pyrenees, Spain: stratigraphical and palaeobiogeographical significance. Geological Magazine, 156, 1069-1091. DOI: https://doi.org/10.1017/S001675681800047X

Sun, S., McDonough, W.F., 1989. Chemical and isotopic systematics of oceanic basalts: implications for mantle composition and processes. In: Saunders, A.D., Norry, M.J. (eds.). Magmatism in the Ocean Basins. London, The Geological Society, 42 (Special Publications), 313-345.

Swanson-Hysell, N.L., Macdonald, F.A., 2017. Tropical weathering of the Taconic orogeny as a driver for Ordovician cooling. Geology, 45, 719-722. DOI: https://doi.org/10.1130/G38985.1

Syahputra, R., Žák, J., Nance, R.D., 2022. Cambrian sedimentary basins of northern Gondwana asgeodynamic markers of incipient opening of the Rheic Ocean. Gondwana Research, 105, 492-513.

Syme, E.C., 1998. Ore-Associated and Barren Rhyolites in the central Flin Flon Belt: Case Study of the Flin Flon Mine Sequence. Manitoba Energy and Mines, Open File Report OF98-9, 1-32.

Talavera, C., Montero, P., Bea, F., González Lodeiro, F., Whitehouse, M., 2013. U–Pb Zircon geochronology of the Cambro-Ordovician metagranites and metavolcanic rocks of central and NW Iberia. Interbnational Journal of Earth Sciene (Geologische Rundschau), 102, 1-23.

Tan, E., Gurnis, M., Han, L., 2002. Slabs in the lower mantle and their modulation of plume formation. Geochemistry, Geophysics, Geosystem, 3(11), 1067. DOI: 10.1029/2001GC000238

Tan, E., Leng, W., Zhong, S., Gurnis, M., 2011. On the location of plumes and lateral movement of thermochemical structures with high bulk modulus in the 3-D compressible mantle. Geochemistry, Geophysics, Geosystems, 12, Q07005. DOI: https://doi.org/10.1029/2011GC003665

Teichmüller, R., 1931. Zur Geolgie des Thyrrhenisgebietes. Teil 1: Alte und junge Krustenbewegungen im südlinchen Sardinien. Nachrichten von der Gesellschaft der Wissenschaften zu Göttingen, Mathematisch-Physikalische Klasse, 3, 857-950.

Teipel, U., Eichhorn, R., Loth, G., Rohrmüller, J., Höll, R., Kennedy, A., 2004. U–Pb SHRIMP and Nd isotopic data from the western Bohemian Massif (Bayerischer Wald, Germany): Implications for Upper Vendian and Lower Ordovician magmatism. International Journal of Earth Sciences, 93, 782-801.

Thiéblemont, D., Guerrot, C., Simien, F., Zammit, C., 2017. A compilation of radiochronological ages obtained before 2016 on the Armoricain Massif. Inventory and data organization, perspectives for future acquisitions. Géologie de la France, 2017(1), 27-46.

Tichomirowa, M., Berger, H.J, Koch, E.A, Belyatski, B., Götze, J., Kempe, U., Nasdala, L., Schaltegger, U., 2001, Zircon ages of high-grade gneisses in the Eastern Erzgebirge (Central European Variscides)—constraints on origin of the rocks and Precambrian to Ordovician magmatic events in the Variscan foldbelt. Lithos, 56, 303-332.

Tichomirowa, M., Sergeev, S., Berger, H.J., Leonhardt, D., 2012, Inferring protoliths of high-grade metamorphic gneisses of the Erzgebirge using zirconology, geochemistry and comparison with lower-grade rocks from Lusatia (Saxothuringia, Germany). Contributions Mineralogy Petrology, 164, 375-396.

Trombetta, A., Cirrincione, R., Corfú, C., Mazzoleni, P., Pezzino, A., 2004. Mid-Ordovician U–Pb ages of porphyroids in the Peloritan Mountains (NE Sicily): palaeogeographical implications for the evolution of the Alboran microplate. Journal of the Geologica Society, 161, 265-276.

Ugidos, J.M., Sánchez-Santos, P., Barba, P., Valladares, M.I., 2010. Upper Neoproterozoic series in the Central Iberian, Cantabrian and West Asturian Leonese Zones (Spain): geochemical data and statistical results as evidence for a shared homogenised source area. Precambrian Research, 178, 51-58.

Uğurcan, O.G., Ustaömer, T., 2024. Late Cambrian-early Ordovician extensional magmatism, uplift and sedimentation of the N Gondwana margin: new field, geochemical and geochronological data from the peri-Gondwanan Central Sakarya Terrane, Sakarya Zone, NW Turkey. International Geology Review, 67(7), 859-889. DOI: https://doi.org/10.1080/00206814.2024.2406012

Valverde-Vaquero, P., Dunning, G.R., 2000. New U–Pb ages for Early Ordovician magmatism in Central Spain. Journal of the Geological Society, 157, 15-26.

Vergés, J., Martínez-Rius, A., Domingo, F., Muñoz, J.A., Losantos, M., Fleta, J., Gisbert, J., 1994. Mapa geológico de España a escala 1:50.000, hoja de La Pobla de Lillet (no. 255). Madrid, Instituto Tecnológico y Geominero de España (ITGE).

Villaseca, C., Barbero, L., Herreros, V., 1998. A re-examination of the typology of peraluminous granite types in intracontinental orogenic belts. Transactions of the Royal Society of Edinburgh: Earth Sciences, 89, 113-119.

Villaseca, C., Castiñeiras, P., Orejana, D., 2015. Early Ordovician metabasites from the Spanish Central System: A remnant of intraplate HP rocks in the Central Iberian Zone. Gondwana Research, 27, 392-409. DOI: http://dx.doi.org/10.1016/j.gr.2013.10.007

Villaseca, C., Merino Martínez, E., Orejana, D., Andersenc, T., Belousova, E., 2016. Zircon Hf signatures from granitic orthogneisses of the Spanish Central System: Significance and sources of the Cambro–Ordovician magmatism in the Iberian Variscan Belt. Gondwana Research, 34, 60-83.

Vinn, O., Colmenar, J., Zamora, S., Pereira, S., Pillola, G.L., Alkahtane, A.A., Al Farraj, S., El Hedeny, M., 2024. Late Ordovician cornulitid tubeworms from high-latitude

peri-Gondwana (Sardinia and the Pyrenees) and their palaeobiogeographic significance. Journal of Paleontology, 13(4), 939-953. DOI: 10.1016/j.jop.2024.08.009

Vitrac-Michard, A., Allègre, C.J., 1975a. Study of the formation and history of a piece of continental crust by 87Rb–86Sr method: the case of the French oriental Pyrenees, Contribution to Mineralogy and Petrology, 50, 257-285.

Vitrac-Michard, A., Allègre, C.J., 1975b. 238U–206Pb, 235U–207Pb, systematics on Pyrenean basement, Contribution to Mineralogy and Petrology, 51, 205-212.

von Quadt, A., 1997, U-Pb zircon and Sr-Nd-Pb whole-rock investigations from the continental deep drilling (KTB). Geologische Rundschau, 86 (Supplement), S258-S271.

Whalen, J.B., Currie, K.L., Chappell, B.W., 1987. A-type granites: geochemical characteristics and discrimination. Contribution to Mineralogy and Petrology, 95, 420-436.

Winchester, J.A., Floyd, P.A., 1977. Geochemical discrimination of different magma series and their differentiation products using immobile elements. Chemical Geology, 20, 325-343.

Wood, D.A., 1980. The application of a Th-Hf-Ta diagram to problems of tectonomagmatic classification and to establishing the nature of crustal contamination of basaltic lavas of the British Tertiary Volcanic Province. Earth and Planetary Science Letters, 50, 11-30. DOI: https://doi.org/10.1016/0012-821X(80)90116-8

Wu, L., Murphy, J.B., Nance, R.D., 2022. Evaluation of paleomagnetic bias in Ediacaran global paleogeographic reconstructions. Geophysical Research Letters, 49, e2022GL100405. DOI: http://doi.org/10.1029/2022GL100405

Yılmaz Şahin, S., Naycı, Ö., Aysal, N., Cansu, Z., Şişman Tükel, F., 2024. Geochemical and geochronological evidences from Cambrian to Ordovician protracted magmatism in the Istranca Massif, NW Türkiye. Geochemistry, 126196. DOI: https://doi.org/10.1016/j.chemer.2024.126196

Žák, J., Sláma, J., Syahputra, R., Nance, R.D., 2023. Dynamics of Cambro–Ordovician rifting of the northern margin of Gondwana as revealed by the timing of subsidence and magmatism in rift-related basins. International Geology Review, 65(19), 3004-3027. DOI: https://doi.org/10.1080/00206814.2023.2172619

Zeck, H.P., Whitehouse, M.J., Ugidos, J.M., 2007. 496±3Ma zircon ion microprobe age for pre-Hercynian granite, Central Iberian Zone, NE Portugal (earlier claimed 618±9Ma). Geological Magazine, 144(1), 21-31.

Zulauf, G., Dörr, W., Fiala, J., Vejnar, Z., 1997. Late Cadomian crustal tilting and Cambrian transtension in the Teplá–Barrandian unit (Bohemian Massif, Central European Variscides). Geologische Rundschau, 86, 571-584.

Manuscript received October 2024;
revision accepted April 2025;
published Online July 2025.

APPENDIX

ANALYTICAL PROCEDURE

X-Ray Fluorescence Analysis was used for the determination of major elements, a fusion with lithium tetraborate in a sample with flux ratio (0.3:5.5) was performed in a PerlX'3 bead maker and measured with wavelength dispersive XRF ZETIUM* from PANalytical with a rhodium tube and Major program.

Sodium determination was analyzed by Atomic Absorption using lithium metaborate fusion. Loss on ignition was performed by gravimetry by calcination at 950ºC. Trace element determination by ICP-MS using s ample digestion with concentrated HF, HNO_3, and $HClO_4$ to dryness and dissolution of the residue with 10% HCl.

Rare Earth Element Analysis by Inductively Coupled Plasma Mass Spectrometry (ICP-MS). Fusion with lithium metaborate (sample-flux ratio 0.2:0.3) and acid digestion. HFSE determination by ICP-MS: Sample fusion with lithium metaborate. The melt is dissolved with mannitol, hydrochloric acid, and hydrofluoric acid. The solution is evaporated to dryness, the residue is collected with 0.125% hydrofluoric acid and made up to 100 mL with 1 mL of concentrated nitric acid.

Additional Sm-Nd isotopic analyses were performed at Centro de Geocronología y Geoquímica Isotópica from the Complutense University, Madrid. They were carried out in whole-rock powders using a ^{150}Nd–^{149}Sm tracer by isotope dilution-thermal ionization mass spectrometry (ID–TIMS). The samples were first dissolved through oven digestion in sealed Teflon bombs with ultra-pure reagents to perform two-stage conventional cation-exchange chromatography for separation of Sm and Nd, and subsequently analysed using a Sector 54 VG-Micromass multicollector spectrometer. The measured $^{143}Nd/^{144}Nd$ isotopic ratios were corrected for possible isobaric interferences from ^{142}Ce and ^{144}Sm (only for samples with $^{147}Sm/^{144}Sm<0.0001$) and normalized to $^{146}Nd/^{144}Nd=0.7219$ to correct for mass fractionation. The Lajolla Nd international isotopic standard was analysed during sample measurement, and gave an average value of $^{143}Nd/^{144}Nd=0.5114840$ for 9 replicas, with an internal precision of ± 0.000032 (2σ). These values were used to correct the measured ratios for possible sample drift. The estimated error for the $^{147}Sm/^{144}Nd$ ratio is 0.1%.

TABLE I. Classification and location of the new collected samples of the Canigó massif

Sample location					
Sample	Rock type	Sampling site	Latitude	Longitude	Altitude
CG-20-02	Gneiss-G1	Queralbs-La Farga	42.213201N	2.102350E	1159m
CG-20-03	Gneiss-G1	Queralbs-La Farga	42.213201N	2.102350E	1159m
CG-20-04	Gneiss-G1	Queralbs-La Farga	42.215231N	2.103158E	1184m
CG-20-06	Gneiss-G1	Road Marialles-Pla Guillem	42.293959N	2.243656E	1776m
CG-19-07	Gneiss-G1	Road Marialles-Pla Guillem	42.293959N	2.243656E	1776m
CG-20-10B	Gneiss-G2	Coll de Jou	42.520919N	2.364915E	1080m
CG-20-11	Gneiss-G2	Road Saorra- Pi	42.310506N	2.223536E	1080m
CG-20-12A	Gneiss-G2	Road Saorra- Pi	42.311680N	2.215592E	767m
CG-20-12B	Gneiss-G2	Road Saorra- Pi	42.311680N	2.215592E	767m
CG-19-08	Gneiss-G2	Road Saorra- Pi	42.311958N	2.215400E	760m
CG-20-07	Gneiss-G3	Road Marialles-Pla Guillem	42.293320N	2.243900E	1798m
CG-19-05	Gneiss-G3	Road Marialles-Pla Guillem	42.293320N	2.243900E	1798m
CG-20-08	Gneiss-Casemí	Marialles hut	42.300207N	2.243436E	1708m
CG-19-04	Gneiss-Casemí	Marialles hut	42.300207N	2.243436E	1708m
CG-19-09	Gneiss-Cadí	Coll de Jou	42.303021N	2.244316E	1229m
CG-20-09	Gneiss-Cadí	Coll de Jou	42.303021N	2.244316E	1229m
CG-24-04	Amphibolites	Cortalets hut road	42.325888N	2.282905E	1984m
CG-19-06	Amphibolites	Road Marialles-Pla Guillem	42.293320N	2.243900E	1798m
CG-20-01	Ignimbrite	Bruguera	42.170373N	2.110544E	1421m
CG-20-05	Granite	Road Ribes-Queralbs	42.190256N	2.100331E	953m

TABLE II. U-Pb ages of the inherited zircon cores in the Ordovician magmatic rocks of the Canigó

				Age of the inherited zircons						
Author	Method	Rock type	Sample	Paleoarchean	Mesoarchean	Neoarchean	Paleoproterozoic	Mesoproterozoic	Neoproterozoic	Cambrian
Deloule *et al.* (2002)	CAMECA	G-1 gneiss	99Py10							516
Deloule *et al.* (2002)	CAMECA	G-1 gneiss	98PY16							527
Deloule *et al.* (2002)	CAMECA	G-1 gneiss	99PY01						575-552	517
Cocherie *et al.* (2005)	SHRIMP	G-1 gneiss	LP 1				2021-2018-1982		630-550	
Cocherie *et al.* (2005)	SHRIMP	G-1 gneiss	LP 2	3244-3404			2477-2433-2240			
							2007-1951			
Castiñeiras *et al.* (2008a)	SHRIMP	G-2 gneiss	RF-5						850-680-640	530
Casas *et al.* (2010)	SHRIMP	Cadí gneiss	CG-07-01						702	
Martínez *et al.* (2011)	SHRIMP	G-1 gneiss	RN-23						905-852-681-589	
Martínez *et al.* (2011)	SHRIMP	G-1 gneiss	RE-4		2852				824-620-571	
Navidad *et al.* (2018)	SHRIMP	CG-20-01	G-2						974-576	
Navidad *et al.* (2018)	SHRIMP	CG-20-02	G-3						976-796-664-584-555	527
Martí *et al.* (2019)	LA	Ignimbr. Campelles	CAM-6			2609-2533-2506	2499-2246-1726		824	
Martí *et al.* (2019)	LA	Ignimbr. Campelles	CAM-7				2313-2303		652	
Martí *et al.* (2019)	LA	Ignimbr. Campelles	CAM-9				2160-1995-1987		988-941-764-746	516
							1961-1852-1701		625-621	
Martí *et al.* (2019)	LA	Ignimbr. Campelles	CAM-18					1059	758-728-647-639-598	
Martí *et al.* (2019)	LA	Ignimbr. Bruguera	CAM-13						759	